

To my parents for their endless love and support

Análise e simulação numérica de escoamentos de fluidos Newtonianos

Resumo

Este trabalho tem como objectivo o estudo matemático e numérico de fluidos Newtonianos incompressíveis em diferentes geometrias bidimensionais para escoamentos não estacionários. Aplicamos o Método de Elementos Finitos para a obtenção de soluções e analisamos a evolução do escoamento ao longo do tempo.

O nosso estudo para estas equações diferenciais parciais não-lineares é dividido em três passos fundamentais. Considera-se em primeiro lugar a análise matemática das propriedades das soluções, tais como a existência, unicidade (bidimensional) e estimativas à priori associadas. A unicidade de solução é ainda um problema em aberto, no caso tridimensional.

Segue-se o estudo de aproximação numérica com resultados de existência e unicidade de soluções aproximadas, bem como estimativas de erro à priori.

Finalmente, apresentamos simulações numéricas que envolvem escoamentos em diferentes geometrias bidimensionais e o comportamento das soluções é discutido.

Palavras-chave: sistema de Navier-Stokes, Método dos Elementos Finitos.

Abstract

The present work concerns the analysis and numerical simulations of incompressible Newtonian fluids in different bidimensional geometries for unsteady flows. We apply the Finite Element Methods to obtain solutions and we analyze the evolution of the flow over time.

Our study for this non-linear partial differential equations is divided into three main steps. The mathematical analysis of the properties of the solutions, such as existence, uniqueness (bidimensional) and associated a-priori estimates have been done. Uniqueness is still an open problem in the three-dimensional case.

Numerical approximation is next considered and results of existence and uniqueness, as well as a-priori error estimates are established.

Finally, numerical simulations involving flows of different bidimensional geometries are presented and the behavior of the solutions is discussed.

Acknowledgement

I feel most fortunate to have had the opportunity to study in the University of Évora and to do my Master's thesis at the Department of Mathematics. I would like to express my sincere gratitude to all who gave me the possibility to complete this thesis. Without them, it would have been much harder to finish this thesis.

First and foremost, I would like to express my deep-felt everlasting gratitude to my mentor, Prof. Dr. Marília da Conceição Valente de Oliveira Pires of the Mathematics Department at the University of Évora, for entrusting me with such an interesting research work from which I have gained tremendous amount of knowledge and experience. I am highly indebted to her for the trust she placed in my thesis and for her advice, continuous guidance, affectionate encouragement, enduring patience, motivation and constant support throughout the period of research and at every stage of my Mathematics and Application study. I finally consider it as a privilege to have had the opportunity to do this thesis under her supervision.

I would like to thank Prof. Dr. Clara Carlota, Prof. Dr. Joaquim Correia and Prof. Dr. Feliz Minhós for their useful scientific and practical advice and encouragement during my thesis and study.

I want to say that I really enjoy the company of wonderful people I have met in the Mathematics department. I am grateful to all the staff in the Mathematics department for their generous assistance, hard work and dedication, providing me the

means to complete my degree. Especially, I would like to thank Prof. Dr. José Carlos Brandão Tiago Oliveira, Prof. Dr. Imme Pieter Van Den Berg, Mrs. Teresa Nogueiro and Mrs. Marta Graça for their untiring suggestions whenever approached them for help and generous encouragement during my whole study period in Portugal.

My special thanks go to those of my friends and colleagues who gave me their precious and long-lasting support from abroad during my academic career, and the non-academic detour.

This research is funded by EMMA in the framework of EU Erasmus Mundus Action-2 programe. I would like to thank Erasmus Mundus Action-2 (EMMA-WEST) project and the University of Évora for awarding me the scholarship which makes possibilities of me coming in University of Évora, Portugal and providing me a helpful research environment.

Last but not the least, I am very much grateful to my parents for their continuous support in every step of my life.

Md. Mahfuzur Rhaman
Évora, Portugal.

Contents

1	Introduction	1
2	Constitutive Equations	3
2.1	Kinematics	3
2.1.1	The motion of continuous medium	3
2.1.2	The velocity	4
2.1.3	The material derivative	5
2.1.4	The acceleration	6
2.1.5	The deformation gradient tensor	6
2.1.6	The strain or rate of deformation tensor	8
2.2	The Conservation Laws	8
2.2.1	Conservation Law of Mass	8
2.2.2	Conservation Law of Momentum	9
2.3	The Constitutive Law	14
2.3.1	Newtonian Fluids	14
2.3.2	Navier-Stokes Equations	16
2.3.3	Dimensionless Navier-Stokes equations	18
2.4	Boundary conditions	19
3	Mathematical Analysis for incompressible Navier-Stokes Equations	23
3.1	Notations and elementary results of functional analysis	23
3.1.1	Continuous functions spaces	24
3.1.2	Lebesgue space	25
3.1.3	Distributions space	26

3.1.4	Sobolev spaces	27
3.1.5	Space-time functions	30
3.2	Weak formulation of Navier-Stokes problem	31
3.2.1	Abstract formulation	35
3.2.2	Existence and uniqueness of solution	39
3.2.3	Energy inequality	41
4	Numerical Analysis for Navier-Stokes Flow	45
4.1	Finite Element Method	46
4.2	Semi-Discrete Navier-Stokes problem	50
4.3	Time discretization	54
4.4	Algorithm and algebraic linear systems	57
5	Numerical results	63
5.1	Choice of solver and code validation	64
5.1.1	Numerical Test	66
5.2	Applications of Newtonian fluids model	71
5.2.1	Mathematical model	72
5.2.2	Variational formulation	73
5.2.3	Discretized problem	74
5.2.4	Stream function	75
5.2.5	Flow in a straight pipe	76
5.2.6	Flow in a deformed pipe	79
6	Conclusions	89
	Bibliography	91
	Appendix	95

List of Figures

4.1	<i>Example of a non polygonal domain discretized by polygons.</i>	46
4.2	<i>Affine map from the reference triangle \hat{T} to the generic element $T \in \mathcal{T}_h$.</i>	48
4.3	<i>$\mathbb{P}_2 - \mathbb{P}_1$ elements: degrees of freedom for the velocity components (on the left) and for the pressure (on the right).</i>	58
5.1	<i>Structured meshes employed on square $[0.25, 1.25] \times [0.5, 1.50]$. The coarse mesh with 2048 elements (on the left) and the fine mesh with 8192 elements (on the right).</i>	64
5.2	<i>Error on the fluid velocity field (on the left) and the pressure (on the right) in L^2-norm for each instant of time, for different Δt using a mesh with 2048 elements.</i>	66
5.3	<i>Error on the fluid velocity field (on the left) and the pressure (on the right) in L^2-norm for each instant of time, for different Δt using a mesh with 8192 elements.</i>	67
5.4	<i>Comparison of errors of the fluid velocity field (on the left) and the pressure (on the right) in L^2-norm for the instant of time $t = 1$, for different Δt using the both meshes.</i>	67
5.5	<i>Comparison of CPU times used as a function of Δt in solving the problem by the method of Crout for the two meshes.</i>	68
5.6	<i>Comparison of errors of the fluid velocity field (on the left) and the pressure (on the right) in L^2-norm for each instant of time, for different Δt using a mesh with 2048 elements, for both methods: Crout and CG.</i>	68

5.7	<i>Comparison of errors of the fluid velocity field (on the left) and the pressure (on the right) in L^2-norm for the instant of time $t = 1$, for different Δt using both methods.</i>	69
5.8	<i>Comparison of errors of the fluid velocity field (on the left) and the pressure (on the right) in L^2-norm for each instant of time, for different Δt using a mesh with 8192 elements, for both methods: Crout and CG.</i>	69
5.9	<i>Comparison of CPU times used for the both methods, as a function of Δt, in solving the problem with the two meshes.</i>	70
5.10	<i>Comparison of CPU times used as a function of Δt in solving the problem by the both method for the two meshes.</i>	70
5.11	<i>Exact solution at $t = 1$. First component of velocity (on the left), second component of velocity (on the center) and pressure (on the right).</i>	71
5.12	<i>Approach solution at $t = 1$. First component of velocity (on the left), second component of velocity (on the center) and pressure (on the right).</i>	71
5.13	<i>The input profile of inflow Neumann boundary condition.</i>	73
5.14	<i>Structured mesh employed, in a straight pipe.</i>	76
5.15	<i>Qualitative behavior of normal velocity (on the left), of tangential velocity (on the center) and pressure (on the right), in a straight pipe.</i>	76
5.16	<i>Contour plots of u_1 (on the left) and of pressure (on the right) at different instants of time, in a straight pipe.</i>	77
5.17	<i>The representative vectorial field of each component of velocity, in a straight pipe.</i>	78
5.18	<i>Variation of magnitude of the normal velocity in function of time, in a straight pipe.</i>	78
5.19	<i>The representative vector plot (on the left) and the streamlines (on the right), in a straight pipe.</i>	79
5.20	<i>The volume flux of fluid $Q^n(x_i)$, at different times, in a straight pipe.</i>	79
5.21	<i>Unstructured mesh employed, in a pipe with concave deformation of the upper wall.</i>	80

5.22	<i>Normal velocity at different instants of time, in a pipe with concave deformation of the upper wall.</i>	80
5.23	<i>Tangential velocity at different instants of time, in a pipe with concave deformation of the upper wall.</i>	80
5.24	<i>The representative vectorial field of each component of velocity, in a pipe with concave deformation of the upper wall.</i>	81
5.25	<i>Pressure at different instants of time, in a pipe with concave deformation of the upper wall.</i>	81
5.26	<i>The average pressure of fluid $\bar{p}^n(x_i)$, at different times, in a pipe with concave deformation of the upper wall.</i>	82
5.27	<i>The whole flow pattern: velocity vector plots and streamlines at five different times, in a pipe with concave deformation of the upper wall.</i>	83
5.28	<i>The volume flux of fluid $Q^n(x_i)$, at different times, in a pipe with concave deformation of the upper wall.</i>	83
5.29	<i>Unstructured mesh employed, in a pipe with convex deformation of the upper wall.</i>	84
5.30	<i>The whole flow pattern: velocity vector plots and streamlines at five different times, in a pipe with convex deformation of the upper wall.</i>	85
5.31	<i>The volume flux of fluid $Q^n(x_i)$, at different times, in a pipe with convex deformation of the upper wall.</i>	86
5.32	<i>Normal velocity at different instants of time, in a pipe with convex deformation of the upper wall.</i>	86
5.33	<i>Tangential velocity at different instants of time, in a pipe with convex deformation of the upper wall.</i>	86
5.34	<i>The representative vectorial field of each component of velocity, in a pipe with convex deformation of the upper wall.</i>	87
5.35	<i>Pressure at different instants of time, in a pipe with convex deformation of the upper wall.</i>	87
5.36	<i>The average pressure of fluid $\bar{p}^n(x_i)$, at different times, in a pipe with convex deformation of the upper wall.</i>	87

Chapter 1

Introduction

The goal of this work is concerned to numerical approach of the unsteady problem that models the motion of incompressible Newtonian fluids, in the bidimensional case. To understand well this subject, we begin by characterizing a fluid and some of its fundamental properties. More detailed information on this can be found in [21].

When we talk about fluids, we talk about a substance which can not resist a shear force or stress without moving as a solid can. Fluids are mainly divided into two categories: liquids and gases.

When fluids are in contact with a surface they exert a normal and tangential force on the surface. This normal force is present in fluids both at rest and in motion, whereas tangential (shearing) forces exist only for fluids in motion. Liquids and gases are unable to exert tensile stresses. Thus the normal force exerted by a fluid on a surface is always compressive, i.e., it is directed towards the surface. The pressure P on a planar surface is defined as the compressive normal force applied by the fluid in the surface, divided by the area of that surface. It is a scalar quantity and its SI unit is Newtons per square meter (Ne/m^2).

When we exert a compressive force on a fluid, its pressure increases while trying to keep its original volume. This property is called compressibility. In general, liquids¹ are called incompressible fluids and gases are compressible fluids.

The viscosity μ is the flow resistance of the fluid which a fluid offers when it is

¹The compression should be taken into account whenever liquids are highly pressurized

subjected to a tangential force. It is a scalar and its SI unit is Pascal second ($Pa\ s = Ne\ s/m^2 = Kg/(ms)$).

The viscosity of a liquid decreases with increasing temperature. The viscosity of fluids also depends on pressure. The relation between shear stress and velocity gradient is known as the Newton's law of viscosity. In general, fluids which obey such relationship are known as Newtonian fluids (see section 2.3.1).

The density of a fluid is a thermodynamic property which depends on the state of the fluid. The density is the mass per unitary volume of material, which is a positive scalar quantity generally denoted by ρ . It is convenient to express the density ρ as a function of pressure and temperature. The SI unit for the density is kilogram per cubic meter (Kg/m^3).

The reciprocal of density, i.e. the volume per unit of mass, is called the specific volume, which is generally expressed by the symbol $\vartheta = \frac{1}{\rho}$.

In this work we study the behavior of solutions of incompressible Newtonian fluids on bidimensional geometries.

Given the complex behavior of this fluids, the second order partial differential governing equations are non-linear and they have the parabolic characteristic. Results of numerical approach such as existence and unicity of approach solution and error estimates are obtained. Through the application of the finite element method for the Navier-Stokes system, we present results of numerical simulations.

The thesis is organized as follows: in chapter 2, we introduce some notions of continuum mechanics and we make the deduction of equations that describe the behavior of fluids under study. In chapter 3, we present the Mathematical Analysis for the Navier-Stokes equations and after that we introduce some results of functional analysis, essential to the mathematical and numerical study of Navier-Stokes equations. The numerical analysis of Navier-Stokes problem is made in chapter 4 and the results of numerical simulations, which were obtained through a code developed in FreeFem++, are presented in chapter 5. In appendix we introduce some notation and results of tensor calculus.

Chapter 2

Constitutive Equations

In this chapter, the deduction of the equations governing the behavior of incompressible Newtonian fluids is done. With this objective we start by introducing some elementary concepts of mechanics of continuous medium. This subject can be found in detail, for example in [30, 10, 8].

2.1 Kinematics

In this section, we will derive the partial differential equations which govern the fluid motion. With this goal, we ignore the molecular structure of the fluid and face it as a *continuous medium*. In the mathematical sense of the term, it means that, assigning to each point, the macroscopic properties of the actual environment, thus the properties of the medium are presented by continuous functions.

2.1.1 The motion of continuous medium

To study the kinematic, the motion of the medium which may be thought as continuously occupying, at each time, a portion of space, we can use one of the two *references* or *frames*: *Lagrangian* or *Eulerian* (spatial). It is important to understand the meaning of each one.

Consider the Euclidean frame \mathbb{R}^d ($d = 2, 3$) and a time interval $I = [t_0, T] \subset \mathbb{R}$. Suppose that the particle of fluid is on position $\xi \in \Omega_0$, Ω_0 being the domain occupied

by the fluid at the reference initial time t_0 , called *initial* or *reference configuration* and at time $t \in I$, the portion of space Ω_t occupied by the fluid, called *current* or *spatial configuration*. The position of this fluid's particle is $\mathbf{x} \in \Omega_t$. We describe the *motion* or *deformation* of each particle by a family mapping

$$\begin{aligned}\chi_t : \Omega_0 &\longrightarrow \Omega_t \\ \xi &\longrightarrow \mathbf{x} = \mathbf{x}(t, \xi) = \chi_t(\xi)\end{aligned}$$

This mapping is called *Lagrangian mapping* at time t .

If V_0 is a region in Ω_0 , then $\chi_t(V_0) = V_t$ is the volume V_0 moving with the fluid.

We assume that χ_t is continuous and invertible on $\overline{\Omega_0}$, with continuous inverse. The pair (t, ξ) is called the *material* or *Lagrangian variables* and (t, \mathbf{x}) is called *spatial* or *Eulerian variables*.

In general, if a function is in the form $\psi = \psi(t, \xi)$ we speak about *Lagrangian description*, on the other hand if the function is in the form $\psi = \psi(t, \mathbf{x})$ we speak about *Eulerian description*.

When using the Eulerian variables as independent variables we are focusing on a position in space $\mathbf{x} \in \Omega_t$ and on the fluid particle which, at that particular time, is located at \mathbf{x} . When using the Lagrangian variables as independent variables we are interested targeting the fluid particle which was located at position ξ at the reference time t_0 . This means that we are following the trajectory T_ξ describe by the particle, which it has occupied the position ξ , given by

$$T_\xi = \{(t, \mathbf{x}(t, \xi)), t \in I\}.$$

Usually, the equations in Mechanics of Continuous Medium are in Eulerian coordinates because they describe the properties of the fluid's motion in the current configuration but by the inverse of the Lagrangian mapping we know them in the reference configuration.

2.1.2 The velocity

The fluid velocity is the major kinematic quantity. It is a vector field defined by

$$\hat{\mathbf{u}}(t, \xi) = \frac{\partial \mathbf{x}}{\partial t}(t, \xi)$$

in the Lagrangian frame and it denotes the time derivative of trajectory T_ξ of the fluid particle which was located at position ξ at the reference time.

In the Eulerian frame the velocity is defined by

$$\mathbf{u}(t, \mathbf{x}) = \hat{\mathbf{u}}(t, \chi_t^{-1}(\mathbf{x})).$$

2.1.3 The material derivative

The material derivative or Lagrangian derivative of a function f is defined as the time derivative in the Lagrangian frame, yet expressed as function of spatial variables. It takes into account the fact that the fluid is moving and the positions of fluid particles are changing along the time.

Let f be a function such that

$$f : I \times \Omega_t \longrightarrow \mathbb{R} \quad \text{and} \quad \hat{f} = f \circ \chi_t$$

then

$$\begin{aligned} \frac{Df}{Dt} : I \times \Omega_t &\longrightarrow \mathbb{R} \\ (t, \mathbf{x}) &\longrightarrow \frac{D\hat{f}}{Dt}(t, \xi), \quad \xi = \chi_t^{-1}(\mathbf{x}). \end{aligned}$$

So

$$\begin{aligned} \frac{Df}{Dt}(t, \mathbf{x}) &= \frac{d}{dt}f(t, \mathbf{x}(t, \xi)) = \left[\frac{\partial}{\partial t}(f \circ \chi_t) \right] \circ \chi_t^{-1}(t, \mathbf{x}) = \\ &= \frac{\partial f}{\partial t}(t, \mathbf{x}) + \sum_{i=1}^d \frac{\partial f}{\partial x_i}(t, \mathbf{x}) \cdot \frac{\partial x_i}{\partial t} = \frac{\partial f}{\partial t}(t, \mathbf{x}) + \sum_{i=1}^d u_i(t, \mathbf{x}) \frac{\partial f}{\partial x_i}(t, \mathbf{x}) \end{aligned}$$

then

$$\frac{Df}{Dt} = \frac{\partial f}{\partial t} + \mathbf{u} \cdot \nabla f$$

describes the rate of variation of f along the trajectory T_ξ . This derivative relates to the time derivatives evaluated on the Lagrangian and Eulerian frames.

A quantity which satisfies $\frac{\partial f}{\partial t} = 0$ is called *stationary*, and a motion for which $\frac{\partial \mathbf{u}}{\partial t} = 0$ is a *stationary motion*.

2.1.4 The acceleration

The acceleration $\widehat{\mathbf{a}}(t, \xi)$ of a material point ξ is a vector field defined through

$$\begin{aligned} \widehat{\mathbf{a}} : I \times \Omega_0 &\longrightarrow \mathbb{R} \\ (t, \xi) &\longrightarrow \widehat{\mathbf{a}}(t, \xi) = \frac{\partial \widehat{\mathbf{u}}}{\partial t}(t, \xi) = \frac{\partial^2 \mathbf{x}}{\partial t^2}(t, \xi) \end{aligned}$$

Using the material derivative we write the acceleration in Eulerian frame as

$$\mathbf{a} = \frac{D\mathbf{u}}{Dt} = \frac{\partial \mathbf{u}}{\partial t} + (\mathbf{u} \cdot \nabla)\mathbf{u}$$

Componentwise,

$$a_i = \frac{\partial u_i}{\partial t} + \sum_{j=1}^d u_j \frac{\partial u_i}{\partial x_j}, \quad i = 1, \dots, d.$$

2.1.5 The deformation gradient tensor

The deformation of a portion of a space can be described by the family mapping $\{\chi_t\}_{t \in [t_0, T]}$, χ_t being the function which gives us the position of its points, at time t , in relation to the reference configuration. The deformation gradient tensor is another kinematic quantity necessary for the derivation of the mathematical model. This second order tensor is defined, at each $t \in I$, as

$$\begin{aligned} \widehat{F}_t : \Omega_0 &\longrightarrow \mathbb{R}^{d \times d} \\ \xi &\longrightarrow \widehat{F}_t(\xi) = \nabla_\xi \chi_t(\xi) = \frac{\partial \mathbf{x}}{\partial \xi}(t, \xi) \end{aligned}$$

where $\nabla_\xi \chi_t$ is the derivative of χ_t in order to Lagrangian variable ξ .

Componentwise,

$$\left[\widehat{F}_t\right]_{ij} = \frac{\partial x_i}{\partial \xi_j}, \quad i, j = 1, \dots, d.$$

In particular, its determinant $J_t = \det \widehat{F}_t > 0$ is called the Jacobian of the mapping χ_t and it preserves the orientation of the boundary of subdomain maintained by mapping. This way, taking $V_t \subset \Omega_t$ and $V_0 = \chi^{-1}(V_t)$ we can write

$$\int_{V_t} f(t, \mathbf{x}) d\mathbf{x} = \int_{V_0} \widehat{f}(t, \xi) J_t(\xi) d\xi.$$

The next lemma, whose proof can be found in [8] tells us how to differentiate $J(t, \xi) = J_t(\xi)$.

Lemma 2.1.1 (*Euler expansion formula*)

$$\frac{D}{Dt} J_t(\xi) = \frac{D}{Dt} J(t, \xi) = J(t, \xi) \nabla \cdot \mathbf{u}(t, \chi_t(\xi)). \quad (2.1)$$

□

With the following theorem we can evaluate the rate of change of a defined integral over V_t as a function of the integrals of volume and boundary. Its proof can be found in [24, 10].

Theorem 2.1.1 (*Reynolds Transport Theorem*)

Let $V_0 \subset \Omega_0$ and $V_t \subset \Omega_t$ be its image under the mapping χ_t . Let $f : I \times \Omega_t \rightarrow \mathbb{R}$ be continuously differentiable with respect to both variables then

$$\frac{d}{dt} \int_{V_t} f = \int_{V_t} \left(\frac{Df}{Dt} + f \nabla \cdot \mathbf{u} \right) = \int_{V_t} \left[\frac{\partial f}{\partial t} + \nabla \cdot (f \mathbf{u}) \right] \quad (2.2)$$

□

By the divergence theorem, we can rewrite (2.2) as

$$\frac{d}{dt} \int_{V_t} f = \int_{V_t} \frac{\partial f}{\partial t} + \int_{\partial V_t} f \mathbf{u} \cdot \mathbf{n}$$

2.1.6 The strain or rate of deformation tensor

The strain tensor or rate of deformation tensor is a kinematic quantity that gives us information about the variation of volume element form along the time without rotation effects. The strain tensor may be defined as such that controls the evolution of the relative positions of points in a fluid element. This tensor is defined by

$$\mathbf{D}(\mathbf{u}) = \frac{1}{2} [\nabla \mathbf{u} + (\nabla \mathbf{u})^t] \quad (2.3)$$

and it is the symmetric part of the velocity gradient.

Componentwise,

$$[\mathbf{D}(\mathbf{u})]_{ij} = \frac{1}{2} \left(\frac{\partial u_i}{\partial x_j} + \frac{\partial u_j}{\partial x_i} \right), \quad i, j = 1, \dots, d.$$

The determinant $|\mathbf{D}(\mathbf{u})|$ gives us the volume variation of the continuous medium by unit of time.

2.2 The Conservation Laws

Taking into account the Lavoisier Law: "*in nature nothing is created, nothing is lost, everything is transformed*", we can deduce the three basics principles of conservation.

2.2.1 Conservation Law of Mass

The conservation law of mass is a fundamental principle of classical mechanics. This means that *the mass is neither created nor destroyed*. This way, during the motion the body's mass is unchanged. So, the mass of material contained in V_0 is the same as the one contained in V_t . Mathematically, we can translate this equality by

$$m(V_0) = m(\chi_t(V_0)) = m(V_t)$$

V_t being the material volume at time t , i.e, $V_t = \chi_t(V_0)$ the image under the Lagrangian mapping of a subdomain $V_0 \subset \Omega_0$.

Consider the mass density $\rho : I \times \Omega_t \longrightarrow \mathbb{R}$, a strictly positive, measurable function such that the mass of fluid contained in V_t is given by

$$\int_{V_t} \rho(t, \mathbf{x}) d\mathbf{x} = m(V_t).$$

Fixed $V_t \subset \Omega_t$ we have

$$0 = \frac{d}{dt} m(V_t) = \frac{d}{dt} \int_{V_t} \rho(t, \mathbf{x}) d\mathbf{x}.$$

Applying (2.2) the Reynold Transport Theorem, we obtain the *integral form of the law of conservation of mass*

$$\int_{V_t} \left(\frac{D\rho}{Dt} + \rho \nabla \cdot \mathbf{u} \right) = \int_{V_t} \left[\frac{\partial \rho}{\partial t} + \nabla \cdot (\rho \mathbf{u}) \right] = 0. \quad (2.4)$$

By the arbitrariness of V_t (2.4) is equivalent to the *differential form of the law of conservation of mass* also known as the *continuity equation*

$$\frac{\partial \rho}{\partial t} + \nabla \cdot (\rho \mathbf{u}) = 0. \quad (2.5)$$

Being $\rho = \text{constant}$, from (2.5) we conclude

$$\nabla \cdot \mathbf{u} = 0 \quad (2.6)$$

This kinematic constraint applied to the Euler expansion formula allows to conclude that $\frac{D}{Dt} J_t = 0$ which is the *incompressibility constraint*. A flow that satisfies the incompressibility constraint is called *incompressible flow*. We remark that all fluid with constant density is an incompressible flow, but the opposite is not true in general. It is easy to show that the only possible motions of an incompressible flow are those which preserve the fluid volume.

2.2.2 Conservation Law of Momentum

The consequences of body motion can not be described simply by velocity, they also depend on the mass. So, we use the *momentum of mass* (mass \times velocity) to relate

them. The *momentum of the mass at times t of the volume V_t* known as *linear momentum* is defined by

$$\int_{V_t} \rho \mathbf{u}$$

where $\rho \mathbf{u}$ is the *density of the momentum*.

The Newton's second law tells us "*force = mass \times acceleration*", i.e., "*the rate of change of momentum of a portion of the fluid equals the force applied to it*".

There are three types of forces acting on a portion of material of a continuum:

- *Body forces* - these forces act on a volume of fluid in such a way that the magnitude of the body force is proportional to the mass or volume of the fluid element. Body forces act on a fluid but are not applied by a fluid. They exert their influence on fluids at rest and in motion without need for physical contact between the fluid and the external source of the body force. In general, a body force must be represented as a function of both position and time by a vector field $\mathbf{f} : I \times \Omega_t \rightarrow \mathbb{R}^d$ called *specific body force* and it is an acceleration, like the gravity. When these forces are applied on a volume V_t , they are expressed by

$$\int_{V_t} \rho \mathbf{f}.$$

- *Surface forces* - these forces act on an element of fluid through physical contact. In general, a surface force must be represented by a vector field $\mathbf{t}^e : I \times \Gamma_t \rightarrow \mathbb{R}^d$ called *applied stresses*, defined on a measurable subset of a domain boundary $\Gamma_t \subset \partial\Omega_t$. These forces exist at every interface involving a fluid, both on a fluid at rest and in a fluid in motion. The total surface force depends on the size, shape, and orientation of the surface on which the force acts, as well as on characteristics of the fluid and its motion. In developing a model for the surface force, we may distinguish three different situations: the surface force exerted by a fluid on a structure, the surface force applied to a

fluid by a structure, and the state of stress in a fluid. The orientation of any surface is specified by the outward unit normal of the surface.

In a fluid in motion, the surface force per unit area acting on an infinitesimal surface, generally has both normal and tangential components. Thus, stress in fluid dynamics is a vector quantity. The surface force acting on a plane surface element depends on the position, and on the size and orientation of the element. The total surface force acting on any surface in contact with fluid is given by

$$\int_{\Gamma_t} \mathbf{t}^e.$$

The total surface force is a vector quantity whose components may be solved in any desired direction.

- *Internal continuity forces* - these forces are exerted between the continuous medium particles and they are responsible for maintaining material continuity during the motion and are modeled taking into account the *Principle of Cauchy*, which tells us the only dependence of the internal forces on the geometry of boundary ∂V_t is through its outward normal \mathbf{n} , and the *Cauchy Stress Tensor Theorem*.

Theorem 2.2.1 (*Principle of Cauchy*)

There exist a vector field, called the Cauchy stress field $\mathbf{t} : I \times \Omega_t \times S_1 \rightarrow \mathbb{R}^d$ with $S_1 = \{\mathbf{n} \in \mathbb{R}^d : \|\mathbf{n}\| = 1\}$ such that its integral on the surface of any material domain $V_t \subset \Omega_t$, is given by

$$\int_{\partial V_t} \mathbf{t}(t, \mathbf{x}, \mathbf{n}) d\Gamma,$$

where $d\Gamma$ is the area element and \mathbf{n} is the outward normal of ∂V_t , is equivalent to the resultant of the material continuity forces acting on V_t .

□

Furthermore, we have $\mathbf{t} = \mathbf{t}^e$ on $\partial V_t \cap \Gamma_t$.

At this point, we can write mathematically the conservation law of linear momentum as

$$\frac{d}{dt} \int_{V_t} \rho \mathbf{u} = \int_{V_t} \rho \mathbf{f} + \int_{\partial V_t} \mathbf{t}(t, \mathbf{x}, \mathbf{n}) \quad (2.7)$$

for a given arbitrary time $t \in I$ and $V_t \subset \Omega_t$. The equality (2.7) tells us that the variation of the linear momentum of V_t defined by

$$\frac{d}{dt} \int_{V_t} \rho \mathbf{u}$$

is balanced by the resultant of the internal and the body forces.

Supposing regularity conditions of the Cauchy stresses, we relate the *internal continuity forces* to a *tensor field*, by the following theorem, whose proof can be found in [29].

Theorem 2.2.2 (*Cauchy Stress Tensor Theorem*)

Being the body forces \mathbf{f} , the density ρ and the fluid acceleration $\frac{D\mathbf{u}}{Dt}$ bounded functions on Ω_t , for any $t \in I$ and the Cauchy stress vector field \mathbf{t} is continuously differentiable with respect to the variable \mathbf{x} for each $\mathbf{n} \in S_1 = \{\mathbf{n} \in \mathbb{R}^d : \|\mathbf{n}\| = 1\}$ and continuous with respect to \mathbf{n} . Then, there exists a continuously differentiable symmetric tensor field, called Cauchy stress tensor

$$\mathbf{T} : I \times \overline{\Omega_t} \longrightarrow \mathbb{R}^{d \times d}$$

such that

$$\mathbf{t}(t, \mathbf{x}, \mathbf{n}) = \mathbf{T}(t, \mathbf{x}) \cdot \mathbf{n}, \quad \forall t \in I, \forall \mathbf{x} \in \Omega_t, \forall \mathbf{n} \in S_1.$$

□

Therefore, under the hypothesis of Cauchy theorem, we have

- The applied surface forces on $\partial V_t \cap \Gamma_t$ can be expressed by $\mathbf{T} \cdot \mathbf{n}$, i.e.,

$$\mathbf{T} \cdot \mathbf{n} = \mathbf{t} = \mathbf{t}^e \text{ on } \partial V_t \cap \Gamma_t. \quad (2.8)$$

- The resultant of the internal forces on V_t can be expressed by $\int_{\partial V_t} \mathbf{T} \cdot \mathbf{n}$, i.e.,

$$\int_{\partial V_t} \mathbf{T} \cdot \mathbf{n} = \int_{\partial V_t} \mathbf{t}^e. \quad (2.9)$$

This allows us to rewrite the principle of linear momentum (2.7) as

$$\frac{d}{dt} \int_{V_t} \rho \mathbf{u} = \int_{V_t} \rho \mathbf{f} + \int_{\partial V_t} \mathbf{T} \cdot \mathbf{n}. \quad (2.10)$$

Supposing that $\nabla \cdot \mathbf{T}$ is integrable, we can apply the divergence theorem and (2.10) becomes

$$\frac{d}{dt} \int_{V_t} \rho \mathbf{u} = \int_{V_t} \rho \mathbf{f} + \int_{V_t} \nabla \cdot \mathbf{T}. \quad (2.11)$$

By Reynolds Transport Theorem 2.1.1 we obtain, since ρ is constant and consequently $\nabla \cdot \mathbf{u} = 0$,

$$\frac{d}{dt} \int_{V_t} \rho \mathbf{u} = \int_{V_t} \left[\frac{D(\rho \mathbf{u})}{Dt} + \rho \mathbf{u} \nabla \cdot \mathbf{u} \right] = \int_{V_t} \rho \frac{D(\mathbf{u})}{Dt}. \quad (2.12)$$

Then, using (2.11) and (2.12), the principle of the linear momentum can be expressed by

$$\int_{V_t} \left(\rho \frac{D\mathbf{u}}{Dt} - \rho \mathbf{f} - \nabla \cdot \mathbf{T} \right) = 0. \quad (2.13)$$

By the arbitrariness of V_t , in Ω_t (2.13) is equivalent to the differential form of the principle of the linear momentum

$$\rho \frac{D\mathbf{u}}{Dt} - \nabla \cdot \mathbf{T} = \rho \mathbf{f} \Leftrightarrow \rho \frac{\partial \mathbf{u}}{\partial t} + \rho(\mathbf{u} \cdot \nabla) \mathbf{u} - \nabla \cdot \mathbf{T} = \rho \mathbf{f}. \quad (2.14)$$

The non linear term $\rho(\mathbf{u} \cdot \nabla) \mathbf{u}$ is called the *convective term*.

Componentwise

$$\rho \frac{\partial u_i}{\partial t} + \rho \sum_{j=1}^d u_j \frac{\partial u_i}{\partial x_j} - \sum_{j=1}^d \frac{\partial T_{ij}}{\partial x_j} = \rho f_i \quad i = 1, \dots, d.$$

2.3 The Constitutive Law

The constitutive law relates the Cauchy stress tensor with the kinematics of different quantities, in particular, the velocity field. This relations allow us to characterize the mechanic behavior of fluid. In this work we are concerned with fluids, obeying a Newtonian behavior.

2.3.1 Newtonian Fluids

As we know, the viscous fluid is characterized by the inability to remain at rest after being subjected to a tension.

The Newtonian fluids are a subclass of isotropic (direction independent) viscous fluids to which the stress tensor \mathbf{T} is the sum of the tension caused by the thermodynamic pressure in the fluid, the tension that causes deformation fluid and the tension due to volumetric expansion. These fluids are called Stokesians Fluids.

For the Newtonian fluids, we assumed that the tension causing both deformation of the fluid and tension due to volumetric expansion depends only on the strain tensor $\mathbf{D}(\mathbf{u})$. This way, for Stokesians fluids the stress tensor is given by

$$\mathbf{T} = -P\mathbf{I} + \mathbf{F}(\mathbf{D}(\mathbf{u}))$$

where P is a scalar function called (*thermodynamic*) *pressure* (the perpendicular force per unit area exerted by the continuous medium outside), \mathbf{I} is the identity matrix and \mathbf{F}^1 is an isotropic tensor.

Newtonian fluids are isotropic viscous fluids to which the stress tensor \mathbf{T} is given by

$$\mathbf{T} = -P\mathbf{I} + \eta\nabla \cdot \mathbf{u} + 2\mu\mathbf{D}(\mathbf{u})$$

where η , the volumic viscosity, multiplies the tension due to volumetric expansion and μ , the hydrodynamic viscosity multiplies the tension which contributes to the motion of the fluid. These viscosities verify the relations $3\eta + 2\mu \geq 0$ and $\mu \geq 0$.

¹Let $\mathcal{O} = \{\text{tensor } \tau : \tau\tau^t = \tau^t\tau = \mathbf{I}\}$. We call isotropic tensor for all tensor σ , which is invariant with respect to \mathcal{O} ($\tau\sigma\tau^t = \sigma, \forall \tau \in \mathcal{O}$)

Intuitively, the viscosity of a fluid is the resistance that it offers to shear stress during movement.

Here are some properties of Newtonian fluid behavior:

- The Newtonian fluid maintains constant viscosity when subjected to the action of the forces of shear stress or shear, i.e., it does not change the viscosity with the variation of shear (tangential component of the strain tensor). The viscosity is independent from kinematic quantities.
- The Newtonian fluid does not deform under the presence of constant tensions.
- The Newtonian fluid relaxes immediately with the tension.
- The Newtonian fluid does not vary the normal tension with the shear rate.
- The Newtonian fluids flow react immediately in the presence of threshold tensions or transfer tensions.

In a Newtonian incompressible fluid, the Cauchy stress tensor is a linear function of the strain tensor. The Cauchy stress tensor can be written in the form

$$\mathbf{T} = -P\mathbf{I} + 2\mu\mathbf{D}(\mathbf{u}) = -P\mathbf{I} + \mu [\nabla\mathbf{u} + (\nabla\mathbf{u})^t] \quad (2.15)$$

where the term $2\mu\mathbf{D}(\mathbf{u})$ is often referred as viscous stress component of the stress tensor. As example of compressible Newtonian fluids, we refer the following gases: oxygen, hydrogen, air, methane and ammonia. As example of incompressible Newtonian fluids we refer the following liquids: water, gasoline, olive oil, ethylic alcohol.

2.3.2 Navier-Stokes Equations

For the Newtonian incompressible fluid, considering that μ is constant, we have (see the appendix (A – 7))

$$\begin{aligned}
 \nabla \cdot \mathbf{T} &= \nabla \cdot [-P\mathbf{I} + \mu [\nabla \mathbf{u} + (\nabla \mathbf{u})^t]] \\
 &= \nabla \cdot (-P\mathbf{I}) + \nabla \cdot [\mu [\nabla \mathbf{u} + (\nabla \mathbf{u})^t]] \\
 &= -P\nabla \cdot \mathbf{I} - \nabla P \cdot \mathbf{I} + \mu \nabla \cdot [\nabla \mathbf{u} + (\nabla \mathbf{u})^t] \\
 &= -\nabla P \cdot \mathbf{I} + \mu \nabla \cdot [\nabla \mathbf{u} + (\nabla \mathbf{u})^t] \\
 &= -\nabla P + \mu \nabla \cdot [\nabla \mathbf{u} + (\nabla \mathbf{u})^t], \tag{2.16}
 \end{aligned}$$

the momentum equation (2.14) may be written as

$$\rho \frac{\partial \mathbf{u}}{\partial t} + \rho(\mathbf{u} \cdot \nabla) \mathbf{u} + \nabla P - \mu \nabla \cdot [\nabla \mathbf{u} + (\nabla \mathbf{u})^t] = \rho \mathbf{f} \Leftrightarrow \tag{2.17}$$

$$\rho \frac{\partial \mathbf{u}}{\partial t} + \rho(\mathbf{u} \cdot \nabla) \mathbf{u} + \nabla P - 2\mu \nabla \cdot \mathbf{D}(\mathbf{u}) = \rho \mathbf{f}.$$

Being ρ constant, we define the kinematic viscosity by $\nu = \frac{\mu}{\rho}$ (m^2/s) and the pressure (scalar) by $p = \frac{P}{\rho}$ (m^2/s^2) and we obtain

$$\frac{\partial \mathbf{u}}{\partial t} + (\mathbf{u} \cdot \nabla) \mathbf{u} + \nabla p - 2\nu \nabla \cdot \mathbf{D}(\mathbf{u}) = \mathbf{f}. \tag{2.18}$$

The system of equations formed by partial differential equations of the law of conservation of mass (2.6) and the momentum equations (2.18)

$$\begin{cases} \frac{\partial \mathbf{u}}{\partial t} + (\mathbf{u} \cdot \nabla) \mathbf{u} + \nabla p - 2\nu \nabla \cdot \mathbf{D}(\mathbf{u}) = \mathbf{f}. \\ \nabla \cdot \mathbf{u} = 0. \end{cases} \tag{2.19}$$

defines the *Navier-Stokes equations* for the incompressible fluids.

As we have (see appendix (A – 11))

$$\nabla \cdot \nabla \mathbf{u} = \Delta \mathbf{u} \tag{2.20}$$

$$\nabla \cdot (\nabla \mathbf{u})^t = \nabla (\nabla \cdot \mathbf{u}) = 0 \tag{2.21}$$

for the incompressible fluid.

Then, the momentum equation for the incompressible Newtonian fluid with constant viscosity is

$$\frac{\partial \mathbf{u}}{\partial t} + (\mathbf{u} \cdot \nabla) \mathbf{u} + \nabla p - \nu \Delta \mathbf{u} = \mathbf{f}. \quad (2.22)$$

Using (2.22) we can rewrite the *Navier-Stokes equations* for the incompressible fluids as following

$$\begin{cases} \frac{\partial \mathbf{u}}{\partial t} + (\mathbf{u} \cdot \nabla) \mathbf{u} + \nabla p - \nu \Delta \mathbf{u} = \mathbf{f} \\ \nabla \cdot \mathbf{u} = 0. \end{cases} \quad (2.23)$$

The Navier-Stokes equations are defined on fixed spatial domain Ω such that $\Omega \subset \Omega_t$, for all $t \in I$, which cover the region of study. The principal unknowns of this system are the velocity field \mathbf{u} and the scaled pressure p .

To solve the problem, we need to define a velocity of fluid for an initial instant time $t = t_0$, called the initial velocity $\mathbf{u}(t_0, \mathbf{x}) = \mathbf{u}_0(\mathbf{x})$, $\mathbf{x} \in \Omega$.

In some cases, when the fluid is highly viscous, the contribution of the non-linear convective term $(\mathbf{u} \cdot \nabla) \mathbf{u}$ is negligible compared to the viscous contribution and may be neglected. We have then the *Stokes equations*

$$\begin{cases} \frac{\partial \mathbf{u}}{\partial t} - \nu \Delta \mathbf{u} + \nabla p = \mathbf{f} & \text{in } \Omega \\ \nabla \cdot \mathbf{u} = 0 & \text{in } \Omega \end{cases}$$

In this case, the motion of the fluid is slow and we consider it highly viscous.

A flow which does not change with time, at any position, is called a steady flow. For example, when water runs out while the handle is stationary, leaving the opening constant, the flow is steady. In this case, we have $\frac{\partial \mathbf{u}}{\partial t} = 0$ and this term disappears in the equations.

2.3.3 Dimensionless Navier-Stokes equations

This thesis is concerned about flows of incompressible viscous fluids of Newtonian type. For these fluids, the Cauchy stress tensor is given by $\mathbf{T} = -p\mathbf{I} + 2\mu\mathbf{D}(\mathbf{u})$, where p represents the pressure. The equations of conservation of momentum and mass hold in the domain Ω ,

$$\frac{\partial \mathbf{u}}{\partial t} + \mathbf{u} \cdot \nabla \mathbf{u} + \nabla p - \nu \Delta \mathbf{u} = \mathbf{f}, \quad \nabla \cdot \mathbf{u} = 0. \quad (2.24)$$

We consider the dimensionless form of this system by introducing the following quantities

$$\mathbf{x} = \frac{\tilde{\mathbf{x}}}{L}, \quad t = \frac{U\tilde{t}}{L}, \quad \mathbf{u} = \frac{\tilde{\mathbf{u}}}{U}, \quad p = \frac{\tilde{p}L}{\nu U}, \quad \mathbf{f} = \frac{\rho \tilde{\mathbf{f}} L^2}{\nu U},$$

where the symbol $\tilde{\cdot}$ is attached to dimensional parameters (L represents a reference length, U a characteristic velocity of the flow, $\frac{L}{\nu U}$ a characteristic hydrostatic pressure and $\frac{\rho L^2}{\nu U}$ a characteristic density of the forces).

We introduce the *Reynolds number*, which is a dimensionless number. It is defined as

$$\mathcal{R}e = \frac{\rho U L}{\nu}.$$

The Reynolds number expresses the viscosity of the fluid. A low value for the Reynolds number identifies a very viscous fluid.

The dimensionless system, defined in $[0, T] \times \Omega$, takes the form

$$\begin{cases} \mathcal{R}e \frac{\partial \mathbf{u}}{\partial t} - \Delta \mathbf{u} + \mathcal{R}e \mathbf{u} \cdot \nabla \mathbf{u} + \nabla p = \mathbf{f}, \\ \nabla \cdot \mathbf{u} = 0, \end{cases} \quad (2.25)$$

with the initial condition $\mathbf{u}(0, \mathbf{x}) = \mathbf{u}_0(\mathbf{x})$, $\mathbf{x} \in \Omega$ and the boundary conditions prescribed.

2.4 Boundary conditions

A *well-posed problem* in sense of Hadamard means that

- A solution exists
- The solution is unique
- The solution must be stable in the sense that it depends continuously on the data. In other words, a small change in the given data must produce a small change in the solution.

To close the mathematical formulation and obtain a well-posed problem it is necessary to introduce the boundary conditions in the fluid domain appropriately. Normally, the boundary conditions are driven by physical considerations:

- Dirichlet boundary conditions - mathematically, translated by imposing on the boundary (or measurable subset), a known velocity field $\mathbf{g} : I \times \Gamma_D \rightarrow \mathbb{R}^3$ where $\Gamma_D \subseteq \partial\Omega$, such that $\mathbf{u} = \mathbf{g}$ on Γ_D . Γ_D is called kinematic boundary.

These boundary conditions should be applied when the fluid is confined to a fixed region of space Ω bounded by $\partial\Omega$, where the fluid cannot cross the rigid boundaries. This means that the normal component of the velocity vector field must vanish on the boundary (*no-penetration condition*) and also that the tangential components of the fluid's velocity are controlled (*no-slip boundary conditions*). For a viscous fluid in contact with a solid boundary, the complete no-slip, no-penetration boundary condition may be summarized by saying that the velocity field of the fluid on the boundary is always equal to the velocity of the boundary at the same point, i.e.,

$$\mathbf{u} = \mathbf{g} \text{ on } \Gamma_D \quad (\text{adherence conditions}).$$

In particular, if the boundary is at rest, then

$$\mathbf{u} = 0 \text{ on } \Gamma_D.$$

and we have homogeneous Dirichlet boundary conditions.

For the incompressible fluids, when $\Gamma_D = \partial\Omega$ we have the compatibility condition

$$\int_{\Gamma_D} \mathbf{g} \cdot \mathbf{n} = 0$$

thanks to the divergence theorem

$$0 = \int_{\Omega} \nabla \cdot \mathbf{u} = \int_{\partial\Omega} \mathbf{u} \cdot \mathbf{n} = \int_{\partial\Omega} \mathbf{g} \cdot \mathbf{n}.$$

The Dirichlet boundary conditions can also be applied in the boundary areas where there is inlet fluid (*inflow conditions*). In the case of Newtonian fluid, just set the velocity or surface forces component on the boundary.

- Neumann boundary conditions - mathematically, translated by imposing the boundary (or measurable subset) the value of normal derivative of velocity field, i.e.,

$$\frac{\partial \mathbf{u}}{\partial \mathbf{n}} = \nabla \mathbf{u} \cdot \mathbf{n} = \mathbf{h} \quad \text{on } \Gamma_N.$$

If $\mathbf{h} = 0$ then we have homogeneous Neumann boundary conditions. Γ_N is called the static boundary.

This boundary conditions gives us the flux across the boundary Γ_N . In particular, when we have homogeneous Neumann boundary conditions (*do-nothing boundary conditions*) it means that there is no-flux on the boundary Γ_N . Do-nothing boundary conditions are probably the best possible general propose boundary condition for using along outflow boundaries and seems to be supported from the mathematical point of view by their simplicity and elegance with the variational framework.

Often these conditions can be combined with the flux and/or pressure drop conditions and apply equally along both inflow and outflow boundaries (boundaries where there are inlet or outlet fluid).

A non-friction condition is given by

$$\mathbf{T} \cdot \mathbf{n} = -p \cdot \mathbf{n} + 2\nu \mathbf{D}(\mathbf{u}) \cdot \mathbf{n} = \mathbf{h} \text{ on } \partial\Omega \quad (2.26)$$

Typically, we have $\mathbf{h} = -p_e \mathbf{n}$, where p_e is the external pressure. This boundary condition can be seen as an inflow or outflow condition on fictitious boundary (for instance, the inlet or the exit, respectively, of a tube). Mathematically, this condition is a Neumann condition for Cauchy tensor.

When $\mathbf{h} = 0$ indicates that there is no normal reaction over the boundary, i.e., the liquid is not forced on Γ_N , it is free (enter or leave the domain).

Remark:

In order to obtain a well-posed initial boundary value problem for the Navier-Stokes equations we do not prescribe the boundary value of the pressure or its initial value because the pressure is in fact fully and uniquely determined by the evolution of the velocity field \mathbf{u} .

Chapter 3

Mathematical Analysis for incompressible Navier-Stokes Equations

In this chapter, we will present the mathematical analysis of the Navier-Stokes equations for constant density (incompressible) fluids. We refer [13, 33] for details. The derivation of this equations was given in the previous chapter. We will do an a-priori estimate for the Navier-Stokes equations. We present some results of existence and unicity to the solution for problems of type (2.23) with appropriate boundary conditions. For this purpose, we introduce some notations and basic concepts of functional analysis, useful to the study that follows.

3.1 Notations and elementary results of functional analysis

More details on the results presented in this section can be found in [5, 4, 36, 1]. Throughout all of our developments, Ω will denote an open bounded domain in Euclidean space \mathbb{R}^d , $d = 2, 3$ with boundary $\partial\Omega$. Generally we will always assume that Ω is simply connected. We will assume also that its boundary $\partial\Omega$ is regular enough, *i.e.*, locally Ω is below of graph of some function ϕ and $\partial\Omega$ is represented by the graph

of ϕ and the regularity of $\partial\Omega$ is determined by ϕ .

Let \mathcal{C} be an arbitrary set of \mathbb{R}^d . We denote by $\bar{\mathcal{C}}$ its closure and by $^\circ\mathcal{C}$ its interior.

We use bold letters to indicate vectors and the same letter in normal typeface to indicate their components. Points in Ω or \mathbb{R}^d will be denoted by $\mathbf{x} = (x_1, \dots, x_d)$, an element of volume by $d\mathbf{x}(=dx_1 \dots dx_d)$ and an element of surface area by ds .

For a real function u in Ω , we denote by $\text{supp}(u)$ the support of u , that is,

$$\text{supp}(u) = \overline{\{\mathbf{x} \in \Omega : u(\mathbf{x}) \neq 0\}}.$$

3.1.1 Continuous functions spaces

Let $\Omega \subset \mathbb{R}^d$, $d = 2, 3$ is an open subset.

We denote by $C^0(\Omega)$ or $C(\Omega)$ the vector space of all continuous functions on Ω .

Let u be a sufficiently smooth function. We define the derivative of order α by

$$D^\alpha u = \frac{\partial^{|\alpha|} u}{\partial x_1^{\alpha_1} \dots \partial x_d^{\alpha_d}}$$

for all multi-index $\alpha = (\alpha_1, \dots, \alpha_d) \in \mathbb{N}_0^d$ with $|\alpha| = \sum_{i=1}^d \alpha_i$.

We denote by $\mathbf{C}^m(\Omega)$ the vector space of all functions u which, with all their partial derivatives D^α of orders $0 \leq |\alpha| \leq m$, are continuous on Ω .

We denote by $\mathbf{C}^m(\bar{\Omega})$ the vector space of all functions u which, with all their partial derivatives D^α of order $\alpha \in \mathbb{N}_0^d$, $|\alpha| = \sum_{i=1}^d \alpha_i$, are bounded and uniformly continuous on $\bar{\Omega}$. $\mathbf{C}^m(\bar{\Omega})$, $m > 0$ is a Banach space with the norm given by

$$\|u\|_{\mathbf{C}^m(\bar{\Omega})} = \max_{0 \leq |\alpha| \leq m} \sup_{\mathbf{x} \in \bar{\Omega}} |(D^\alpha u)(\mathbf{x})|.$$

We denote by $C^\infty(\Omega)$ the linear space of infinitely differentiable functions. In fact,

$$C^\infty(\Omega) = \bigcap_{m=0}^{\infty} C^m(\Omega).$$

We denote by $C_0^m(\Omega)$ the subspace of function in $C^m(\Omega)$ with compact support.

3.1.2 Lebesgue space

Let $\Omega \subset \mathbb{R}^d$, $d = 2, 3$ is an open, bounded subset with smooth boundary $\partial\Omega$ and $\mathbf{x} = (x_1, \dots, x_d)$ is the point of Ω .

We denote by $L^p(\Omega)$, $1 \leq p < \infty$, Lebesgue space of real functions defined on Ω with the p -integrable functions for the Lebesgue measure $d\mathbf{x} = dx_1, \dots, dx_d$ i.e.,

$$L^p(\Omega) = \left\{ u : \Omega \rightarrow \mathbb{R} \mid \int_{\Omega} |u(\mathbf{x})|^p d\mathbf{x} < \infty \right\}, \quad 1 \leq p < \infty,$$

The space $L^p(\Omega)$ is a Banach space for the norm

$$\|u\|_{L^p(\Omega)} = \left(\int_{\Omega} |u(\mathbf{x})|^p d\mathbf{x} \right)^{1/p}.$$

This norm verifies the Hölder inequality:

$$\int_{\Omega} |uv| d\mathbf{x} \leq \|u\|_{L^p(\Omega)} \|v\|_{L^q(\Omega)} \quad (3.1)$$

for all functions $u \in L^p(\Omega)$, $v \in L^q(\Omega)$ such that $1/p + 1/q = 1$. When $p = q = 2$, Hölder inequality reduces to Schwarz inequality (see appendix (A – 1)).

For $p = \infty$, $L^\infty(\Omega)$ is a Banach space of essentially bounded real functions with norm

$$\|u\|_{L^\infty} = \sup_{\mathbf{x} \in \Omega} |u(\mathbf{x})| = \inf \{ \lambda \in \mathbb{R} : |u(\mathbf{x})| \leq \lambda, \text{ a.e. } \mathbf{x} \in \Omega \}$$

We denote by $\mathbf{L}^p(\Omega)$ ($1 \leq p < \infty$) the space of vector field functions $\mathbf{u} : \Omega \rightarrow \mathbb{R}^d$ whose components belongs to $L^p(\Omega)$, equipped with the norm

$$\|\mathbf{u}\|_{\mathbf{L}^p(\Omega)} = \left(\sum_{i=1}^d \|u_i\|_{L^p(\Omega)} \right)^{1/p}, \quad 1 \leq p < \infty$$

and

$$\|\mathbf{u}\|_{\mathbf{L}^\infty(\Omega)} = \inf \{ C \in \mathbb{R} : |u_i(\mathbf{x})| \leq C, \quad i = 1, \dots, d, \text{ a.e. } \mathbf{x} \in \Omega \}$$

We denote by $[L^p(\Omega)]^{d \times d}$ ($1 \leq p < \infty$) the space of tensors fields $\mathbf{T} : \Omega \rightarrow \mathbb{R}^{d \times d}$ whose components T_{ij} belongs to $L^p(\Omega)$, equipped with the norm

$$\|\mathbf{T}\|_{\mathbf{L}^p(\Omega)} = \left(\sum_{i=1}^d \sum_{j=1}^d \|T_{ij}\|_{L^p(\Omega)} \right)^{1/p}.$$

If $\mathbf{T}, \mathbf{G} \in [L^2(\Omega)]^{d \times d}$ then we define the scalar product by

$$(\mathbf{T}, \mathbf{G})_{\mathbf{L}^2(\Omega)} = \int_{\Omega} \mathbf{T} : \mathbf{G} d\mathbf{x} = \int_{\Omega} \sum_{i=1}^d \sum_{j=1}^d T_{ij} G_{ij} d\mathbf{x}.$$

Another important space is the space of functions in $L^p(\Omega)$ with null measure, i.e.,

$$L_0^p(\Omega) = \left\{ u \in L^p(\Omega) : \int_{\Omega} u d\mathbf{x} = 0 \right\}.$$

This space is equivalent to the space $L^p(\Omega)/\mathbb{R}$ of functions in $L^p(\Omega)$ defined within a constant.

We denote by $L_{loc}^p(\Omega)$ the linear space of measurable functions locally p -integrable in Ω .

We shall need the Young inequality in dealing with integral estimates

$$ab \leq \frac{a^p}{p} + \frac{b^q}{q}, \quad \forall a, b, p, q \in \mathbb{R}^+ \text{ such that } \frac{1}{p} + \frac{1}{q} = 1 \quad (3.2)$$

Replacing a by $\varepsilon^{1/p}a$ and b by $\varepsilon^{-1/p}a$ for positive ε we obtain an useful interpolation inequality

$$ab \leq \frac{\varepsilon a^p}{p} + \frac{\varepsilon^{-q/p} b^q}{q} \leq \varepsilon a^p + \varepsilon^{-q/p} b^q \quad (3.3)$$

3.1.3 Distributions space

Denote the space $C_0^\infty(\Omega)$ by $\mathcal{D}(\Omega)$. It is called the test functions space. In $\mathcal{D}(\Omega)$ we define the following topology: a sequence $\{v_n\} \subset \mathcal{D}(\Omega)$ converge to $v \in \mathcal{D}(\Omega)$ if there is a closed bounded subset $K \subset \mathcal{D}(\Omega)$ such that $\{v_n\}$ vanish out of K for each n and the sequence $D^\alpha v_n$ converge uniformly to $D^\alpha v$ in Ω for all α .

Let $\mathcal{D}'(\Omega)$ be the space of continuous linear forms in $\mathcal{D}(\Omega)$ for the topology defined in $\mathcal{D}(\Omega)$, i.e, the dual space of $\mathcal{D}(\Omega)$. For each $v \in \mathcal{D}(\Omega)$ and $T \in \mathcal{D}'(\Omega)$, we define $\langle T, v \rangle$ the value of T in v .

For each function $u \in L^1_{loc}(\Omega)$ we associate a *distribution* $T_u \in \mathcal{D}'(\Omega)$ defined by

$$\langle T_u, v \rangle = \int_{\Omega} u(\mathbf{x})v(\mathbf{x})d\mathbf{x}, \quad v \in \mathcal{D}(\Omega).$$

The function u can be identified with the distribution T_u . So, if $u \in L^2(\Omega)$ we have, for all $v \in \mathcal{D}(\Omega)$

$$\langle u, v \rangle = \int_{\Omega} u(\mathbf{x})v(\mathbf{x})d\mathbf{x}.$$

The space $\mathcal{D}'(\Omega)$ is called the space of distribution.

We define the derivative of order α of distribution T , $D^\alpha T$ as being the distribution defined by

$$\langle D^\alpha T, v \rangle = (-1)^{|\alpha|} \langle T, D^\alpha v \rangle, \quad \forall v \in \mathcal{D}(\Omega).$$

If there is a function $v_\alpha \in L^p(\Omega)$ such that

$$\langle D^\alpha T, v \rangle = \int_{\Omega} v_\alpha(\mathbf{x})v(\mathbf{x})d\mathbf{x}$$

for all $v \in \mathcal{D}(\Omega)$ then we say that $D^\alpha T$ is a function in $L^p(\Omega)$.

3.1.4 Sobolev spaces

The Sobolev space $H^m(\Omega)$, with m being a non-negative integer is the space of functions $v \in L^2(\Omega)$ such that all the distributional derivatives of v of order up to m are a function of $L^2(\Omega)$, i.e.,

$$H^m(\Omega) = \{v \in L^2(\Omega) : D^\alpha v \in L^2(\Omega), \forall \alpha \text{ such that } |\alpha| \leq m\}$$

We observe that $H^0(\Omega) = L^2(\Omega)$.

$H^m(\Omega)$ is a Banach space with respect to the norm

$$\|v\|_{H^m(\Omega)} = \left(\sum_{|\alpha| \leq m} \|D^\alpha v\|_{L^2(\Omega)}^2 \right)^{1/2}$$

In particular,

$$\|v\|_{H^1(\Omega)} = \left(\|v\|_{L^2(\Omega)}^2 + \|\nabla v\|_{L^2(\Omega)}^2 \right)^{1/2} \quad (3.4)$$

Further, its seminorm is defined as follows:

$$|v|_{H^m(\Omega)} = \left(\sum_{|\alpha|=m} \|D^\alpha v\|_{L^2(\Omega)}^2 \right)^{1/2}$$

In particular,

$$|v|_{H^1(\Omega)} = \|\nabla v\|_{L^2(\Omega)} \quad (3.5)$$

Notice that $H^m(\Omega)$ is indeed an Hilbert space with respect to the scalar product

$$(u, v)_{H^m(\Omega)} = \sum_{|\alpha| \leq m} \int_{\Omega} D^\alpha u D^\alpha v d\mathbf{x}$$

Finally, we denote by $H_0^m(\Omega)$ the closure of $C_0^\infty(\Omega)$ with respect to the norm $\|\cdot\|_{H^m(\Omega)}$ and with $H^{-m}(\Omega)$ the dual space of $H_0^m(\Omega)$.

If Ω has a Lipschitz continuous boundary, $H^m(\Omega)$ is indeed the closure of $C^\infty(\overline{\Omega})$ with respect to the norm $\|\cdot\|_{H^m(\Omega)}$. In other words, $C^\infty(\overline{\Omega})$ is dense in $H^m(\Omega)$.

We denote by $\mathbf{H}^m(\Omega)$, $m \in \mathbb{N}_0$ the space of vector functions $\mathbf{u} : \Omega \rightarrow \mathbb{R}^d$ whose components are in $H^m(\Omega)$ and whose norm is defined as

$$\|\mathbf{u}\|_{\mathbf{H}^m(\Omega)} = \left(\sum_{i=1}^d \|u_i\|_{H^m(\Omega)}^2 \right)^{1/2}.$$

Its semi-norm is $|\mathbf{u}|_{\mathbf{H}^m(\Omega)} = \left(\sum_{i=1}^d |u_i|_{H^m(\Omega)}^2 \right)^{1/2}$.

The space $\mathbf{H}^m(\Omega)$ is equipped with the scalar product

$$(\mathbf{u}, \mathbf{v})_{\mathbf{H}^m(\Omega)} = \sum_{i=1}^d (u_i, v_i)_{H^m(\Omega)}, \quad \mathbf{u}, \mathbf{v} \in \mathbf{H}^m(\Omega)$$

is an Hilbert space.

Considering the important theorems that follows, whose proof can be found in [5, 4].

Theorem 3.1.1 (*Sobolev embeddings*)

Let Ω be a bounded domain in \mathbb{R}^d with Lipschitz continuous boundary $\partial\Omega$. The following continuous embeddings hold

- If $0 \leq s < \frac{d}{2}$, $\mathbf{H}^s(\Omega) \hookrightarrow \mathbf{L}^p(\Omega)$, $p = \frac{2d}{d-2s}$,
- If $s = \frac{d}{2}$, $\mathbf{H}^s(\Omega) \hookrightarrow \mathbf{L}^q(\Omega)$, $2 \leq q < \infty$,
- If $s > \frac{d}{2}$, $\mathbf{H}^s(\Omega) \hookrightarrow \mathbf{C}^0(\Omega)$, $2 \leq q < \infty$,

□

Theorem 3.1.2 (*Green integration formula*)

Let Ω be a bounded domain in \mathbb{R}^d , ($d = 2, 3$) with Lipschitz continuous boundary $\partial\Omega$ and \mathbf{n} be an unit outer normal along $\partial\Omega$. Let $u, v \in H^1(\Omega)$ then for each component n_i ($i = 1, \dots, d$) of \mathbf{n} there exist the integral and is finite

$$\int_{\partial\Omega} uvn_i.$$

Moreover, we have

$$\int_{\Omega} \frac{\partial u}{\partial x_i} v = - \int_{\Omega} u \frac{\partial v}{\partial x_i} + \int_{\partial\Omega} uvn_i \quad (3.6)$$

and if $u \in H^2(\Omega)$ then for all $v \in H^1(\Omega)$ we obtain

$$\sum_{i=1}^d \int_{\Omega} \frac{\partial u}{\partial x_i} \frac{\partial v}{\partial x_i} = - \sum_{i=1}^d \int_{\Omega} \frac{\partial^2 u}{\partial x_i^2} v + \sum_{i=1}^d \int_{\partial\Omega} n_i \frac{\partial u}{\partial x_i} v \quad (3.7)$$

□

Theorem 3.1.3 (*Poincaré inequality*)

Let Ω be a connected bounded (in at least one direction) subset of \mathbb{R}^d , ($d = 2, 3$). Then for all $k > 0$, there exists a constant $c = C(d, k, \Omega)$ such that

$$\|u\|_{H^k(\Omega)} \leq c \|\nabla u\|_{H^k(\Omega)}, \quad \forall u \in H_0^k(\Omega) \quad (3.8)$$

□

In particular, $\|\nabla u\|_{L^2(\Omega)} = \|u\|_{H^1(\Omega)}$ is a norm on $H_0^1(\Omega)$ which is equivalent to the norm $\|u\|_{H^1(\Omega)}$; over $H_0^1(\Omega)$ the integral $\int_{\Omega} \nabla u : \nabla v$ is a scalar product which induces the norm $\|\nabla u\|_{L^2(\Omega)}$ equivalent to the norm $\|u\|_{H^1(\Omega)}$.

Theorem 3.1.4 (*Korn inequality*)

Let Ω be a connected bounded (in at least one direction) subset of \mathbb{R}^d , ($d = 2, 3$). Suppose that velocity field $\mathbf{u} \in \mathbf{H}^1(\Omega)$ is null on $\Gamma \subset \partial\Omega$ ($\text{meas}(\Gamma) > 0$). Then, there exists a constant $C_k > 0$ such that the following equality is verified

$$\int_{\Omega} \mathbf{D}(\mathbf{u}) : \mathbf{D}(\mathbf{u}) = \int_{\Omega} |\mathbf{D}(\mathbf{u})|^2 \geq C_k \|\nabla \mathbf{u}\|_{\mathbf{L}^2(\Omega)}^2. \quad (3.9)$$

□

The proof can be found in [7].

3.1.5 Space-time functions

Consider the space-time functions $\mathbf{v}(t, \mathbf{x})$, $(t, \mathbf{x}) \in [t_0, T] \times \Omega$ and V be a Banach space. We define, for all $p \in [1, \infty[$ the Banach space

$$L^p(t_0, T; V) = \left\{ \mathbf{v} : [t_0, T] \rightarrow V : \mathbf{v} \text{ is measurable and } \left(\int_{t_0}^T \|\mathbf{v}(t)\|_V^p dt \right)^{\frac{1}{p}} < \infty \right\}$$

endowed with the norm

$$\|\mathbf{v}\|_{L^p(t_0, T; V)} = \left(\int_{t_0}^T \|\mathbf{v}(t)\|_V^p dt \right)^{\frac{1}{p}}$$

In a similar way, we can define $L^\infty(t_0, T; V)$:

$$L^\infty(t_0, T; V) = \left\{ \mathbf{v} : [t_0, T] \rightarrow V : \mathbf{v} \text{ is measurable and } \sup_{t_0 \leq t \leq T} \|\mathbf{v}(t)\|_V \right\}$$

endowed with the norm

$$\|\mathbf{v}\|_{L^\infty(t_0, T; V)} = \sup_{t_0 \leq t \leq T} \|\mathbf{v}(t)\|_V$$

We define the space $H^1(t_0, T; V)$ as follows:

$$H^1(t_0, T; V) = \left\{ \mathbf{v} \in L^2(t_0, T; V) : \frac{\partial \mathbf{v}}{\partial t} \in L^2(t_0, T; V) \right\}$$

where $\frac{\partial \mathbf{v}}{\partial t}$ is the derivative in the sense of distribution with value in V . For instance, when $V = L^2(\Omega)$, $H^1(t_0, T; L^2(\Omega))$ is the space of functions $L^2([t_0, T] \times \Omega)$ having the distributional time-derivative in $L^2(\Omega)$.

3.2 Weak formulation of Navier-Stokes problem

Without loss of generality, we consider an incompressible fluid confined into a domain Ω with fixed boundary. Mathematically, for each $t \in [t_0, T]$ (to simplify, we take from now $t_0 = 0$), we write the unsteady Navier-Stokes equations with the homogeneous Dirichlet boundary conditions defined over Ω , a bounded domain of \mathbb{R}^d ($d = 2, 3$), with a Lipschitz continuous boundary $\partial\Omega$. For reasons that will appear clear later on we prefer to use the Navier-Stokes equation in the form (2.19). So,

$$\left\{ \begin{array}{ll} \frac{\partial \mathbf{u}}{\partial t} + (\mathbf{u} \cdot \nabla) \mathbf{u} + \nabla p - 2\nu \nabla \cdot \mathbf{D}(\mathbf{u}) = \mathbf{f}, & \text{in } [0, T] \times \Omega \\ \nabla \cdot \mathbf{u} = 0, & \text{in } [0, T] \times \Omega \\ \mathbf{u} = 0, & \text{on } [0, T] \times \partial\Omega \\ \mathbf{u}(t = 0, \mathbf{x}) = \mathbf{u}_0(\mathbf{x}), & \forall \mathbf{x} \in \Omega \end{array} \right. \quad (3.10)$$

where \mathbf{f} is a given external force field per unity mass, \mathbf{u} is the velocity field, \mathbf{u}_0 is the known initial velocity field and like we defined in section 2.3.2 p is the rate between

the pressure and the density, ν is the constant kinematic viscosity.

The weak formulation, called variational formulation, of Navier-Stokes problem, consists on the integral equations over Ω obtained by integration, after multiply the momentum equation and continuity equation by appropriate test functions.

Let us suppose that $\mathbf{u} \in \mathbf{C}^2([0, T] \times \bar{\Omega})$ and $p \in C^1([0, T] \times \bar{\Omega})$ are the classical (or strong) solution of (3.10). Consider the space $\mathbf{V} = \mathbf{H}_0^1(\Omega)$ and take $\mathbf{v} \in \mathbf{V}$ an arbitrary test function. Taking the scalar product between the momentum equation and \mathbf{v} , we obtain

$$\int_{\Omega} \frac{\partial \mathbf{u}}{\partial t} \cdot \mathbf{v} + \int_{\Omega} (\mathbf{u} \cdot \nabla) \mathbf{u} \cdot \mathbf{v} + \int_{\Omega} \nabla p \cdot \mathbf{v} - 2\nu \int_{\Omega} \nabla \cdot \mathbf{D}(\mathbf{u}) \cdot \mathbf{v} = \int_{\Omega} \mathbf{f} \cdot \mathbf{v} \quad (3.11)$$

Applying the Green's formulas (theorem 3.1.2) to (3.11) we have

$$\begin{aligned} \int_{\Omega} \frac{\partial \mathbf{u}}{\partial t} \cdot \mathbf{v} + \int_{\Omega} (\mathbf{u} \cdot \nabla) \mathbf{u} \cdot \mathbf{v} - \int_{\Omega} p \nabla \cdot \mathbf{v} + \int_{\partial \Omega} \mathbf{v} \cdot p \mathbf{n} + 2\nu \int_{\Omega} \mathbf{D}(\mathbf{u}) : \nabla \mathbf{v} - \\ \int_{\partial \Omega} (2\nu \mathbf{D}(\mathbf{u}) \cdot \mathbf{n}) \cdot \mathbf{v} = \int_{\Omega} \mathbf{f} \cdot \mathbf{v} \Leftrightarrow \\ \int_{\Omega} \frac{\partial \mathbf{u}}{\partial t} \cdot \mathbf{v} + \int_{\Omega} (\mathbf{u} \cdot \nabla) \mathbf{u} \cdot \mathbf{v} - \int_{\Omega} p \nabla \cdot \mathbf{v} + 2\nu \int_{\Omega} \mathbf{D}(\mathbf{u}) : \nabla \mathbf{v} = \\ = \int_{\Omega} \mathbf{f} \cdot \mathbf{v} + \int_{\partial \Omega} \mathbf{v} \cdot (2\nu \mathbf{D}(\mathbf{u}) \cdot \mathbf{n} - p \mathbf{n}) \end{aligned} \quad (3.12)$$

Taking into account \mathbf{v} vanish on the boundary, the variational form to the momentum equation is

$$\int_{\Omega} \frac{\partial \mathbf{u}}{\partial t} \cdot \mathbf{v} + \int_{\Omega} (\mathbf{u} \cdot \nabla) \mathbf{u} \cdot \mathbf{v} - \int_{\Omega} p \nabla \cdot \mathbf{v} + 2\nu \int_{\Omega} \mathbf{D}(\mathbf{u}) : \nabla \mathbf{v} = \int_{\Omega} \mathbf{f} \cdot \mathbf{v} \quad (3.13)$$

Knowing that (see appendix (A - 12))

$$\int_{\Omega} \mathbf{D}(\mathbf{u}) : \nabla \mathbf{v} = \int_{\Omega} \mathbf{D}(\mathbf{u}) : \mathbf{D}(\mathbf{v}) \quad (3.14)$$

we rewrite the variational form of the momentum equation as

$$\int_{\Omega} \frac{\partial \mathbf{u}}{\partial t} \cdot \mathbf{v} + \int_{\Omega} (\mathbf{u} \cdot \nabla) \mathbf{u} \cdot \mathbf{v} - \int_{\Omega} p \nabla \cdot \mathbf{v} + 2\nu \int_{\Omega} \mathbf{D}(\mathbf{u}) : \mathbf{D}(\mathbf{v}) = \int_{\Omega} \mathbf{f} \cdot \mathbf{v} \quad (3.15)$$

As we take a Dirichlet problem, the pressure is determined only up to a constant¹, since it appears in the equations only through its gradient. So, we consider the space $Q = L^2_0(\Omega)$ and take $q \in Q$ and we multiply the continuity equation by q and integrate over Ω . Then, we obtain

$$\int_{\Omega} \nabla \cdot \mathbf{u} q = 0 \quad (3.16)$$

The variational form to Navier-Stokes problem reads:

$\forall t \in [0, T]$, given $\mathbf{f} \in L^2(0, T; \mathbf{H}^{-1}(\Omega))$ and $\mathbf{u}_0 \in \mathbf{H}_0^1(\Omega)$ with $\nabla \cdot \mathbf{u}_0 = 0$, find $(\mathbf{u}, p) \in L^2(0, T; \mathbf{V}) \times L^2(0, T; Q)$ such that

$$\left\{ \begin{array}{l} \int_{\Omega} \frac{\partial \mathbf{u}}{\partial t} \cdot \mathbf{v} + \int_{\Omega} (\mathbf{u} \cdot \nabla) \mathbf{u} \cdot \mathbf{v} - \int_{\Omega} p \nabla \cdot \mathbf{v} + 2\nu \int_{\Omega} \mathbf{D}(\mathbf{u}) : \mathbf{D}(\mathbf{v}) = \int_{\Omega} \mathbf{f} \cdot \mathbf{v}, \quad \forall \mathbf{v} \in \mathbf{V} \\ \int_{\Omega} q \nabla \cdot \mathbf{u} = 0, \quad \forall q \in Q \\ \mathbf{u}(0) = \mathbf{u}_0 \end{array} \right. \quad (3.17)$$

Lemma 3.2.1

Problem (3.10) and Problem (3.17) are equivalent. \square

Proof

Taking into account the following inclusions $L^2(0, T; \mathbf{V}) \subset C^2([0, T] \times \overline{\Omega})$ and $L^2(0, T; Q) \subset C^1([0, T] \times \overline{\Omega})$, it is immediate that a smooth solution (\mathbf{u}, p) of (3.10) is the solution of (3.17), i.e., (\mathbf{u}, p) is also a weak solution of the Navier-Stokes problem.

Conversely, considering $(\mathbf{u}, p) \in L^2(0, T; \mathbf{V}) \times L^2(0, T; Q)$, solution of (3.17). Let t be arbitrarily fixed, hence $\mathbf{u} \equiv \mathbf{u}(t) \in \mathbf{V}$ and $p \equiv p(t) \in Q$. Taking a test function

¹To compute an unique value for the pressure it is necessary to fix a constant with a zero-mean constraint.

$\mathbf{v} \in \mathcal{D}(\Omega)$, using (3.14), by applying Green's formula

$$\begin{aligned} \int_{\Omega} \frac{\partial \mathbf{u}}{\partial t} \cdot \mathbf{v} + \int_{\Omega} (\mathbf{u} \cdot \nabla) \mathbf{u} \cdot \mathbf{u} - \int_{\Omega} p \nabla \cdot \mathbf{v} + 2\nu \int_{\Omega} \mathbf{D}(\mathbf{u}) : \mathbf{D}(\mathbf{v}) &= \int_{\Omega} \mathbf{f} \cdot \mathbf{v} \Leftrightarrow \\ \int_{\Omega} \frac{\partial \mathbf{u}}{\partial t} \cdot \mathbf{v} + \int_{\Omega} (\mathbf{u} \cdot \nabla) \mathbf{u} \cdot \mathbf{v} - \int_{\Omega} \nabla p \cdot \mathbf{v} + 2\nu \int_{\Omega} \nabla \cdot \mathbf{D}(\mathbf{u}) \cdot \mathbf{v} &= \\ &= \int_{\Omega} \mathbf{f} \cdot \mathbf{v} - \int_{\partial\Omega} \mathbf{v} \cdot (2\nu \mathbf{D}(\mathbf{u}) \cdot \mathbf{n} - p \mathbf{n}). \end{aligned}$$

As $\text{supp}(\mathbf{v})$ is compact then results $\int_{\partial\Omega} \mathbf{v} \cdot (2\nu \mathbf{D}(\mathbf{u}) \cdot \mathbf{n} - p \mathbf{n}) = 0$, so

$$\int_{\Omega} \frac{\partial \mathbf{u}}{\partial t} \cdot \mathbf{v} + \int_{\Omega} (\mathbf{u} \cdot \nabla) \mathbf{u} \cdot \mathbf{v} - \int_{\Omega} p \nabla \cdot \mathbf{v} + 2\nu \int_{\Omega} \mathbf{D}(\mathbf{u}) : \nabla \mathbf{v} = \int_{\Omega} \mathbf{f} \cdot \mathbf{v}, \quad \forall \mathbf{v} \in \mathcal{D}(\Omega).$$

By density,

$$\int_{\Omega} \frac{\partial \mathbf{u}}{\partial t} \cdot \mathbf{v} + \int_{\Omega} (\mathbf{u} \cdot \nabla) \mathbf{u} \cdot \mathbf{v} - \int_{\Omega} p \nabla \cdot \mathbf{v} + 2\nu \int_{\Omega} \mathbf{D}(\mathbf{u}) : \nabla \mathbf{v} = \int_{\Omega} \mathbf{f} \cdot \mathbf{v} \Leftrightarrow$$

$$\int_{\Omega} \left(\frac{\partial \mathbf{u}}{\partial t} + (\mathbf{u} \cdot \nabla) \mathbf{u} - \nabla p + 2\nu \mathbf{D}(\mathbf{u}) - \mathbf{f} \right) \cdot \mathbf{v} = 0, \quad \forall \mathbf{v} \in \mathbf{L}^2(\Omega) \Leftrightarrow$$

$$\frac{\partial \mathbf{u}}{\partial t} + (\mathbf{u} \cdot \nabla) \mathbf{u} - \nabla p + 2\nu \mathbf{D}(\mathbf{u}) - \mathbf{f} = 0 \text{ a.e. in } \Omega$$

i.e.

$$\frac{\partial \mathbf{u}}{\partial t}(t) + (\mathbf{u}(t) \cdot \nabla) \mathbf{u}(t) - \nabla p(t) + 2\nu \mathbf{D}(\mathbf{u}(t)) - \mathbf{f}(t) = 0 \text{ a.e. in } \Omega$$

Given the arbitrariness of t we conclude

$$\frac{\partial \mathbf{u}}{\partial t} + (\mathbf{u} \cdot \nabla) \mathbf{u} - \nabla p + 2\nu \mathbf{D}(\mathbf{u}) - \mathbf{f} = 0 \text{ a.e. in } [0, T] \times \Omega$$

As $\mathbf{u} \in L^2(0, T; \mathbf{V})$ then $\mathbf{u} = 0$ on $[0, T] \times \partial\Omega$.

We conclude this way that the solution of 3.17 is also a (weak) solution of Problem (3.10). ■

3.2.1 Abstract formulation

Define as follows forms:

$$a(\mathbf{u}, \mathbf{v}) = 2\nu (\mathbf{D}(\mathbf{u}), \mathbf{D}(\mathbf{v})) = 2\nu \int_{\Omega} \mathbf{D}(\mathbf{u}) : \mathbf{D}(\mathbf{v}) \quad (3.18)$$

$$b(\mathbf{v}, p) = -(p, \nabla \cdot \mathbf{v}) = - \int_{\Omega} p \nabla \cdot \mathbf{v} \quad (3.19)$$

$$c(\mathbf{w}, \mathbf{u}, \mathbf{v}) = ((\mathbf{w} \cdot \nabla) \mathbf{u}, \mathbf{v}) = \int_{\Omega} (\mathbf{w} \cdot \nabla) \mathbf{u} \cdot \mathbf{v} \quad (3.20)$$

Lemma 3.2.2

The forms $a : \mathbf{V} \times \mathbf{V} \longrightarrow \mathbb{R}$ and $b : \mathbf{V} \times Q \longrightarrow \mathbb{R}$, defined by (3.18) and (3.19) respectively, are continuous with respect to their arguments. Moreover, $a(\cdot, \cdot)$ is coercive (\mathbf{V} -elliptic), i.e.,

$$\exists \alpha > 0 : a(\mathbf{v}, \mathbf{v}) \geq \alpha \|\mathbf{v}\|_{\mathbf{H}^1(\Omega)}^2, \quad \forall \mathbf{v} \in \mathbf{V}.$$

□

Proof

Let $\mathbf{u}, \mathbf{v} \in \mathbf{V}$ be arbitrary vector field functions. Using the equality (see appendix (A – 13))

$$\int_{\Omega} \mathbf{D}(\mathbf{u}) : \mathbf{D}(\mathbf{v}) = \int_{\Omega} \nabla \mathbf{u} : \nabla \mathbf{v}. \quad (3.21)$$

the continuity of bilinear form $a(\cdot, \cdot)$ is an immediate consequence of Hölder inequality with $p = q = 2$ (Cauchy-Schwarz inequality). So,

$$|a(\mathbf{u}, \mathbf{v})| = \left| 2\nu \int_{\Omega} \mathbf{D}(\mathbf{u}) : \mathbf{D}(\mathbf{v}) \right| = \left| 2\nu \int_{\Omega} \nabla \mathbf{u} : \nabla \mathbf{v} \right| \underbrace{\leq}_{\text{Holder}} 2\nu \|\nabla \mathbf{u}\|_{\mathbf{L}^2(\Omega)} \|\nabla \mathbf{v}\|_{\mathbf{L}^2(\Omega)} \underbrace{\leq}_{\text{def. norm } \mathbf{H}^1} \nu \|\mathbf{u}\|_{\mathbf{H}^1(\Omega)} \|\mathbf{v}\|_{\mathbf{H}^1(\Omega)} \quad (3.22)$$

Considering $q \in L_0^2(\Omega)$ an arbitrary function, we have by Hölder inequality with $p = q = 2$

$$|b(\mathbf{u}, q)| = \left| \int_{\Omega} \nabla \cdot \mathbf{u} q \right| \underbrace{\leq}_{\text{Holder}} \|\nabla \cdot \mathbf{u}\|_{\mathbf{L}^2(\Omega)} \|q\|_{\mathbf{L}^2(\Omega)} \underbrace{\leq}_{\text{def. norm } \mathbf{H}^1} \|\mathbf{u}\|_{\mathbf{H}^1(\Omega)} \|q\|_{\mathbf{L}^2(\Omega)}. \quad (3.23)$$

To prove the coercivity of bilinear form $a(\cdot, \cdot)$ we take an arbitrary vector field functions \mathbf{v} in \mathbf{V} and \mathbf{u} in \mathbf{V} such that $\nabla \cdot \mathbf{u} = 0$. By the inequalities of Korn (3.9) and Poincaré (3.8) we obtain

$$a(\mathbf{u}, \mathbf{u}) = 2\nu \int_{\Omega} |\mathbf{D}(\mathbf{u})|^2 \geq 2\nu C_k |\mathbf{u}|_{\mathbf{H}^1(\Omega)} \geq \frac{2\nu C_k}{c_p^2 + 1} \|\mathbf{u}\|_{\mathbf{H}^1(\Omega)}$$

being C_k and c_p the constants in Korn and Poincaré inequality respectively. \blacksquare

Lemma 3.2.3

The form $c : \mathbf{V} \times \mathbf{V} \times \mathbf{V} \rightarrow \mathbb{R}$, defined by (3.20), is continuous with respect to its arguments. \square

Proof

Let $\mathbf{u}, \mathbf{v}, \mathbf{w} \in \mathbf{V}$ be arbitrary functions. So, $\nabla \mathbf{u} \in \mathbf{L}^2(\Omega)$. From theorem 3.1.1, we have $\mathbf{H}^1(\Omega) \hookrightarrow \mathbf{L}^6(\Omega)$ for $d = 2, 3$ and consequently $\mathbf{H}^1(\Omega) \hookrightarrow \mathbf{L}^4(\Omega)$. Then, $\mathbf{w}, \mathbf{v} \in \mathbf{L}^4(\Omega)$ hence $\mathbf{wv} \in \mathbf{L}^2(\Omega)$.

Considering the $c(\mathbf{w}, \mathbf{u}, \mathbf{v}) = \int_{\Omega} (\mathbf{w} \cdot \nabla) \mathbf{u} \cdot \mathbf{v}$ componentwise, we have, by Cauchy-Schwarz inequality

$$\begin{aligned} \int_{\Omega} w_i \frac{\partial u_k}{\partial x_i} v_k &\leq \left[\int_{\Omega} (w_i v_k)^2 \right]^{\frac{1}{2}} \left[\int_{\Omega} \left(\frac{\partial u_k}{\partial x_i} \right)^2 \right]^{\frac{1}{2}} \\ &\leq \left(\int_{\Omega} w_i^4 \right)^{\frac{1}{4}} \left(\int_{\Omega} v_k^4 \right)^{\frac{1}{4}} \left[\int_{\Omega} \left(\frac{\partial u_k}{\partial x_i} \right)^2 \right]^{\frac{1}{2}} \\ &\leq \|w_i\|_{L^4(\Omega)} \|v_k\|_{L^4(\Omega)} \|u_k\|_{H_0^1(\Omega)} \end{aligned}$$

Thanks to the continuous embedding $H^1(\Omega) \hookrightarrow L^4(\Omega)$, there is a positive constant C such that

$$\int_{\Omega} w_i \frac{\partial u_k}{\partial x_i} v_k \leq C^2 \|w_i\|_{H^1(\Omega)} \|v_k\|_{H^1(\Omega)} \|u_k\|_{H_0^1(\Omega)} \leq C^2 \|w_i\|_{H^1(\Omega)} \|v_k\|_{H^1(\Omega)} \|u_k\|_{H^1(\Omega)}$$

It follows that, there is a positive constant K such that

$$|c(\mathbf{w}, \mathbf{u}, \mathbf{v})| \leq K \|\mathbf{w}\|_{\mathbf{H}^1(\Omega)} \|\mathbf{u}\|_{\mathbf{H}^1(\Omega)} \|\mathbf{v}\|_{\mathbf{H}^1(\Omega)} \quad \forall \mathbf{u}, \mathbf{v}, \mathbf{w} \in \mathbf{H}^1(\Omega). \quad (3.24)$$

■

Lemma 3.2.4

Let $\mathbf{v}, \mathbf{w} \in \mathbf{H}^1(\Omega)$ with $\nabla \cdot \mathbf{w} = 0$ in Ω and $\mathbf{w} \cdot \mathbf{n} = 0$ on $\partial\Omega$, $\forall t \in [0, T]$. Then, we have

$$c(\mathbf{w}, \mathbf{v}, \mathbf{v}) = 0. \quad (3.25)$$

and

$$c(\mathbf{w}, \mathbf{u}, \mathbf{v}) = -c(\mathbf{w}, \mathbf{v}, \mathbf{u}). \quad (3.26)$$

□

Proof

Let $\mathbf{v} \in \mathcal{D}(\overline{\Omega})$ and $\mathbf{w} \in \mathbf{H}^1(\Omega)$. By Green's theorem,

$$\begin{aligned} c(\mathbf{w}, \mathbf{v}, \mathbf{v}) &= \sum_{i,j=1}^d \int_{\Omega} w_j \frac{\partial v_i}{\partial x_j} v_i = \sum_{i,j=1}^d \int_{\Omega} w_j \frac{1}{2} \frac{\partial v_i^2}{\partial x_j} \\ &= -\frac{1}{2} \sum_{i,j=1}^d \left(\int_{\Omega} \frac{\partial w_j}{\partial x_j} v_i + \int_{\partial\Omega} w_j n_j v_i \right) \end{aligned}$$

By hypothesis $\nabla \cdot \mathbf{w} = 0$ and $\mathbf{w} \cdot \mathbf{n} = 0$ on $\partial\Omega$ then we have

$$c(\mathbf{w}, \mathbf{v}, \mathbf{v}) = 0.$$

Consider (3.25) and replace \mathbf{v} by $\mathbf{u} + \mathbf{v}$. By definition of $c(\cdot, \cdot, \cdot)$ results

$$0 = c(\mathbf{w}, \mathbf{u} + \mathbf{v}, \mathbf{u} + \mathbf{v}) \Leftrightarrow c(\mathbf{w}, \mathbf{u}, \mathbf{v}) + c(\mathbf{w}, \mathbf{v}, \mathbf{u}) \Leftrightarrow c(\mathbf{w}, \mathbf{u}, \mathbf{v}) = -c(\mathbf{w}, \mathbf{v}, \mathbf{u})$$

■

Taking into account the definition of forms $a(\cdot, \cdot)$, $b(\cdot, \cdot)$ and $c(\cdot, \cdot, \cdot)$, we can reformulate the variational formulation of Navier-stokes problem as follows:

$\forall t \in [0, T]$, given $\mathbf{f} \in L^2(0, T; \mathbf{H}^{-1}(\Omega))$ and $\mathbf{u}_0 \in \mathbf{H}_0^1(\Omega)$ with $\nabla \cdot \mathbf{u}_0 = 0$, find $(\mathbf{u}, p) \in L^2(0, T; \mathbf{V}) \times L^2(0, T; Q)$ such that

$$\begin{cases} \left(\frac{\partial \mathbf{u}}{\partial t}, \mathbf{v} \right) + a(\mathbf{u}, \mathbf{v}) + c(\mathbf{u}, \mathbf{u}, \mathbf{v}) + b(\mathbf{v}, p) = (\mathbf{f}, \mathbf{v}), & \forall \mathbf{v} \in \mathbf{V} \\ b(\mathbf{u}, q) = 0 & \forall q \in Q \\ \mathbf{u}(0) = \mathbf{u}_0 \end{cases} \quad (3.27)$$

We define $\mathbf{V}_{div} = \{\mathbf{v} \in \mathbf{H}_0^1(\Omega) : \nabla \cdot \mathbf{v} = 0\}$. Taking $\mathbf{v} \in \mathbf{V}_{div}$ results the bilinear form $b(\mathbf{v}, p) = 0$. This suggests the following weak formulation of the problem (3.27):

Given $\mathbf{f} \in L^2(0, T; \mathbf{H}^{-1}(\Omega))$ and $\mathbf{u}_0 \in \mathbf{V}_{div}$, find $(\mathbf{u}, p) \in L^2(0, T; \mathbf{V}_{div}) \times L^2(0, T; Q)$ such that

$$\begin{cases} \left(\frac{\partial \mathbf{u}}{\partial t}, \mathbf{v} \right) + a(\mathbf{u}, \mathbf{v}) + c(\mathbf{u}; \mathbf{u}, \mathbf{v}) = (\mathbf{f}, \mathbf{v}) & \forall \mathbf{v} \in \mathbf{V}_{div} \\ \mathbf{u}(0) = \mathbf{u}_0 \end{cases} \quad (3.28)$$

The following lemma guarantees that Problem (3.27) is equivalent to Problem (3.28).

Lemma 3.2.5

Any solution of Problem (3.27) is a solution of Problem (3.28); the inverse is also verified. \square

Proof

It is trivial that any solution of Problem (3.27) is an also solution of Problem (3.28), since if \mathbf{u} satisfies (3.27) then $\mathbf{u} \in \mathbf{V}_{div} \subset \mathbf{V}$ satisfies (3.28).

To demonstrate the inverse we need the following lemma whose proof can be found in [13].

Lemma 3.2.6

Let Ω be a domain of \mathbb{R} ($d=2,3$) and let $l \in \mathbf{V}'^2$. Then $l(\mathbf{v}) = 0, \forall \mathbf{v} \in \mathbf{V}_{div}$ if and only if there exists an unique function $p \in L_0^2(\Omega)$ such that

$${}^2\mathbf{V}' = (\mathbf{H}_0^1(\Omega))' = \mathbf{H}^{-1}$$

$$l(\mathbf{v}) = (p, \nabla \cdot \mathbf{v}) = \int_{\Omega} p \nabla \cdot \mathbf{v}, \quad \forall \mathbf{v} \in \mathbf{V}. \quad (3.29)$$

□

Let \mathbf{u} be a solution of Problem (3.28). We consider the linear functional

$$l : \mathbf{v} \longrightarrow l(\mathbf{v}) = \left(\frac{\partial \mathbf{u}}{\partial t}, \mathbf{v} \right) + a(\mathbf{u}, \mathbf{v}) + c(\mathbf{u}, \mathbf{u}, \mathbf{v}) - (\mathbf{f}, \mathbf{v}), \quad \forall \mathbf{v} \in \mathbf{V}$$

The functional l is continuous over \mathbf{V} , since by the triangular, Cauchy-Schwarz and Poincaré's inequality, (3.22) and (3.24)

$$\begin{aligned} |l(\mathbf{v})| &\leq \left\| \frac{\partial \mathbf{u}}{\partial t} \right\|_{\mathbf{V}} \|\mathbf{v}\|_{\mathbf{V}} + 2\nu \|\mathbf{u}\|_{\mathbf{V}} \|\mathbf{v}\|_{\mathbf{V}} + K \|\mathbf{u}\|_{\mathbf{V}} \|\mathbf{u}\|_{\mathbf{V}} \|\mathbf{v}\|_{\mathbf{V}} + \|\mathbf{f}\|_{\mathbf{L}^2(\Omega)} \|\mathbf{v}\|_{\mathbf{V}} \\ &\leq \left(\left\| \frac{\partial \mathbf{u}}{\partial t} \right\|_{\mathbf{V}} + 2\nu \|\mathbf{u}\|_{\mathbf{V}} + K \|\mathbf{u}\|_{\mathbf{V}} \|\mathbf{u}\|_{\mathbf{V}} + \|\mathbf{f}\|_{\mathbf{L}^2(\Omega)} \right) \|\mathbf{v}\|_{\mathbf{V}} \end{aligned} \quad (3.30)$$

So, it is clear that $l \in \mathbf{V}'$, being a linear continuous functional on \mathbf{V} .

As \mathbf{u} is solution of Problem (3.28), we have $l(\mathbf{v}) = 0$ over \mathbf{V} .

By lemma 3.2.6 there is an unique $p \in L_0^2(\Omega)$ such that $l(\mathbf{v}) = (p, \nabla \cdot \mathbf{v})$, then

$$\begin{aligned} (p, \nabla \cdot \mathbf{v}) &= \left(\frac{\partial \mathbf{u}}{\partial t}, \mathbf{v} \right) + a(\mathbf{u}, \mathbf{v}) + c(\mathbf{u}, \mathbf{u}, \mathbf{v}) - (\mathbf{f}, \mathbf{v}), \quad \forall \mathbf{v} \in \mathbf{V} \Leftrightarrow \\ \left(\frac{\partial \mathbf{u}}{\partial t}, \mathbf{v} \right) &+ a(\mathbf{u}, \mathbf{v}) + c(\mathbf{u}, \mathbf{u}, \mathbf{v}) - (p, \nabla \cdot \mathbf{v}) = (\mathbf{f}, \mathbf{v}), \quad \forall \mathbf{v} \in \mathbf{V} \end{aligned}$$

So we conclude that \mathbf{u} is solution of 3.27. ■

3.2.2 Existence and uniqueness of solution

In three-dimensional case there is a gap between the class functions where the existence is known, and the smaller classes, where uniqueness is proved due to lack of information concerning the regularity of the weak solutions.

For this dimension, Martine Marion and Roger Temam stated that:

- There exists for all time a weak (nonsmooth) solution, but it may not be unique;
- If a strong (smooth) solution exists for all time then it is unique; but we do not know if such a solution exists for all time;

- A strong solution exists on a certain interval of time $[0, t_1]$, where t_1 depends on the data; Furthermore on $[0, t_1]$, the solution can be as smooth as the data permits;
- When a strong solution exists on an interval of time, then no other weak solution exists on the same interval of time.

The solution's regularity in three-dimensional case that we can prove, is weaker than those of two-dimensional case. More details on these issues, as well as the existence and uniqueness theorems for $d = 3$ can be found in [13, 33].

In this section, we limit ourselves to present two theorems of existence and uniqueness of the bidimensional Navier-Stokes problem without proof. Other theorems can be proven to be more regular solutions since we assume more regularity in the data [13, 33].

Theorem 3.2.1

Let $k \geq -1$ be an integer and Ω a bounded domain in \mathbb{R}^2 of class C^m , $m = \max\{k + 2, 2\}$. Then, for any $\mathbf{f} \in L^2(0, T; \mathbf{H}^k(\Omega))$ and $\mathbf{u}_0 \in \mathbf{H}^1(\Omega)$. Then Problem (3.27) admits an unique solution (\mathbf{u}, p) such that

$$\mathbf{u} \in L^\infty(0, T; \mathbf{H}^{k+2} \cap \mathbf{H}_0^1(\Omega)), \quad p \in C(0, T; \mathbf{H}^{k+1} \cap L_0^2(\Omega)) \quad (3.31)$$

□

Theorem 3.2.2

Let Ω be an open Lipschitz subset of \mathbb{R}^2 bounded and the space $\mathbf{H} = \{\mathbf{u} \in \mathbf{L}^2(\Omega) : \nabla \cdot \mathbf{u} = 0\}$. Consider the given $\mathbf{f} \in L^2(0, T; \mathbf{H}^{-1}(\Omega))$ and $\mathbf{u}_0 \in \mathbf{H}(\Omega)$. Then there exists and it is unique $\mathbf{u} \in L^2(0, T; \mathbf{V})$ which is solution of Problem (3.28). Moreover,

$$\mathbf{u} \in L^\infty(0, T; \mathbf{H}) \quad (3.32)$$

and \mathbf{u} is continuous from $[0, T]$ into \mathbf{H} .

□

3.2.3 Energy inequality

The stability criterion is essential for physical problems. A mathematical problem is usually considered physically realistic if a small change in given data produces correspondingly a small change in the solution, i.e, the solution depends continuously on the data. We can use energy inequality to see if the mathematical problem (3.10) is physically realistic.

Lemma 3.2.7 (*Energy inequality*)

Let $\mathbf{u} \in L^2(0, T; \mathbf{V})$ be a solution of (3.27), $\forall t > 0$ then the following inequality holds

$$\|\mathbf{u}(t)\|_{\mathbf{L}^2(\Omega)}^2 + 2\nu C_k \int_0^t \|\nabla \mathbf{u}(\sigma)\|_{\mathbf{L}^2(\Omega)}^2 d\sigma \leq \frac{C_p}{2\nu C_k} \int_0^t \|\mathbf{f}(\sigma)\|_{\mathbf{L}^2(\Omega)}^2 d\sigma + \|\mathbf{u}_0\|_{\mathbf{L}^2(\Omega)}^2 \quad (3.33)$$

□

Remark:

For all $t > 0$, $\mathbf{u} \in L^2(0, T; \mathbf{V}_{div})$ the solution of (3.28) verifies also (3.33) This inequality provides an a-priori stability for the solution of Navier-stokes equations.

Proof

Multiplying the first of (3.10) by \mathbf{u} and integrating over the domain Ω we obtain

$$\int_{\Omega} \frac{\partial \mathbf{u}}{\partial t} \cdot \mathbf{u} + \int_{\Omega} (\mathbf{u} \cdot \nabla) \mathbf{u} \cdot \mathbf{u} + \int_{\Omega} \nabla p \cdot \mathbf{u} - 2\nu \int_{\Omega} \nabla \cdot \mathbf{D}(\mathbf{u}) \cdot \mathbf{u} = \int_{\Omega} \mathbf{f} \cdot \mathbf{u} \quad (3.34)$$

By Reynolds Transport Theorem 2.1.1 the kinetic energy of the fluid (energy associated with fluid in motion) holds³

$$\begin{aligned} e(\mathbf{u}) &= \int_{\Omega} \frac{\partial \mathbf{u}}{\partial t} \cdot \mathbf{u} = \int_{\Omega} \frac{1}{2} \left(2 \frac{\partial \mathbf{u}}{\partial t} \cdot \mathbf{u} \right) = \frac{1}{2} \int_{\Omega} \frac{\partial}{\partial t} |\mathbf{u}|^2 \\ &= \frac{1}{2} \frac{d}{dt} \int_{\Omega} |\mathbf{u}|^2 - \int_{\partial\Omega} \mathbf{u} |\mathbf{u}|^2 \cdot \mathbf{n} = \frac{1}{2} \frac{d}{dt} \int_{\Omega} |\mathbf{u}|^2 = \frac{1}{2} \frac{d}{dt} \|\mathbf{u}\|_{\mathbf{L}^2(\Omega)}^2 \end{aligned} \quad (3.35)$$

³with the calculations that follow we can conclude that $(\frac{\partial \mathbf{u}}{\partial t}, \mathbf{v}) = \int_{\Omega} \frac{\partial \mathbf{u}}{\partial t} \cdot \mathbf{v} = \frac{d}{dt} \int_{\Omega} \mathbf{u} \cdot \mathbf{v} = \frac{d}{dt} (\mathbf{u}, \mathbf{v})$.

and by Korn inequality (3.9)⁴

$$-\int_{\Omega} \nabla \cdot \mathbf{D}(\mathbf{u}) \cdot \mathbf{u} = \int_{\Omega} \mathbf{D}(\mathbf{u}) : \nabla \mathbf{u} + \int_{\Omega} \mathbf{D}(\mathbf{u}) \cdot \mathbf{u} \cdot \mathbf{u} = \int_{\Omega} |\mathbf{D}(\mathbf{u})|^2 \geq C_k \|\nabla \mathbf{u}\|_{\mathbf{L}^2(\Omega)}^2. \quad (3.36)$$

By (3.25) we conclude that the term

$$\int_{\Omega} (\mathbf{u} \cdot \nabla) \mathbf{u} \cdot \mathbf{u} = 0. \quad (3.37)$$

Finally the term

$$\int_{\Omega} \nabla p \cdot \mathbf{u} = -\int_{\Omega} p \nabla \cdot \mathbf{u} + \int_{\partial\Omega} p \mathbf{n} \cdot \mathbf{u} = 0 \quad (3.38)$$

By (3.35), (3.36) (3.37) and (3.38), applying (3.3) we obtain

$$\begin{aligned} \frac{d}{dt} \|\mathbf{u}\|_{\mathbf{L}^2(\Omega)}^2 + 4\nu C_k \int_{\Omega} \|\nabla \mathbf{u}\|_{\mathbf{L}^2(\Omega)}^2 &\leq \frac{d}{dt} \|\mathbf{u}\|_{\mathbf{L}^2(\Omega)}^2 + 4\nu C_k \int_{\Omega} |\mathbf{D}(\mathbf{u})|^2 = \\ &= \int_{\Omega} \frac{\partial \mathbf{u}}{\partial t} \cdot \mathbf{u} + \int_{\Omega} (\mathbf{u} \cdot \nabla) \mathbf{u} \cdot \mathbf{u} + \int_{\Omega} \nabla p \cdot \mathbf{u} - 2\nu \int_{\Omega} \nabla \cdot \mathbf{D}(\mathbf{u}) \cdot \mathbf{u} = \\ &= 2 \int_{\Omega} \mathbf{f} \cdot \mathbf{u} \leq \frac{1}{\varepsilon} \|\mathbf{f}\|_{\mathbf{L}^2(\Omega)}^2 + \varepsilon \|\mathbf{u}\|_{\mathbf{L}^2(\Omega)}^2 \\ &\leq \frac{1}{\varepsilon} \|\mathbf{f}\|_{\mathbf{L}^2(\Omega)}^2 + \varepsilon \|\mathbf{u}\|_{\mathbf{H}^1(\Omega)}^2, \quad \forall \varepsilon > 0 \end{aligned} \quad (3.39)$$

Applying (3.8) and taking $\varepsilon = \frac{2\nu C_k}{C_p}$ (with C_k and C_p the Korn's and Poincaré's constants, respectively), we obtain

$$\frac{d}{dt} \|\mathbf{u}\|_{\mathbf{L}^2(\Omega)}^2 + 2\nu C_k \int_{\Omega} \|\nabla \mathbf{u}\|_{\mathbf{L}^2(\Omega)}^2 \leq \frac{C_p}{2\nu C_k} \|\mathbf{f}\|_{\mathbf{L}^2(\Omega)}^2 \quad (3.40)$$

⁴In fact, we limit inferiorly the enstrophy $E(\mathbf{u})$ (quantity directly related to the kinetic energy in the flow model that corresponds to dissipation effects in the fluid), since $E(\mathbf{u}) = \int_{\Omega} |\nabla \mathbf{u}|^2 = \int_{\Omega} 2|\mathbf{D}(\mathbf{u})|^2$ by (A-13)

By integrating between 0 and t we have

$$\int_0^t \frac{d}{dt} \|\mathbf{u}(\sigma)\|_{\mathbf{L}^2(\Omega)}^2 d\sigma + 2\nu C_k \int_0^t \|\nabla \mathbf{u}(\sigma)\|_{\mathbf{L}^2(\Omega)}^2 d\sigma \leq \frac{C_p}{2\nu C_k} \int_0^t \|\mathbf{f}(\sigma)\|_{\mathbf{L}^2(\Omega)}^2 d\sigma \Leftrightarrow$$

$$\Leftrightarrow \|\mathbf{u}(t)\|_{\mathbf{L}^2(\Omega)}^2 - \|\mathbf{u}(0)\|_{\mathbf{L}^2(\Omega)}^2 + 2\nu C_k \int_0^t \|\nabla \mathbf{u}(\sigma)\|_{\mathbf{L}^2(\Omega)}^2 d\sigma \leq \frac{C_p}{2\nu C_k} \int_0^t \|\mathbf{f}(\sigma)\|_{\mathbf{L}^2(\Omega)}^2 d\sigma$$

$$\Leftrightarrow \|\mathbf{u}(t)\|_{\mathbf{L}^2(\Omega)}^2 + 2\nu C_k \int_0^t \|\nabla \mathbf{u}(\sigma)\|_{\mathbf{L}^2(\Omega)}^2 d\sigma \leq \frac{C_p}{2\nu C_k} \int_0^t \|\mathbf{f}(\sigma)\|_{\mathbf{L}^2(\Omega)}^2 d\sigma + \|\mathbf{u}_0\|_{\mathbf{L}^2(\Omega)}^2$$

■

Chapter 4

Numerical Analysis for Navier-Stokes Flow

In this chapter, the analysis of an approximate problem corresponding to the unsteady Navier-Stokes model with a constant viscosity is carried out. Existence and uniqueness of approximate solutions are proved and corresponding estimates are given.

Our aim here is the numerical analysis of an approximate problem corresponding to the continuous system (2.23) studied in chapter 2, in the case of a bidimensional classical Navier-Stokes model.

In the next section, we introduce some basic concepts about Finite Element Method (FEM). The FEM is a method which approaches the solution of partial differential equations (PDEs) and is a general technique for constructing approximate solutions to boundary value problems in dimension d ($d \leq 3$). Finite element method is widely used in diverse fields to solve static and dynamic problems – solid mechanics, fluid mechanics, electromagnetics, biomechanics, etc.

All results will be presented here for the two-dimensional case, where we will do the application of these concepts and present of numerical simulations.

Although there are several types of finite elements, in the following, we deal only with the discretization of the Navier-Stokes problem, using a Lagrange Finite Element of type $\mathbb{P}_2 - \mathbb{P}_1$.

4.1 Finite Element Method

The solution (\mathbf{u}, p) of the problem (3.27) lives in a space of infinite dimension. In this circumstance, it is generally impossible to calculate the exact solution. Then we determine an approximation of \mathbf{u} and p , respectively \mathbf{u}_h and p_h , each one defined in finite dimensional appropriate spaces V_h , such that $\dim V_h = I(h)$ ($\lim_{h \rightarrow 0} I(h) = +\infty$) and dependent on a parameter $h > 0$. These spaces are formed by polynomials and for all function v_h in V_h (in particular \mathbf{u}_h and p_h for the appropriate spaces) we have $v_h = \sum_{i=1}^I \alpha_i \phi_i$, $\alpha_i \in \mathbb{R}$, $i = 1, \dots, I$ where $\{\phi_1, \dots, \phi_I\}$ is a basis of V_h . This is the principle of the Finite Element Method.

The FEM can be studied in details in [3, 24, 26, 2, 13]. Here we introduce a few basic concepts. Consider m distinct points p_i ($i = 1, \dots, m$) in $\bar{\Omega}$ and decompose the domain Ω into finite number of subdomains Ω_e with vertices in the set $\{p_1, \dots, p_m\}$. The union of these subdomains, called finite elements, such that $\bar{\Omega} = \bigcup_{e=1}^N \Omega_e = \bar{\Omega}_h$, is called the mesh of Ω and the m points p_i are called the nodes of Ω . Here Ω_e may or may not be polygon. If Ω_e is a polygon and Ω is not then we can not approach the boundary very well and we have $\Omega_h = \bigcup_{e=1}^N \Omega_e \subset \bar{\Omega}$. In this case we must take into account the error of discretization.

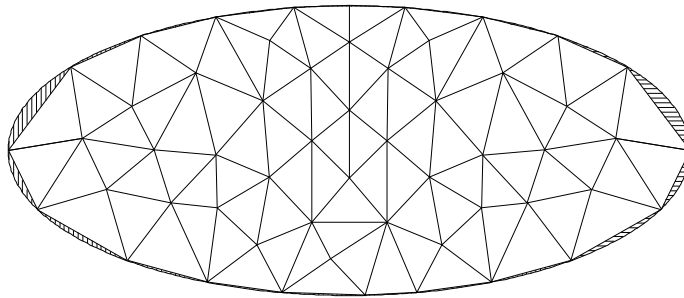


Figure 4.1: Example of a non polygonal domain discretized by polygons.

For sake of clarity, we assume that $\bar{\Omega} = \bigcup_{e=1}^N \Omega_e = \bar{\Omega}_h$. So we consider each subdomain as a triangle T with non-empty interior such that the interior of two distinct triangles

T_i and T_j are disjoint ($i \neq j; i, j = 1, \dots, N$) and every boundary of T_i is a boundary of another triangle (the triangles are adjacent or part of boundary $\partial\Omega$), *i.e.*, we consider a triangulation \mathcal{T}_h of Ω constructed by non degenerated triangles. The parameter h is the diameter of the triangulation \mathcal{T}_h given by $h = \max_{T \in \mathcal{T}_h} h_T$, where h_T is the diameter of the circumscribed circle into T .

For the following we consider an uniform regular mesh \mathcal{T}_h . This means that all the triangles have approximately the same size. In this circumstance there exists positive constants C_1, C_2 independent of h and T such that

$$\frac{h_T}{\rho_T} \leq C_1, \quad \forall T \in \mathcal{T}_h,$$

where ρ_T is the diameter of the inscribed circle into T and

$$C_2 h \leq h_T, \quad \forall T \in \mathcal{T}_h$$

For this mesh we define a set of appropriate basis functions $\{\phi_1(x, y), \dots, \phi_m(x, y)\}$ such that for all function v in \mathcal{T}_h we define the interpolation as

$$v(x, y) = \sum_{i=1}^m v_i \phi_i(x, y) \quad (4.1)$$

where, for all $i \in \{1, \dots, m\}$, v_i is the value of the function ϕ at the node i of the mesh and the basis function ϕ_i has the following property ($i, j = 1, \dots, m$)

$$\phi_i(x_j, y_j) = \delta_{ij} \quad (\delta_{ij} \text{ is the Kronecker symbol})$$

To avoid setting m basis functions we introduce the master element as the triangle \hat{T} with the vertices $\hat{\mathbf{a}}_1 = (0, 0)$, $\hat{\mathbf{a}}_2 = (1, 0)$ and $\hat{\mathbf{a}}_3 = (0, 1)$. Given an arbitrary triangle T with vertices $\mathbf{a}_i = (x_i, y_i)$, $i = 1, 2, 3$, there exist only one invertible affine transformation (figure 4.2)

$$F_T : \mathbb{R}^2 \rightarrow \mathbb{R}^2$$

$$\hat{\mathbf{x}} \rightarrow B_T \hat{\mathbf{x}} + b_T = \mathbf{x}$$

with inverse $F_T^{-1}(\mathbf{x}) = B_T^{-1}(\mathbf{x} - b_T)$ where $B_T = \begin{bmatrix} x_2 - x_1 & x_3 - x_1 \\ y_2 - y_1 & y_3 - y_1 \end{bmatrix}$ is an invertible

matrix and $b_T = \begin{bmatrix} x_1 \\ y_1 \end{bmatrix}$ is a vector, such that $F_T(\hat{\mathbf{a}}_i) = \mathbf{a}_i, i = 1, 2, 3$.

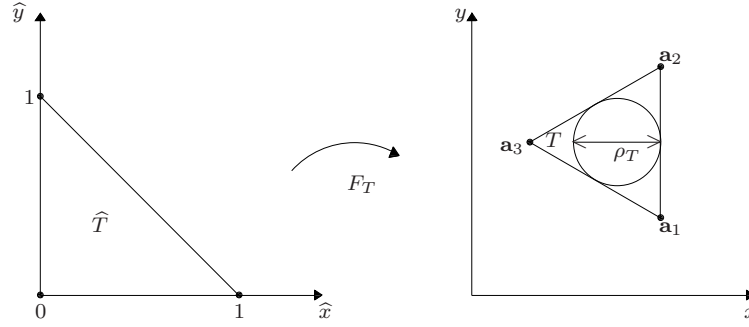


Figure 4.2: Affine map from the reference triangle \hat{T} to the generic element $T \in \mathcal{T}_h$.

For all function v defined over T , we associate bijectively the function \hat{v} defined over \hat{T} by

$$\forall \hat{\mathbf{x}} \in \hat{T}, \quad \hat{v}(\hat{\mathbf{x}}) = v(\mathbf{x}) = v(F_T(\hat{\mathbf{x}})) = v \circ F_T(\hat{\mathbf{x}}).$$

As F_T is invertible, we have also

$$\forall \mathbf{x} \in T, \quad v(\mathbf{x}) = \hat{v}(\hat{\mathbf{x}}) = \hat{v}(F_T^{-1}(\mathbf{x})) = \hat{v} \circ F_T^{-1}(\mathbf{x})$$

This way we can work only over master triangle \hat{T} .

We can prove (see [24]) that there exists a constant $C = C(k)$ such that

$$|\hat{v}|_{H^k(\hat{T})} \leq C \|B_T\|^k |\det B_T|^{-1/2} |v|_{H^k(T)}, \quad \forall v \in H^k(T)$$

and

$$|v|_{H^k(T)} \leq C \|B_T^{-1}\|^k |\det B_T|^{1/2} |\hat{v}|_{H^k(\hat{T})}, \quad \forall \hat{v} \in H^k(\hat{T})$$

where $\|\cdot\|$ is the matrix norm associated to the Euclidean norm in \mathbb{R}^2 . In terms of geometric quantities of T we have the following estimates ([24, 26])

$$\|B_T\| \leq \frac{h_T}{\hat{\rho}}, \quad \|B_T^{-1}\| \leq \frac{\hat{h}}{\rho_T},$$

where $\hat{\rho}$ and \hat{h} are, respectively, the diameters of inscribed and circumscribed circle and the into \hat{T} . Moreover,

$$|\det(B_T)| = \frac{\text{Area}(T)}{\text{Area}(\hat{T})} = 2\text{Area}(T) \neq 0.$$

For each triangle T we consider the finite set $\Sigma_T = \{\mathbf{a}_i\}_{i=1}^n$ of distinct points of T and a finite dimensional vectorial space P_T of functions defined over T with real values. We say that Σ are P -unisolvent if and only if all the function in P_T is uniquely determined by its values at points in Σ_T , *i.e*

$$\forall \alpha_i \in \mathbb{R}, p(\mathbf{a}_i) = \alpha_i \quad (i = 1, \dots, n).$$

In this case, the triplex (T, P_T, Σ_T) is a finite element of Lagrange.

We call finite elements space to the discrete space $V_h = \{v_h \in V : v_h|_T \in P_T, \forall T \in \mathcal{T}_h\}$ where V is an infinite dimensional space of functions defined over Ω .

To determine a basis of V_h we need to define the compatibility conditions between two finite elements:

(H1) For all pair $\{T_1, T_2\}$ of adjacents triangles of \mathcal{T}_h , with a common side $T' = T_1 \cap T_2$ there is $P_{T_1|_{T'}} = P_{T_2|_{T'}}$ and $\Sigma_{T_1} \cap T' = \Sigma_{T_2} \cap T'$.

(H2) For all $T \in \mathcal{T}_h$, the finite element (T, P_T, Σ_T) is of class C^0 . This means that $P_T \subset C(T)$ and for any side T' of T , the set $\Sigma' = \Sigma_T \cap T'$ is P' -unisolvent where $P' = \{p|_{T'} : p \in P_T\}$

Given a finite element (T, P_T, Σ_T) there exists one and only one function $\phi_i \in P_T$ for all $i = 1, \dots, n$ such that $\phi_i(\mathbf{a}_j) = \delta_{ij}$, for all $j = 1, \dots, n$ and the only function in P_T which vanishes on Σ_T is the null function. They are the basis functions of V_h . So, for any function $v \in V_h$ we have

$$v = \sum_{i=1}^N v(\mathbf{a}_i) \phi_i.$$

The scalars $v(\mathbf{a}_i), i = 1, \dots, N$ are called degrees of freedom of the function v in V_h . The set of elements $T \in \mathcal{T}_h$ for which the node \mathbf{a}_i belongs on $\text{supp}(\phi_i)$. The restriction of ϕ_i for each of these elements T is a basis function of finite element (T, P_T, Σ_T) .

For each T we define the P -interpolation operator of Lagrange such that for all function $v \in C(\overline{\Omega})$, this operator associates the function $\Pi_h^T(v)$ defined by

$$\Pi_h^T(v) = \sum_{i=1}^N v(\mathbf{a}_i) \phi_i.$$

$$\text{So, } \Pi_T v(\mathbf{a}_j) = \sum_{i=1}^n v(\mathbf{a}_i) p_i(\mathbf{a}_j) = \sum_{i=1}^n v(\mathbf{a}_i) \delta_{ij} = v(\mathbf{a}_j).$$

The interpolant $\Pi_h^T(v)$ is the unique function in V_h which takes the same values of the given function v at all nodes \mathbf{a}_i . We can introduce a local interpolation operator with $\alpha_i, 1 \leq i \leq N_T$ nodes of T as

$$\Pi_T(v) = \sum_{i=1}^{N_T} v(\alpha_i) \phi_{i|_T}, \quad \forall v \in C(T)$$

It can be verified at once that $\Pi_h^T(v)|_T = \Pi_T(v|_T) \quad \forall T \in \mathcal{T}_h, v \in C(\bar{\Omega})$.

We have the following theorem [24, 26] that gives us an estimate for the interpolation error.

Theorem 4.1.1

Suppose that $\{\mathcal{T}_h\}_{h>0}$ is a regular triangulations's family of $\bar{\Omega}$ whose elements verifies **(H1)** and **(H2)**. Let $k \geq 1$ be an integer. For $m \in \{0, 1\}$, there is a constant C , independent of h , such that

$$|v - \Pi_T(v)|_{H^m(\Omega)} \leq Ch^{k+1-m} |v|_{H^{k+1}(\Omega)} \quad \forall v \in H^{k+1}(\Omega). \quad (4.2)$$

Moreover,

$$\inf_{v_h \in V_h} |v - v_h|_{H^m(\Omega)} \leq Ch^{k+1-m} |v|_{H^{k+1}(\Omega)} \quad \forall v \in H^{k+1}(\Omega). \quad (4.3)$$

□

4.2 Semi-Discrete Navier-Stokes problem

We consider *Galerkin's method* for constructing approximate solutions to the variational boundary-value problem (3.17) or its abstract formulation (3.27). Galerkin's method consists of seeking an approximate solution (3.17) in a finite-dimensional subspace V_h of the space of admissible functions where the solution lies in this subspace rather than in the whole space.

The natural Galerkin approximation for problem (3.10) is a mixed method which is based on Lagrange multiplier formulations of constrained problems. We refer to mixed approximation methods as those associated to the approximation of saddle point problems, in which there are two bilinear forms and two approximation spaces satisfying a compatibility condition.

Let $(\mathcal{T}_h)_h$ be a family of triangulations and h the parameter of discretization. Consider $\mathbf{V}_h \subset \mathbf{H}^1(\Omega)$ and $Q_h \subset L_0^2(\Omega)$ two finite dimensional spaces for the velocity field and the pressure, respectively. We take

$$\mathbf{V}_h^0 = \mathbf{V}_h \cap \mathbf{H}_0^1(\Omega) \quad \text{and} \quad M_h = Q_h \cap L_0^2(\Omega).$$

This pair of discrete spaces (\mathbf{V}_h^0, M_h) verifies a compatibility condition known as the *discrete LBB* (or *inf-sup*) *condition*, which reads as follows:

There exists $\beta > 0$ (independent of h) such that

$$\inf_{q_h \in Q_h \setminus \{0\}} \sup_{\mathbf{v}_h \in \mathbf{V}_h^0 \setminus \{0\}} \frac{|(q_h, \nabla \cdot \mathbf{v}_h)|}{\|\mathbf{v}_h\|_{\mathbf{V}_h^0} \|q_h\|_{Q_h}} \geq \beta. \quad (4.4)$$

We remind that this property is necessary for the well posedness of discrete problem. The result, stated below, is classical and can be found in [?].

Theorem 4.2.1

Suppose that \mathcal{T}_h is non-degenerate and has no triangle with two edges on $\partial\Omega$. Then the LBB-condition (4.4) is satisfied.

□

To problem (3.27), for each $h > 0$, we associate the following approximated problem

for each $t \in [0, T]$, $\mathbf{u}_{0,h} \in \mathbf{V}_h^0$, find $(\mathbf{u}_h, p_h) \equiv (\mathbf{u}_h(t, \cdot), p_h(t, \cdot)) \in \mathbf{V}_h^0 \times M_h$ such

that

$$\begin{cases} \frac{d}{dt} (\mathbf{u}_h, \mathbf{v}_h) + a(\mathbf{u}_h, \mathbf{v}_h) + c(\mathbf{u}_h, \mathbf{u}_h, \mathbf{v}_h) + b(\mathbf{v}_h, p_h) = (\mathbf{f}, \mathbf{v}_h), & \forall \mathbf{v}_h \in \mathbf{V}_h^0 \\ b(\mathbf{u}_h, q_h) = 0 & \forall q_h \in M_h \\ \mathbf{u}_h(0) = \mathbf{u}_{0,h} \end{cases} \quad (4.5)$$

The existence of solution of the problem (4.5) is guaranteed by the choice of spaces, \mathbf{V}_h^0 and M_h , which verify the LBB condition.

Using (4.4) and some space properties we can prove the following result:

Lemma 4.2.1

Problem (4.5) has an unique solution $(\mathbf{u}_h, p_h) \in \mathbf{V}_h^0 \times M_h$.

Moreover,

$$\inf_{\mathbf{u}_h \in \mathbf{V}_h} \|\mathbf{u} - \mathbf{u}_h\|_{\mathbf{H}^1(\Omega)} + \inf_{p_h \in Q_h} \|p - p_h\|_{L^2(\Omega)} = O(h), \quad (4.6)$$

i.e.,

$$\lim_{h \rightarrow 0} \|\mathbf{u} - \mathbf{u}_h\|_{\mathbf{H}^1(\Omega)} + \lim_{h \rightarrow 0} \|p - p_h\|_{L^2(\Omega)} = 0 \quad (4.7)$$

□

The following lemma deals with error estimate of (4.5). The proof can be found in [24].

Lemma 4.2.2

Let \mathbf{V}_h^0 and M_h be a couple of finite element spaces that satisfy the compatibility condition and $\mathbf{u} \in \mathbf{V}$, $p \in M$ and $\mathbf{u}_0 \in \mathbf{V}_{div}$ then

$$\|\mathbf{u} - \mathbf{u}_h\|_{\mathbf{L}^2(\Omega)} \leq C_1(t)h^2, \quad \|p - p_h\|_{L^2(\Omega)} \leq C_1(t)h \quad (4.8)$$

□

Now we are going to study the stability. As pointed out in section 3.2.3 the convective term $\int_{\Omega} (\mathbf{u} \cdot \nabla) \mathbf{u} \cdot \mathbf{v}$ does not contribute to energy system at differential level in (3.17) or equivalently (3.27) or (3.28). Indeed, taking $\mathbf{v} = \mathbf{u}$ he have

$$\int_{\Omega} (\mathbf{u} \cdot \nabla) \mathbf{u} \cdot \mathbf{u} = \frac{1}{2} \int_{\Omega} \mathbf{u} \cdot \nabla |\mathbf{u}|^2 = -\frac{1}{2} \int_{\Omega} \nabla \cdot \mathbf{u} |\mathbf{u}|^2 + \frac{1}{2} \int_{\partial\Omega} \mathbf{u} \cdot \mathbf{n} |\mathbf{u}|^2 = -\frac{1}{2} \int_{\Omega} \nabla \cdot \mathbf{u} |\mathbf{u}|^2 \quad (4.9)$$

Thanks to the second equation in (3.17) the last term is zero. This property is not true at discrete level in (4.5) due to discretization. Nonetheless, we can modify (4.5) in a consistent way by adding to the first equation the term

$$\frac{1}{2} ((\nabla \cdot \mathbf{u}_h) \mathbf{u}_h, \mathbf{v}) = \frac{1}{2} \int_{\Omega} (\nabla \cdot \mathbf{u}_h) \mathbf{u}_h \cdot \mathbf{v}. \quad (4.10)$$

So, it is possible to recover the same stability property feature at differential level. We underline the fact that this modification is consistent since the exact solution satisfies $\nabla \cdot \mathbf{u} = 0$.

As follows, we will consider always this modified problem that we rewrite hereafter for the sake of clarity:

$$\begin{cases} \text{for each } t \in [0, T], \text{ find } (\mathbf{u}_h, p_h) \equiv (\mathbf{u}_h(t, \cdot), p_h(t, \cdot)) \in \mathbf{V}_h^0 \times M_h \text{ such that} \\ \left. \begin{aligned} \frac{d}{dt} (\mathbf{u}_h, \mathbf{v}_h) + a(\mathbf{u}_h, \mathbf{v}_h) + c(\mathbf{u}_h, \mathbf{u}_h, \mathbf{v}_h) + \frac{1}{2} ((\nabla \cdot \mathbf{u}_h) \mathbf{u}_h, \mathbf{v}_h) + b(\mathbf{v}_h, p_h) &= (\mathbf{f}, \mathbf{v}_h), \\ &\forall \mathbf{v}_h \in \mathbf{V}_h^0 \\ b(\mathbf{u}_h, q_h) &= 0, \\ &\forall q_h \in M_h \\ \mathbf{u}_h(0) &= \mathbf{u}_{0,h} \end{aligned} \right\} \end{cases} \quad (4.11)$$

Now we can prove that (4.11) is stable.

Lemma 4.2.3

For each fixed t , $\mathbf{u}_h \in \mathbf{V}_h^0$ solution of (4.11), verifies the following inequality

$$\|\mathbf{u}_h(t)\|_{\mathbf{L}^2(\Omega)}^2 + 2\nu C_k \int_0^t \|\nabla \mathbf{u}(\sigma)\|_{\mathbf{L}^2(\Omega)}^2 d\sigma \leq \frac{C_p}{2\nu C_k} \int_0^t \|\mathbf{f}(\sigma)\|_{\mathbf{L}^2(\Omega)}^2 d\sigma + \|\mathbf{u}_{0,h}\|_{\mathbf{L}^2(\Omega)}^2 \quad (4.12)$$

□

Proof

For each fixed $t \in [0, T]$, we take $\mathbf{v}_h = \mathbf{u}_h$ in first of (4.11). Using (4.10) results

$$c(\mathbf{u}_h, \mathbf{u}_h, \mathbf{u}_h) + \frac{1}{2}((\nabla \cdot \mathbf{u}_h) \mathbf{u}_h, \mathbf{u}_h) = 0$$

and using reasoning analogous to that applied in the proof of lemma 3.2.7 we obtain (4.12). ■

The inequality (4.12) is the discrete counterpart of (3.33) and provides the stability estimate.

4.3 Time discretization

There are several methods of time discretization. Here we describe only one, the method that we used in numerical simulations.

We used *backward Euler scheme* of first order defined by

$$\frac{\partial \mathbf{u}}{\partial t}(t^{n+1}, \cdot) = \frac{\mathbf{u}(t^{n+1}, \cdot) - \mathbf{u}(t^n, \cdot)}{t^{n+1} - t^n} \quad (4.13)$$

associated to *Characteristic Galerkin Method*. The Characteristic Galerkin Method evaluates time derivatives of vector field on Lagrangian frame, appealing to characteristic lines or trajectories described by a material particle when it has been driven by the field at the velocity of the field (see section 2.1.1).

We described the motion of material particle of Newtonian fluid during the time interval $[t_0, t_1] \subset [0, T]$, ($T > 0$), which was on position ξ at instant t_0 by

$$\chi_{t;t_0} : \xi \longrightarrow \chi(t; t_0, \xi) \quad (4.14)$$

and define its characteristic line or trajectory, with the same flow direction, by the only solution of Cauchy Problem¹ following:

¹This Cauchy problem have one and only one solution, since \mathbf{u} is continuous in $[0, T] \times \bar{\Omega}$ and Lipschitz continuous in $\bar{\Omega}$, uniformly with respect to $t \in [0, T]$.

$$\begin{cases} \frac{d\chi}{dt}(t; t_0, \xi) = \mathbf{u}(t; \chi(t; t_0, \xi)), t \in]0, T[\\ \chi(t_0; t_0, \xi) = \xi. \end{cases} \quad (4.15)$$

Observe that by uniqueness of trajectory, the position, at instant t , of a particle that was on position ξ at instant t_0 and which was on position \mathbf{x} at instant $t = t_1$, i.e., $\mathbf{x} = \chi(t_1; t_0, \xi)$, is the same position of the particle which was on ξ at instant t_0 . That means

$$\chi(t; t_1, \mathbf{x}) = \chi(t; t_1, \chi(t_1; t_0, \xi)) = \chi(t; t_0, \xi). \quad (4.16)$$

Hence, we conclude

$$\chi(t; t_1, \chi(t_1; t, \xi)) = \chi(t; t, \xi) = \xi. \quad (4.17)$$

So, we can define the inverse mapping of $\chi : \xi \longrightarrow \chi(t; t_0, \xi)$ as

$$\chi_{t; t_0}^{-1} : \xi \longrightarrow \chi(t_0; t, \xi) = \chi_{t_0; t}(\xi) \quad (4.18)$$

Consider

$$\mathbf{u}(t, \mathbf{x}) = \widehat{\mathbf{u}}(t, \chi_{t; 0}^{-1}(\mathbf{x})) = \widehat{\mathbf{u}}(t, \chi(0; t, \xi)). \quad (4.19)$$

or equivalently

$$\widehat{\mathbf{u}}(t, \mathbf{x}) = \mathbf{u}(t, \chi(t; 0, \xi)). \quad (4.20)$$

From (4.15) results

$$\begin{aligned} \frac{\partial \widehat{\mathbf{u}}}{\partial t}(t, \mathbf{x}) &= \frac{d\mathbf{u}}{dt}(t; \chi(t; 0, \mathbf{x})) = \\ &= \frac{\partial \mathbf{u}}{\partial t}(t, \chi(t; 0, \mathbf{x})) + \sum_{i=1}^2 \frac{\partial \mathbf{u}}{\partial x_i}(t; \chi(t; 0, \mathbf{x})) \frac{\partial x_i}{\partial t}(t; \chi(t; 0, \mathbf{x})) \\ &= \frac{\partial \mathbf{u}}{\partial t}(t, \mathbf{x}) + \sum_{i=1}^2 \frac{\partial \mathbf{u}}{\partial x_i}(t; \mathbf{x}) u_i(t, \mathbf{x}) = \frac{D\mathbf{u}}{Dt}(t, \mathbf{x}) \end{aligned} \quad (4.21)$$

the material derivatives of \mathbf{u} , representing the rate of variation of \mathbf{u} along the trajectory $\chi_{t;0}$.

Taking an uniform mesh of $[0, T]$ defined by $t^n = n\Delta t$, $n = 0, \dots, T/\Delta t$, Δt being the time step and applying the backward Euler scheme we have

$$\begin{aligned}
\frac{\partial \widehat{\mathbf{u}}}{\partial t}(t^{n+1}, \mathbf{x}) &\approx \frac{\widehat{\mathbf{u}}(t^{n+1}, \mathbf{x}) - \widehat{\mathbf{u}}(t^n, \mathbf{x})}{t^{n+1} - t^n} = \\
&= \frac{\mathbf{u}(t^{n+1}, \chi(0; t^{n+1}, \mathbf{x})) - \mathbf{u}(t^n, \chi(0; t^{n+1}, \mathbf{x}))}{\Delta t} = \\
&= \frac{\mathbf{u}(t^{n+1}, \mathbf{x}) - \mathbf{u}(t^n, \chi(t^n; t^{n+1}, \mathbf{x}))}{\Delta t} \\
&= \frac{\mathbf{u}(t^{n+1}, \mathbf{x}) - \mathbf{u}^n \circ \chi^n(\mathbf{x})}{\Delta t}
\end{aligned} \tag{4.22}$$

where $\mathbf{u}^n \approx \mathbf{u}(t^n, \cdot)$ and $\chi^n(\mathbf{x}) \approx \chi(t^n; t^{n+1}, \mathbf{x})$, $n = 0, \dots, T/\Delta t$.

Applying the backward Euler scheme also for discretizing

$$\frac{d\chi}{dt}(t; t^{n+1}, \mathbf{x}) = \mathbf{u}(t, \chi(t; t^{n+1}, \mathbf{x})) \tag{4.23}$$

we obtain a second order approximation of $\chi(t; t^{n+1}, \mathbf{x})$ given by

$$\chi(t; t^{n+1}, \mathbf{x}) \approx \mathbf{x} - \mathbf{u}(t^{n+1}, \mathbf{x}) \Delta t \tag{4.24}$$

At this point, we can write the scheme for the problem (3.10), denoting $\mathbf{u}^n \circ \chi^n(\mathbf{x}) \approx \mathbf{u}^n(\mathbf{x} - \Delta t \mathbf{u}(t^{n+1}, \mathbf{x})) = \mathbf{u}^n(\mathbf{x}^*)$.

$$\left\{ \begin{array}{ll}
\mathbf{u}^{n+1} + \Delta t \nabla p^{n+1} - 2\nu \Delta t \nabla \cdot \mathbf{D}(\mathbf{u}^{n+1}) + \frac{\Delta t}{2} (\nabla \cdot \mathbf{u}^{**}) \mathbf{u}^{n+1} = \Delta t \mathbf{f}^{n+1} + \mathbf{u}^n(\mathbf{x}^*), & \text{in } \Omega \\
\nabla \cdot \mathbf{u}^{n+1} = 0, & \text{in } \Omega \\
\mathbf{u}^{n+1} = 0, & \text{on } \partial\Omega \\
\mathbf{u}^0 = \mathbf{u}_0, & \text{in } \Omega
\end{array} \right. \tag{4.25}$$

If $\mathbf{u}^{**} = \mathbf{u}^{n+1}$ we obtain an implicit method. However, we can linearize by doing $\mathbf{u}^{**} = \mathbf{u}^n$.

Lemma 4.3.1

Using piecewise linear finite elements in space applied to Navier-Stokes problem, the error behavior of the characteristic scheme is

$$\|\mathbf{u}^n - \mathbf{u}(t^n)\|_{\mathbf{L}^2(\Omega)} = O\left(h + \Delta t + \frac{h^2}{\Delta t}\right) \quad (4.26)$$

uniformly with respect to ν (kinematic viscosity). □

Introducing the notations

$$\mathbf{w} = \mathbf{u}^{n+1}$$

$$\pi = p^{k+1}$$

$$\mathbf{g}^{n+1} = \Delta t \mathbf{f}^{n+1} + \mathbf{u}^n(\mathbf{x}^*)$$

and choosing the previous finite dimensional spaces \mathbf{V}_h^0 and M_h , the problem (4.25) admits discrete variational formulation:

$$\left\{ \begin{array}{l} \frac{1}{\Delta t} (\mathbf{w}_h, \mathbf{v}_h) + a(\mathbf{w}_h, \mathbf{v}_h) + \frac{1}{2} ((\nabla \cdot \mathbf{u}_h) \mathbf{u}_h, \mathbf{v}_h) + b(\mathbf{v}_h, \pi_h) = (\mathbf{g}^{n+1}, \mathbf{v}_h), \quad \forall \mathbf{v}_h \in \mathbf{V}_h^0 \\ b(\mathbf{w}_h, q_h) = 0 \quad \forall q_h \in M_h \end{array} \right. \quad (4.27)$$

With the previous discrete spaces, the discrete problem (4.27) has an unique solution which converge to the solution of continuous problem.

4.4 Algorithm and algebraic linear systems

Among the choices that satisfy (4.4), we choose the *Hood-Taylor* finite elements $\mathbb{P}_2 - \mathbb{P}_1$.



Figure 4.3: $\mathbb{P}_2 - \mathbb{P}_1$ elements: degrees of freedom for the velocity components (on the left) and for the pressure (on the right).

To clarify we fixed some notations:

Let \mathcal{T}_h , $h > 0$ be a regular triangulation defined over the domain Ω . We define \mathbb{P}_k the polynomials space constitute by the polynomial function from \mathbb{R}^2 into \mathbb{R} of degree less than or equal to k ($k \geq 0$). We denote by $\mathbb{P}_k(T)$ the restriction to $T \in \mathcal{T}_h$ of \mathbb{P}_k . Consider the following finite element spaces

$$V_h^0 = \{v_h \in \mathbf{C}(\bar{\Omega}) \cap H_0^1(\Omega) \mid v_{h|T} \in \mathbb{P}_2(T), \forall T \in \mathcal{T}_h\} \subset V, \quad (4.28)$$

$$M_h = \{q_h \in C(\bar{\Omega}) \cap L_0^2(\Omega) \mid q_{h|T} \in \mathbb{P}_1(T), \forall T \in \mathcal{T}_h\} \subset Q. \quad (4.29)$$

such that

- $\dim(V_h^0) = N_h$, being N_h the total number of vertices and the midpoints of mesh's triangles in interior of Ω (not belong to the boundary $\partial\Omega$, since we have a Dirichlet problem, being known the velocity over $\partial\Omega$).
- $\dim(M_h) = m_h$, being m_h the total number of vertices of mesh's triangles.

Let $\mathbf{V}_h^0 = V_h^0 \times V_h^0$. This pair of spaces (\mathbf{V}_h^0, M_h) corresponds to the *Hood-Taylor* finite element method, and verifies a compatibility condition known as the *discrete LBB*.

We want to solve the approximated problem following (discrete variational formulation of (4.25)):

For each $t^{n+1} = (n+1)\Delta t \in [0, T]$, ($n \in \mathbb{N}_0$) given $\mathbf{u}_h^0 = \mathbf{u}_h(0)$, find $(\mathbf{u}_h^{n+1}, p_h^{n+1}) \in \mathbf{V}_h^0 \times M_h$ such that

$$\begin{cases} (\mathbf{u}_h^{n+1}, \mathbf{v}_h) - \Delta t (p_h^{n+1}, \nabla \cdot \mathbf{v}_h) + 2\nu \Delta t (\mathbf{D}(\mathbf{u}_h^{n+1}), \mathbf{D}(\mathbf{v}_h)) + \frac{\Delta t}{2} ((\nabla \cdot \mathbf{u}_h^n) \mathbf{u}_h^{n+1}, \mathbf{v}_h) = (\mathbf{g}, \mathbf{v}_h) & \text{in } \Omega \\ (\nabla \cdot \mathbf{u}_h^{n+1}, q_h^{n+1}) = 0, & \text{in } \Omega \end{cases} \quad (4.30)$$

Let $\{\varphi_i, i = 1, \dots, N_h\}$ be the Lagrange basis associated to \mathbf{V}_h^0 and $\{\psi_j, j = 1, \dots, m_h\}$ be the Lagrange basis associated to M_h . Given \mathbf{u}_h^n , we express the corresponding approximate solutions $\mathbf{u}_h^{n+1} = (u_{1,h}^{n+1}, u_{2,h}^{n+1})$ and p_h^{n+1} in the basis of V_h^0 and M_h

$$u_{1,h}^{n+1} = \sum_{j=1}^{N_h} u_{1,j}^{n+1} \varphi_j, \quad u_{2,h}^{n+1} = \sum_{j=1}^{N_h} u_{2,j}^{n+1} \varphi_j, \quad p_h^{n+1} = \sum_{k=1}^{m_h} p_k^{n+1} \psi_k. \quad (4.31)$$

Being the degrees of freedom referred as:

- the approximation of component k ($k=1, 2$) of velocity the values $u_{k,i}^{n+1} \approx u_k(t^{n+1}, (x_1^i, x_2^i))$, with (x_1^i, x_2^i) the coordinates of \mathbb{P}_2 - mesh nodes, i. e., the values of each component of velocity into vertices and the midpoints of edges of each triangle.
- the pressure approximation the values $p_j^{n+1} \approx p(t^{n+1}, (x_1^j, x_2^j))$ with (x_1^j, x_2^j) the coordinates of \mathbb{P}_1 - mesh nodes, i. e., the values of each component of velocity into vertices of each triangle.

With (4.31) and tests functions $\varphi_i \in \mathbf{V}_h^0$ and $\psi_k \in M_h$ we obtain the following linear system

$$\left\{ \begin{aligned}
& \int_{\Omega} \left\{ \left(\sum_{j=1}^{N_h} u_{1,j}^{n+1} \varphi_j \right) \varphi_i - \Delta t \sum_{k=1}^{m_h} p_k^{n+1} \psi_k \frac{\partial \varphi_i}{\partial x} + \right. \\
& \quad + \nu \Delta t \left[2 \left(\sum_{j=1}^{N_h} u_{1,j}^{n+1} \frac{\partial \varphi_j}{\partial x} \right) \frac{\partial \varphi_i}{\partial x} + \left(\sum_{j=1}^{N_h} u_{1,j}^{n+1} \frac{\partial \varphi_j}{\partial y} + \sum_{j=1}^{N_h} u_{2,j}^{n+1} \frac{\partial \varphi_j}{\partial x} \right) \frac{\partial \varphi_i}{\partial y} \right] + \\
& \quad \left. + \frac{\Delta t}{2} \left(\sum_{k=1}^{N_h} u_{1,k}^n \frac{\partial \varphi_k}{\partial x} + \sum_{k=1}^{N_h} u_{2,k}^n \frac{\partial \varphi_k}{\partial y} \right) \left(\sum_{j=1}^{N_h} u_{1,j}^{n+1} \varphi_j \right) \varphi_i \right\} = \int_{\Omega} g_{1,i}^{n+1} \varphi_i, \\
& \hspace{20em} i = 1, \dots, N_h \\
& \int_{\Omega} \left\{ \left(\sum_{j=1}^{N_h} u_{2,j}^{n+1} \varphi_j \right) \varphi_i - \Delta t \left(\sum_{k=1}^{m_h} p_k^{n+1} \psi_k \right) \frac{\partial \varphi_i}{\partial y} + \right. \\
& \quad + \nu \Delta t \left[2 \left(\sum_{j=1}^{N_h} u_{2,j}^{n+1} \frac{\partial \varphi_j}{\partial y} \right) \frac{\partial \varphi_i}{\partial y} + \left(\sum_{j=1}^{N_h} u_{1,j}^{n+1} \frac{\partial \varphi_j}{\partial y} + \sum_{j=1}^{N_h} u_{2,j}^{n+1} \frac{\partial \varphi_j}{\partial x} \right) \frac{\partial \varphi_i}{\partial x} \right] \\
& \quad \left. + \frac{\Delta t}{2} \left(\sum_{k=1}^{N_h} u_{1,k}^n \frac{\partial \varphi_k}{\partial x} + \sum_{k=1}^{N_h} u_{2,k}^n \frac{\partial \varphi_k}{\partial y} \right) \left(\sum_{j=1}^{N_h} u_{2,j}^{n+1} \varphi_j \right) \varphi_i \right\} = \int_{\Omega} g_{2,i}^{n+1} \varphi_i, \\
& \hspace{20em} i = 1, \dots, N_h \\
& \int_{\Omega} \left[\left(\sum_{j=1}^{N_h} u_{1,j}^{n+1} \varphi_j \right) \frac{\partial \psi_k}{\partial x} + \left(\sum_{j=1}^{N_h} u_{2,j}^{n+1} \varphi_j \right) \frac{\partial \psi_k}{\partial y} \right] = 0, \quad k = 1, \dots, m_h
\end{aligned} \right. \tag{4.32}$$

The linear system can be written in matricial form

$$\begin{bmatrix} \mathbf{A}_1 & \mathbf{A}_2 & \mathbf{B}_x \\ \mathbf{A}_2^t & \mathbf{A}_1 & \mathbf{B}_y \\ \mathbf{B}_x^t & \mathbf{B}_y^t & 0 \end{bmatrix} \begin{bmatrix} \mathbf{u}_1^{n+1} \\ \mathbf{u}_2^{n+1} \\ \mathbf{p}^{n+1} \end{bmatrix} = \begin{bmatrix} \mathbf{b}_1 \\ \mathbf{b}_2 \\ 0 \end{bmatrix} \tag{4.33}$$

where $\mathbf{u}_k^{n+1} = [u_{k,1}^{n+1}, \dots, u_{k,N_h}^{n+1}]^t$ and $\mathbf{p}^{n+1} = [p_1^{n+1}, \dots, p_{m_h}^{n+1}]^t$ are the vectors of unknown degree of freedom and

$$\mathbf{A}_1 = [\mathbf{A}_{1ij}]_{N_h \times N_h} = \left[\int_{\Omega} \left[\varphi_i \varphi_j + \nu \Delta t \left(2 \frac{\partial \varphi_i}{\partial x} \frac{\partial \varphi_j}{\partial x} + \frac{\partial \varphi_i}{\partial y} \frac{\partial \varphi_j}{\partial y} \right) + \right. \right. \\
\left. \left. \frac{\Delta t}{2} \left(\sum_{k=1}^{N_h} u_{1,k}^n \frac{\partial \varphi_k}{\partial x} + \sum_{k=1}^{N_h} u_{2,k}^n \frac{\partial \varphi_k}{\partial y} \right) \varphi_i \varphi_j \right] \right]_{N_h \times N_h}$$

$$\begin{aligned}\mathbf{A}_2 &= [\mathbf{A}_{2ij}]_{N_h \times N_h} = \left[\int_{\Omega} \frac{\partial \varphi_i}{\partial x} \frac{\partial \varphi_j}{\partial y} \right]_{N_h \times N_h} \\ \mathbf{B}_x &= [\mathbf{B}_{xjk}]_{N_h \times m_h} = \left[- \int_{\Omega} \frac{\partial \varphi_j}{\partial x} \psi_k \right]_{N_h \times m_h} \\ \mathbf{B}_y &= [\mathbf{B}_{yjk}]_{N_h \times m_h} = \left[- \int_{\Omega} \frac{\partial \varphi_j}{\partial y} \psi_k \right]_{N_h \times m_h} \\ \mathbf{b}_i &= \left[\int_{\Omega} g_{i,j}^{n+1} \varphi_i \right]_{N_h \times 1}.\end{aligned}$$

We can write the above matricial equation in a more simple way

$$\begin{bmatrix} \mathbf{A} & \mathbf{B} \\ \mathbf{B}^t & 0 \end{bmatrix} \begin{bmatrix} \mathbf{u} \\ \mathbf{p} \end{bmatrix} = \begin{bmatrix} \mathbf{b} \\ 0 \end{bmatrix} \quad (4.34)$$

$$\text{with } \mathbf{A} = \begin{bmatrix} \mathbf{A}_1 & \mathbf{A}_2 \\ \mathbf{A}_2^t & \mathbf{A}_1 \end{bmatrix}, \mathbf{B} = \begin{bmatrix} \mathbf{B}^x \\ \mathbf{B}^y \end{bmatrix}, \mathbf{u} = \begin{bmatrix} \mathbf{u}_1 \\ \mathbf{u}_2 \end{bmatrix} \text{ and } \mathbf{b} = \begin{bmatrix} \mathbf{b}_1 \\ \mathbf{b}_2 \end{bmatrix}.$$

The matrix \mathbf{A} is symmetric positive definite over $\mathbb{R}^{N_h \times N_h}$ and the matrix \mathbf{B} is resulting from a linear injective form therefore the system (4.34) has an unique solution.

Introducing the space

$$\mathbf{V} = \{ \mathbf{v} \in \mathbb{R}^{N_h} : \mathbf{B}^t \mathbf{v} = 0 \} = Ker(\mathbf{B}^t) \quad (4.35)$$

we guarantee that the matrix \mathbf{V} is not singular, if $Ker(\mathbf{B}^t) = \{0\}$. In this case the compatibility condition (4.4) is satisfied. The details can be found in [13].

The solution can be evaluated using a direct method or iterative method applied to symmetric matrices as CG (conjugate gradient method). Details can be found in [28].

The solution of problem (4.25) is obtained by an iterative method in time

Initialization:

- Given : $\mathbf{u}^0 = \mathbf{u}_0$
- Define: $\Delta T = \frac{T}{N}$

Loop: for n from 0 to N

- Solve the system $\begin{bmatrix} \mathbf{A} & \mathbf{B} \\ \mathbf{B}^t & 0 \end{bmatrix} \begin{bmatrix} \mathbf{u} \\ \mathbf{p} \end{bmatrix} = \begin{bmatrix} \mathbf{b} \\ 0 \end{bmatrix}$ by the chosen method .
- $t = t + \Delta t$.

end of loop

We remind that \mathbf{b} depends on the solution at the previous moment through $\mathbf{u}(t^n, \chi(t^n; t^{n+1}, \mathbf{x}))$.

Chapter 5

Numerical results

This chapter is concerned with the application of Finite Element Methods to obtain solutions for unsteady Newtonian flows in different geometries.

All meshes and simulations were done in FreeFem++, a free software with its own high level programming language based on the Finite Element Method to solve partial differential equations.

FreeFem++ uses an automatic mesh generator based on Delaunay-Voronoi algorithm where the number of internal points are proportional to the number of points on the boundaries.

The graphics were generated by Mathematica and FreeFem++.

The calculation of $\mathbf{b}_i = \left[\int_{\Omega} g_{i,j}^{n+1} \varphi_i \right]_{N_h \times 1}$ of (4.34) needs to evaluate the numerical integration of the term

$$\int_{\Omega} \mathbf{u}_h^n \circ \chi^n(\mathbf{x}).$$

It requires knowledge of the value of $\mathbf{u}_h^n \circ \chi^n$ in some nodal points. This means that for any fixed node \mathbf{x}_k , it is necessary to know which triangle $K \in \mathcal{T}_h$ contains the point $\chi^n(\mathbf{x}_k)$. FreeFem++ solves this question. In FreeFem++ there exists an operator $\text{convect}([u_1, u_2], \Delta t, w)$ which computes $w \circ \chi_{\Delta t; 0}$ where $\chi_{\Delta t; 0}$ is the convect field defined by $\chi(\Delta t; 0, \mathbf{x})$ and where $\chi(\tau; 0, \mathbf{x})$ is particle path in the steady state velocity field $\mathbf{u} = [u_1, u_2]$ starting at point \mathbf{x} at time $\tau = 0$ (see section 4.3). When \mathbf{u} is piecewise constant, this is possible because $\chi(\Delta t; 0, \mathbf{x})$ is a polygonal curve which

can be computed exactly and the solution always exists when \mathbf{u} is divergence free. The comand *convect* returns

$$w(\chi(\Delta t; 0, \mathbf{x})).$$

5.1 Choice of solver and code validation

Towards the validation of the code, choosing solver and error analysis, we consider the Kim-Moin model problem with known exact solution given by

$$\mathbf{u}(t, \mathbf{x}) = \left(-\cos(2\pi x)\sin(2\pi y)e^{-8\pi^2\nu t}, \sin(2\pi x)\cos(2\pi y)e^{-8\pi^2\nu t} \right) \quad (5.1)$$

$$p(t, \mathbf{x}) = -\frac{1}{4} \left(\cos(4\pi x) + \cos(4\pi y)e^{-16\pi^2\nu t} \right) \quad (5.2)$$

The velocity and pressure field remain in space and decrease monolithically with time. The Kim-Moin model problem is solved on the unit square $\Omega = [0.25, 1.25] \times [0.5, 1.5]$ and prescribes the exact velocity according to (5.1) and (5.2) along the boundary of the fluid domain. The calculations have been performed with a kinematic viscosity of $\nu = 0.01$ which results the null external force.

The problem has been discretized in space with two meshes with 2048 and 8192 Hood-Taylor elements. For the coarse mesh we have 4225 nodes \mathbb{P}_2 for the velocity and 1089 nodes \mathbb{P}_1 for the pressure. For the finer mesh we have 16641 nodes \mathbb{P}_2 for the velocity and 4225 nodes \mathbb{P}_1 for the pressure.



Figure 5.1: *Structured meshes employed on square $[0.25, 1.25] \times [0.5, 1.50]$. The coarse mesh with 2048 elements (on the left) and the fine mesh with 8192 elements (on the right).*

The time interval $[0, 1]$ was discretized into subintervals, of equal amplitude $\Delta t = 2^{-k}$ with $k = 5, 6, 7, 8$, of type $[t^n, t^{n+1}]$ ($n = 0, \dots, 2^k - 1$). At each time instant $t^n = n\Delta t$ the numerical solution was determined, from the solution an instant before, to evaluate the term $\int_{\Omega} \nabla \cdot \mathbf{u}_h^n \mathbf{u}_h^{n+1} \cdot \mathbf{v}_h$ and the term $\int_{\Omega} \mathbf{u}_h^n \circ \chi^n(\mathbf{x})$ using the command `convect`.

We use a linear direct and an iterative solver available in FreeFem++:

- *Crout method* which is a direct method. It is a variant of the factorization method \mathbf{LU} where $\mathbf{U} = [u_{ij}]_{n \times n}$ is an upper triangular matrix with unitary diagonal and $\mathbf{L} = [l_{ij}]_{n \times n}$ matrix is a lower triangular, with its coefficients defined by

$$l_{ij} = a_{ij} - \sum_{k=1}^{j-1} l_{ik} u_{kj}, \quad j \leq i$$

$$u_{ij} = \frac{a_{ij} - \sum_{k=1}^{i-1} l_{ik} u_{kj}}{l_{ii}}, \quad j > i$$

being \mathbf{A} a nonsingular matrix, as well as the matrix \mathbf{L} and \mathbf{U} , in this way the diagonal elements are not null.

In this case, we can split the system $\mathbf{Ax} = \mathbf{b}$ into triangular systems of simpler resolution as follows

$$\mathbf{Ax} = \mathbf{b} \Leftrightarrow \mathbf{LUx} = \mathbf{b} \Leftrightarrow \begin{cases} \mathbf{Ly} = \mathbf{b} \\ \mathbf{Ux} = \mathbf{y} \end{cases}$$

- *Conjugate Gradient method (CG)* is an iterative method that applies to linear systems in which the matrix is symmetric positive definite. This method is normally used in large sparse matrices. This method can be described as follows [28]:

Initialization:

- Take a vector \mathbf{x}_0 be an approximate initial solution.
- Take a tolerance for error ε .

– Evaluate:

$$* \mathbf{r}_0 = \mathbf{b} - \mathbf{A}\mathbf{x}_0$$

$$* \mathbf{p}_0 = \mathbf{r}_0$$

– Take $k = 0$.

Loop: For $k = 1, \dots$, while $\|\mathbf{r}^{k+1}\| > \varepsilon \|\mathbf{r}^k\|$ do

$$- \alpha_k = \frac{\mathbf{r}_k^t \mathbf{r}_k}{\mathbf{p}_k^t \mathbf{A} \mathbf{p}_k}$$

$$- \mathbf{x}_{k+1} = \mathbf{x}_k + \alpha_k \mathbf{p}_k$$

$$- \mathbf{r}_{k+1} = \mathbf{r}_k - \alpha_k \mathbf{A} \mathbf{p}_k$$

$$- \beta_k = \frac{\mathbf{r}_{k+1}^t \mathbf{r}_{k+1}}{\mathbf{r}_k^t \mathbf{r}_k}$$

$$- \mathbf{p}_{k+1} = \mathbf{r}_{k+1} + \beta_k \mathbf{p}_k$$

End do.

5.1.1 Numerical Test

First test case: In this test case, we take the mesh with 2048 elements and $\Delta t = 2^{-k}$ with $k = 5, 6, 7, 8$ and solve the problem with Crout method. The figure 5.2 shows the errors of the fluid velocity field and the pressure for each instant of time evaluated in the L^2 -norm, i.e, $ev_{2048}(t^n) = \|\mathbf{u} - \mathbf{u}_h\|_{L^2(\Omega)} = \left(\sum_{i=1}^2 \int_{\Omega} (u_i - u_{h,i})^2 \right)^{1/2}$ and $ep_{2048}(t^n) = \|p - p_h\|_{L^2(\Omega)} = \left(\int_{\Omega} (p - p_h)^2 \right)^{1/2}$.

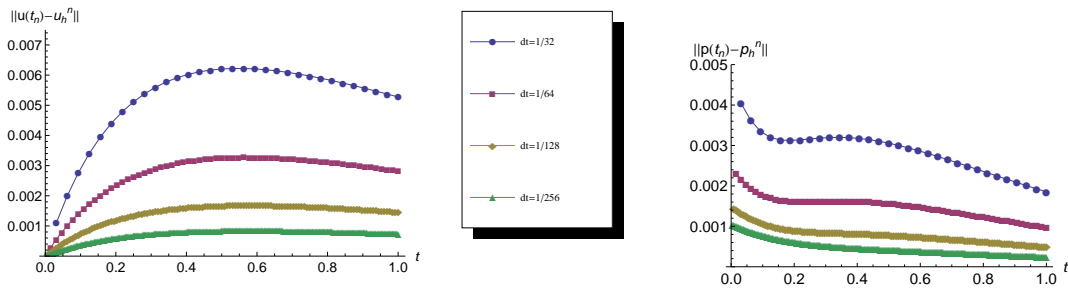


Figure 5.2: Error on the fluid velocity field (on the left) and the pressure (on the right) in L^2 -norm for each instant of time, for different Δt using a mesh with 2048 elements.

Second test case: In this test case, we take the mesh with 8192 elements and $\Delta t = 2^{-k}$ with $k = 5, 6, 7, 8$ and solve the problem with Crout method. The figure 5.3 shows the $ev_{8192}(t^n)$ and $ep_{8192}(t^n)$, the errors of the fluid velocity field and pressure respectively for each instant of time evaluated in the L^2 -norm.

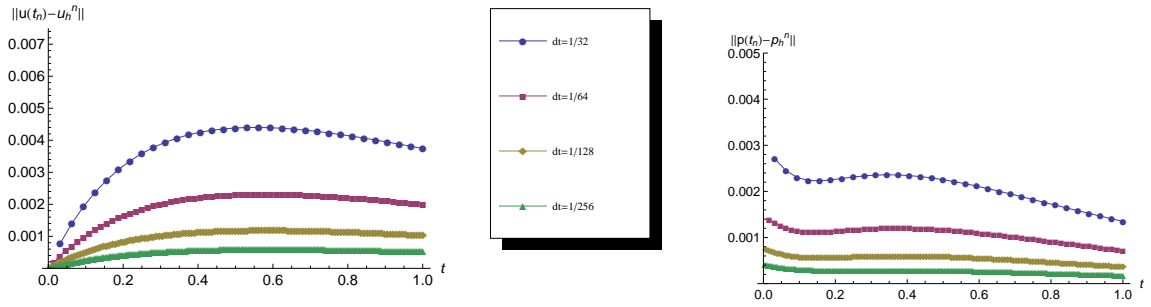


Figure 5.3: Error on the fluid velocity field (on the left) and the pressure (on the right) in L^2 -norm for each instant of time, for different Δt using a mesh with 8192 elements.

Comparison of both tests: Comparing the solutions computed by the two meshes for different time steps Δt , we notice that there is no remarkable difference between both solutions, although the L^2 error is decreasing which can be observed from the figure 5.2 and figure 5.3, which we can easily conclude from the figure 5.4. The figure 5.4 shows the error $ev_{2048}(1)$ and $ev_{8192}(1)$ of the fluid velocity field (on the left) and the error $ep_{2048}(1)$ and $ep_{8192}(1)$ of the pressure (on the right) for the instant of time $t = 1$ evaluated in the L^2 -norm.

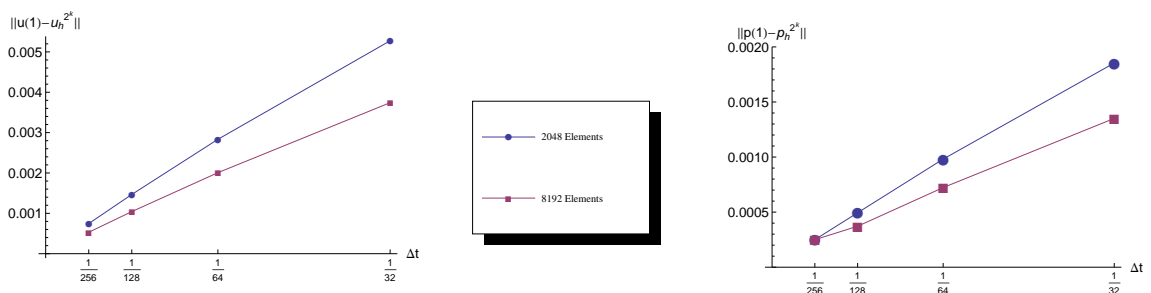


Figure 5.4: Comparison of errors of the fluid velocity field (on the left) and the pressure (on the right) in L^2 -norm for the instant of time $t = 1$, for different Δt using the both meshes.

Given the behavior of the error we can speculate that when $\Delta t \rightarrow 0$ we have $e_{2048}(1) \approx e_{8192}(1)$. Comparing the CPU time for each test, clearly the fine mesh demands for a large CPU time, for different time steps (figure 5.5). From the point of view of CPU time, it is better to employ a mesh less refined and a smaller Δt to achieve the same accuracy level.

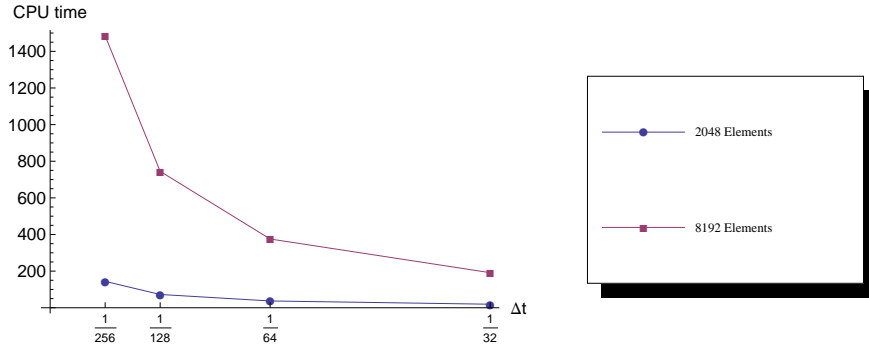


Figure 5.5: Comparison of CPU times used as a function of Δt in solving the problem by the method of Crout for the two meshes.

Third test case: In this test case, we take the mesh with 2048 elements and $\Delta t = 2^{-k}$ with $k = 5, 6, 7, 8$ and solve the problem with CG method. We compared the results with the first test. The figure 5.6 shows the comparison of errors of the fluid velocity field and pressure for each instant of time evaluated in the L^2 -norm, for the both methods: Crout and CG. It is evident that they present the same behavior and the same precision. The difference of error values between the Crout method and CG method are of the order 10^{-7} .

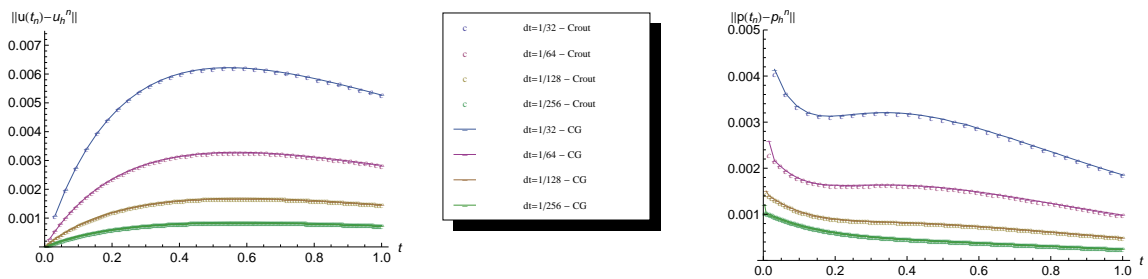


Figure 5.6: Comparison of errors of the fluid velocity field (on the left) and the pressure (on the right) in L^2 -norm for each instant of time, for different Δt using a mesh with 2048 elements, for both methods: Crout and CG.

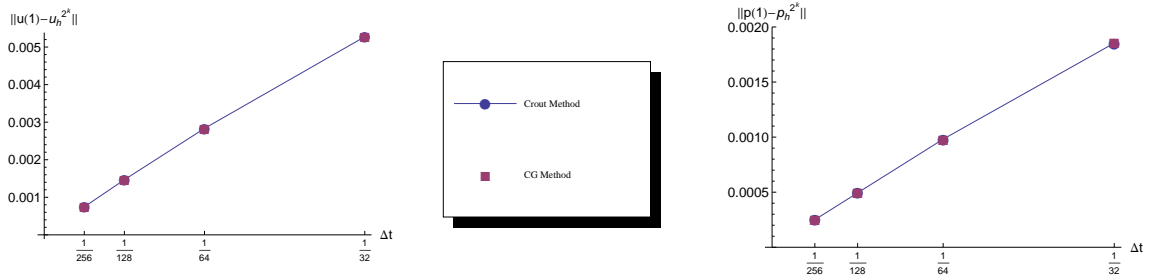


Figure 5.7: Comparison of errors of the fluid velocity field (on the left) and the pressure (on the right) in L^2 -norm for the instant of time $t = 1$, for different Δt using both methods.

As it was expected, by a-priori estimates for the error in time, we obtain a linear convergence in order to time (figure 5.7).

Fourth test case: In this test case, we take the mesh with 8192 elements and $\Delta t = 2^{-k}$ with $k = 5, 6, 7, 8$ and solve the problem with CG method. We compared the results with the third test. We notice that, also for this method, there is no remarkable difference between both solutions, although the error L^2 decreases. The figure 5.8 shows the comparison of errors of the fluid velocity field and pressure for each instant of time evaluated in the L^2 -norm, for the both methods (Crout and CG) with the same mesh. It is evident that they present the same behavior and the same precision. The difference of error values between the Crout method and CG method are of the order 10^{-7} .

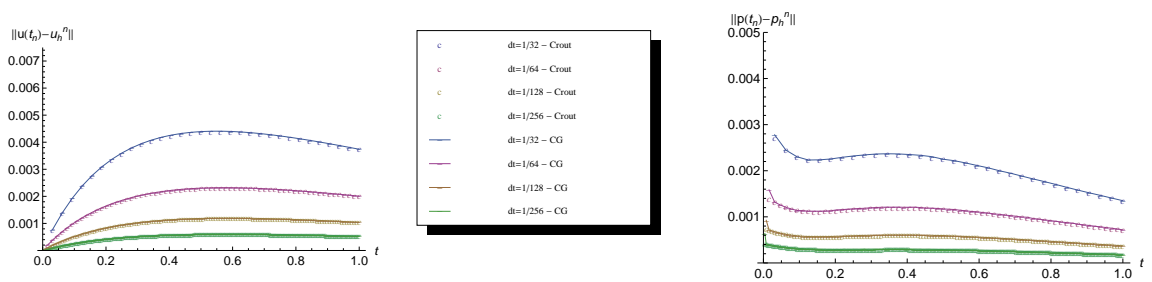


Figure 5.8: Comparison of errors of the fluid velocity field (on the left) and the pressure (on the right) in L^2 -norm for each instant of time, for different Δt using a mesh with 8192 elements, for both methods: Crout and CG.

Since both methods have the same accuracy, we have to decide which method to use based on CPU time. As we can see (figure 5.9), the method CG expends much CPU

time than the method Crout, in the case of mesh to be refined. In the case of less fine mesh, the time spent by the two methods are approximately equal, although in this case the Crout method is slightly faster (figure 5.10).

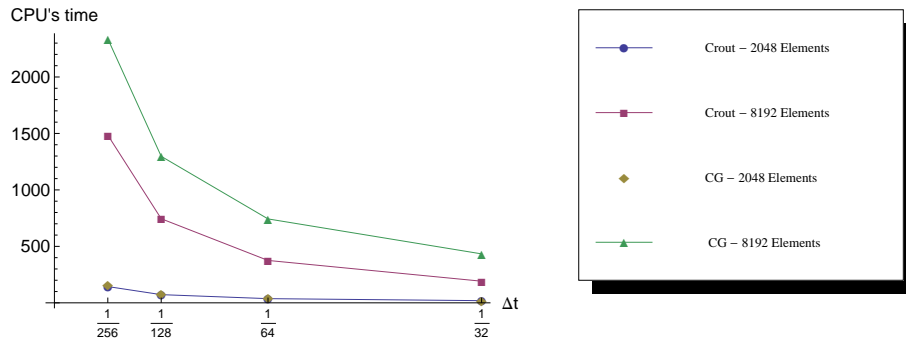


Figure 5.9: Comparison of CPU times used for the both methods, as a function of Δt , in solving the problem with the two meshes.

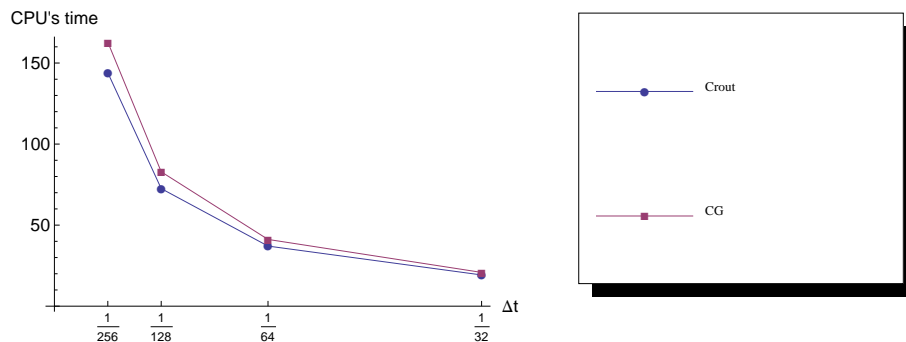
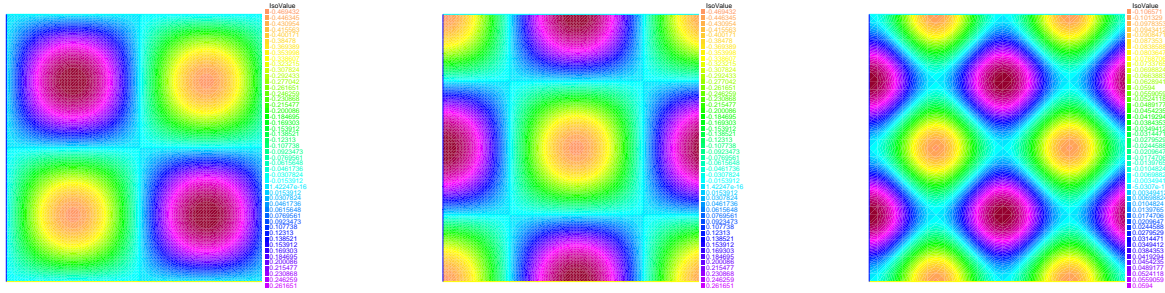


Figure 5.10: Comparison of CPU times used as a function of Δt in solving the problem by the both method for the two meshes.

In large sparse matrix, the Conjugate Gradient method should be more efficient than the method of Crout, but we don't know if the implementation of this solver is optimized. Given the previous study we choose to use the method of Crout.

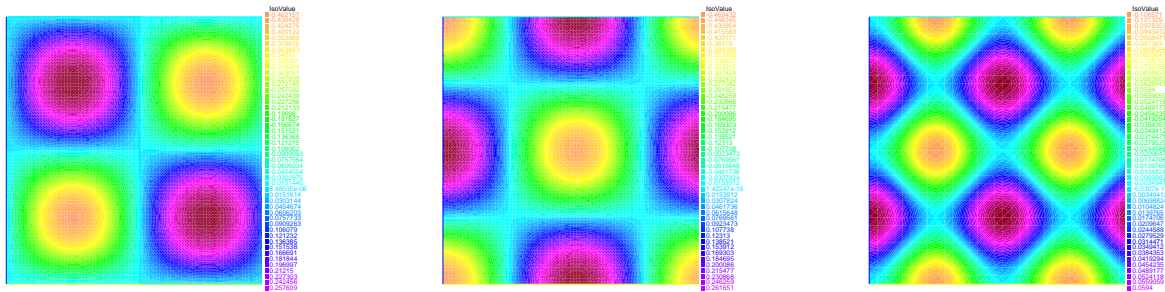
The following figures illustrate the exact solution and corresponding approximation obtained for a mesh with 2048 elements and $\Delta t = 1/128$ at time $t = 1$.



(a) $u(1,x,y) = -\cos(2\pi x)\sin(2\pi y)e^{-0.08\pi^2}$ (b) $v(1,x,y) = \sin(2\pi x)\cos(2\pi y)e^{-0.08\pi^2}$ (c)

$$p(1,x,t) = -\frac{1}{4}(\cos(4\pi x) + \cos(4\pi y))e^{-0.16\pi^2}$$

Figure 5.11: Exact solution at $t = 1$. First component of velocity (on the left), second component of velocity (on the center) and pressure (on the right).



(a) $u_h(1, x, y) \approx u(1, x, y)$ (b) $v_h(1, x, y) \approx v(1, x, y)$ (c) $p_h(1, x, y) \approx p(1, x, y)$

Figure 5.12: Approach solution at $t = 1$. First component of velocity (on the left), second component of velocity (on the center) and pressure (on the right).

5.2 Applications of Newtonian fluids model

From a wide range of applications of Newtonian fluids we can mention in particular the behavior of blood in large arteries, since blood can be considered an homogeneous and incompressible Newtonian fluid. For this reason we have chosen some fictitious geometries similar to existent in some areas of cardio-vascular system as well as geometries corresponding to pathological situations. To simulate blood flow in the cardiovascular system we would have to solve a problem of fluid structure interaction. Leaving it out of the scope of this work, it may be a future work to develop because matter of great interest in the timeliness and has great impact in medicine and because of the techniques of mathematical analysis, numerical analysis and scientific computing involves.

5.2.1 Mathematical model

With this aim we consider the fluid confined in a domain with upper and lower boundary as rigid walls denoted by Γ^w , an upstream section S_1 and downstream section S_2 through which the fluid enters and leaves Ω respectively. An inflow parabolic profile with respect to time is prescribed on upstream section, while on downstream section homogeneous Neumann conditions are assigned. S_1 and S_2 are fictitious boundaries, since the vascular system is closed and there is no such boundaries. We also assume that the flow tends smoothly to equilibrium as $t \rightarrow +\infty$, which mathematically translated by $\mathbf{f} = 0$.

Combined form of above boundary conditions can be provided as follows:

$$\begin{cases} \mathbf{u} = 0, & \text{on } \Gamma^w \\ \mathbf{T} \cdot \mathbf{n} = \sigma \mathbf{n} = -\frac{P_{in}}{2} [1 - \cos(\frac{\pi t}{2.5})] \mathbf{n} & \text{on } S_1 \\ \mathbf{T} \cdot \mathbf{n} = 0 & \text{on } S_2 \end{cases} \quad (5.3)$$

\mathbf{T} being the Cauchy stress tensor defined by (2.15). The first condition of (5.3) guarantees the perfect adherence of the fluid to the wall while the second stages of the fluid enters with a pressure given by $-\frac{P_{in}}{2} [1 - \cos(\frac{\pi t}{2.5})]$ and the last indicates that there is no normal reaction over the boundary.

We suppose that the fluid is initially at rest, although some time-varying transition should be expected before reaching the time-periodic regime, the main characteristics of the flow patterns are present even when starting the simulation from the at-rest state.

The input profile $\mathbf{T} \cdot \mathbf{n}$ on S_1 is shown in figure 5.13

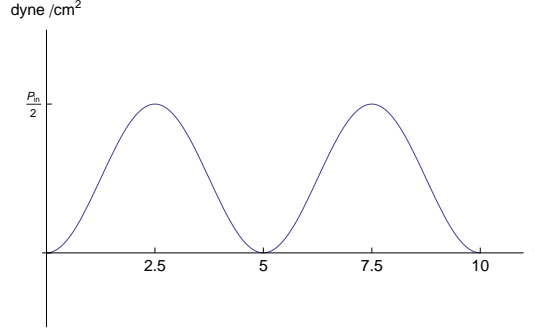


Figure 5.13: *The input profile of inflow Neumann boundary condition.*

For the sake of clarity we write the problem:

$$\left\{ \begin{array}{ll} \frac{\partial \mathbf{u}}{\partial t} + (\mathbf{u} \cdot \nabla) \mathbf{u} + \nabla p - 2\nu \nabla \cdot \mathbf{D}(\mathbf{u}) = 0, & \text{in } [0, T] \times \Omega \\ \nabla \cdot \mathbf{u} = 0, & \text{in } [0, T] \times \Omega \\ \mathbf{u} = 0, & \text{on } \Gamma^w \\ \mathbf{T} \cdot \mathbf{n} = -\frac{P_{in}}{2} [1 - \cos(\frac{\pi t}{2.5})] \mathbf{n} & \text{on } S_1 \\ \mathbf{T} \cdot \mathbf{n} = 0 & \text{on } S_2 \\ \mathbf{u}(t = 0, \mathbf{x}) = 0, & \forall \mathbf{x} \in \Omega \end{array} \right. \quad (5.4)$$

It is possible to prove (see [16]) that the solution of problem (5.4) exists and is unique for all $t \geq 0$.

5.2.2 Variational formulation

Taking the test function $\mathbf{v} \in \mathbf{V} = \{\mathbf{v} \in \mathbf{H}^1(\Omega) : \mathbf{v} = 0 \text{ on } \Gamma^w\}$ and applying the Green's formula results

$$\int_{\Omega} \frac{\partial \mathbf{u}}{\partial t} \cdot \mathbf{v} + \int_{\Omega} (\mathbf{u} \cdot \nabla) \mathbf{u} \cdot \mathbf{v} - \int_{\Omega} p \nabla \cdot \mathbf{v} + \int_{\Omega} 2\nu \mathbf{D}(\mathbf{u}) : \mathbf{D}(\mathbf{v}) - \int_{\partial \Omega} \mathbf{T} \cdot \mathbf{n} \cdot \mathbf{v} = 0 \Leftrightarrow \quad (5.5)$$

$$\Leftrightarrow \int_{\Omega} \frac{\partial \mathbf{u}}{\partial t} \cdot \mathbf{v} + \int_{\Omega} (\mathbf{u} \cdot \nabla) \mathbf{u} \cdot \mathbf{v} - \int_{\Omega} p \nabla \cdot \mathbf{v} + \int_{\Omega} 2\nu \mathbf{D}(\mathbf{u}) : \mathbf{D}(\mathbf{v}) - \int_{\partial\Omega} \mathbf{T} \cdot \mathbf{n} \cdot \mathbf{v} = 0 \Leftrightarrow \quad (5.6)$$

$$\Leftrightarrow \int_{\Omega} \frac{\partial \mathbf{u}}{\partial t} \cdot \mathbf{v} + \int_{\Omega} (\mathbf{u} \cdot \nabla) \mathbf{u} \cdot \mathbf{v} - \int_{\Omega} p \nabla \cdot \mathbf{v} + \int_{\Omega} 2\nu \mathbf{D}(\mathbf{u}) : \mathbf{D}(\mathbf{v}) = \int_{S_1} \sigma \mathbf{n} \cdot \mathbf{v} \quad (5.7)$$

So, the problem (5.4) admits discrete variational formulation:

Find $(\mathbf{u}, p) \in L^2(0, T; \mathbf{V}) \times L^2(0, T; Q)$, with $\mathbf{u}(0, \mathbf{x}) = 0, \forall \mathbf{x} \in \Omega$ such that:

$$\left\{ \begin{array}{l} \int_{\Omega} \frac{\partial \mathbf{u}}{\partial t} \cdot \mathbf{v} + \int_{\Omega} (\mathbf{u} \cdot \nabla) \mathbf{u} \cdot \mathbf{v} - \int_{\Omega} p \nabla \cdot \mathbf{v} + \int_{\Omega} 2\nu \mathbf{D}(\mathbf{u}) : \mathbf{D}(\mathbf{v}) = \int_{S_1} \sigma \mathbf{n} \cdot \mathbf{v}, \quad \forall \mathbf{v} \in \mathbf{V} \\ \int_{\Omega} \mathbf{u} \cdot \mathbf{q} = 0 \quad \forall \mathbf{q} \in Q \end{array} \right. \quad (5.8)$$

5.2.3 Discretized problem

Applying the arguments used in the section 4.2 and in the section 4.3, and using the spaces \mathbf{V}_h^0 and M_h defined by (4.28) and (4.29), respectively, we obtain the following discretized problem:

for each $t^{n+1} \in [0, T]$, find $(\mathbf{u}_h^{n+1}, p_h^{n+1}) \in \mathbf{V}_h^0 \times M_h$ such that

$$\left\{ \begin{array}{l} \int_{\Omega} \mathbf{u}_h^{n+1} \cdot \mathbf{v}_h - \Delta t \int_{\Omega} p_h^{n+1} \nabla \cdot \mathbf{v}_h + 2\nu \Delta t \int_{\Omega} \mathbf{D}(\mathbf{u}_h^{n+1}) : \mathbf{D}(\mathbf{v}_h) + \frac{\Delta t}{2} \int_{\Omega} (\nabla \cdot \mathbf{u}_h^n) \mathbf{u}_h^{n+1} \cdot \mathbf{v}_h = \\ \quad = \int_{S_1} -\frac{P_{in}}{2} \left[1 - \cos \left(\frac{\pi t}{2.5} \right) \right] \cdot \mathbf{n} \cdot \mathbf{v}_h, \quad \forall \mathbf{v}_h \in \mathbf{V}_h^0 \\ \int_{\Omega} \mathbf{u}_h^{n+1} \cdot \mathbf{q}_h = 0, \quad \forall \mathbf{q}_h \in M_h \\ \mathbf{u}_h(0) = 0 \quad \text{on } \Gamma^w \end{array} \right. \quad (5.9)$$

Given Δt , for each $t^{n+1} = (n+1)\Delta t$, ($n = 0, \dots, T/\Delta t$), we take $u_{1,h}^{n+1}$, $u_{2,h}^{n+1}$ and p_h^{n+1} as (4.31), we obtain a system as (4.34) with

$$\mathbf{b}_1 = \left[\int_{S_1} -\frac{P_{in}}{2} \left[1 - \cos \left(\frac{\pi t^{n+1}}{2.5ms} \right) \right] \cdot \mathbf{n} \cdot \varphi_i \right]_{N_h \times 1}$$

5.2.4 Stream function

In bidimensional case, we can use the continuity equation

$$\nabla \cdot \mathbf{u} = \frac{\partial u_1}{\partial x} + \frac{\partial u_2}{\partial y} = 0$$

to introduce a stream function ψ such that

$$\frac{\partial \psi}{\partial x} = -u_2, \quad \frac{\partial \psi}{\partial y} = u_1. \quad (5.10)$$

Setting the stream function equal to a constant defines a streamline in the flow. The streamline is a curve formed by the velocity vectors of each fluid particle at a certain time. In other words, it is the curve where the tangent at each point indicates the direction of flow at that point.

The numerical value of the stream function on a given streamline has no meaning by itself, the difference in the stream function values on different streamlines, $\psi_2 - \psi_1$, represents the volume flow rate per unit time crossing the surface defined by the path connecting a point A over $\psi_1 = \psi$ and B over $\psi_2 = \psi + d\psi$, i.e.,

$$DQ = u_1 dy - u_2 dx = \frac{\partial \psi}{\partial y} dy + \frac{\partial \psi}{\partial x} dx = d\psi.$$

The volume flow rate Q of fluid flowing between two streamlines ψ_1 and ψ_2 is given by

$$Q = \int dQ = \int_{\psi_1}^{\psi_2} d\psi = \psi_2 - \psi_1 \quad (5.11)$$

One consequence of this observation is that when adjacent streamlines are closer to each other the average fluid velocity is larger. If adjacent streamlines diverge from one another, the average velocity is smaller. By plotting a family of streamlines, we

create a flow visualization that immediately tells us how fast the fluid is moving at different points.

5.2.5 Flow in a straight pipe

We simulate the flow in a straight pipe whose boundary is made up of two rigid wall. This simulations would represent the propagation of a Newtonian fluid in a straight pipe of length $L = 6$ by imposition of two fictitious borders $S_1 = \{0\} \times [0, 1]$ and $S_2 = \{6\} \times [0, 1]$ with a pulsatile pressure type on inlet $\frac{P_{in}}{2} [1 - \cos(\frac{\pi t}{2.5})]$. With this aim, we have taken the 2D rectangle $\Omega = [0, 6] \times [0, 1]$, and solved the problem with the Crout method on a structured mesh of 1200 elements, with 2541 nodes \mathbb{P}_2 for the velocity and 671 nodes \mathbb{P}_1 for the pressure (Figure 5.14).

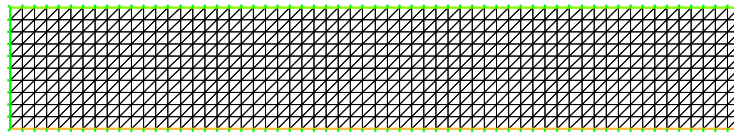


Figure 5.14: *Structured mesh employed, in a straight pipe.*

We take a step time $\Delta t = 0.01 \text{ ms}$ and the interval of time $[0, 10 \text{ ms}]$; a kinematic viscosity $\nu = 1 \text{ poise}$ and $P_{in} = 20000 \text{ dynes/cm}^2$.

The figure 5.15 shows the qualitative behavior of normal and tangential velocity and pressure inside the pipe.

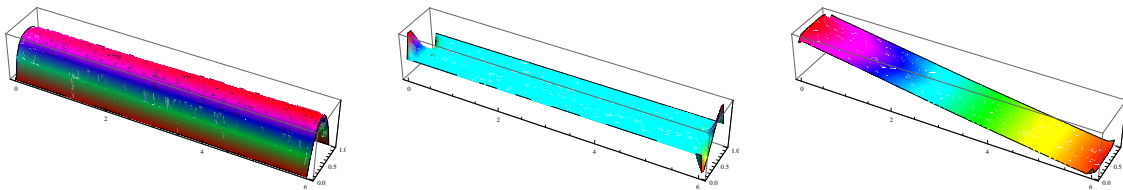


Figure 5.15: *Qualitative behavior of normal velocity (on the left), of tangential velocity (on the center) and pressure (on the right), in a straight pipe.*

The normal velocity increases from the walls until the center, from inlet to outlet (figure 5.16 - column at the left), along the pipe, symmetrically relative to the longi-

tudinal axis as a consequence of the propagation of the impulse of the pressure within the pipe. In tangential velocity we can identify an antisymmetrical behavior with respect to the longitudinal axis of symmetry of the pipe.

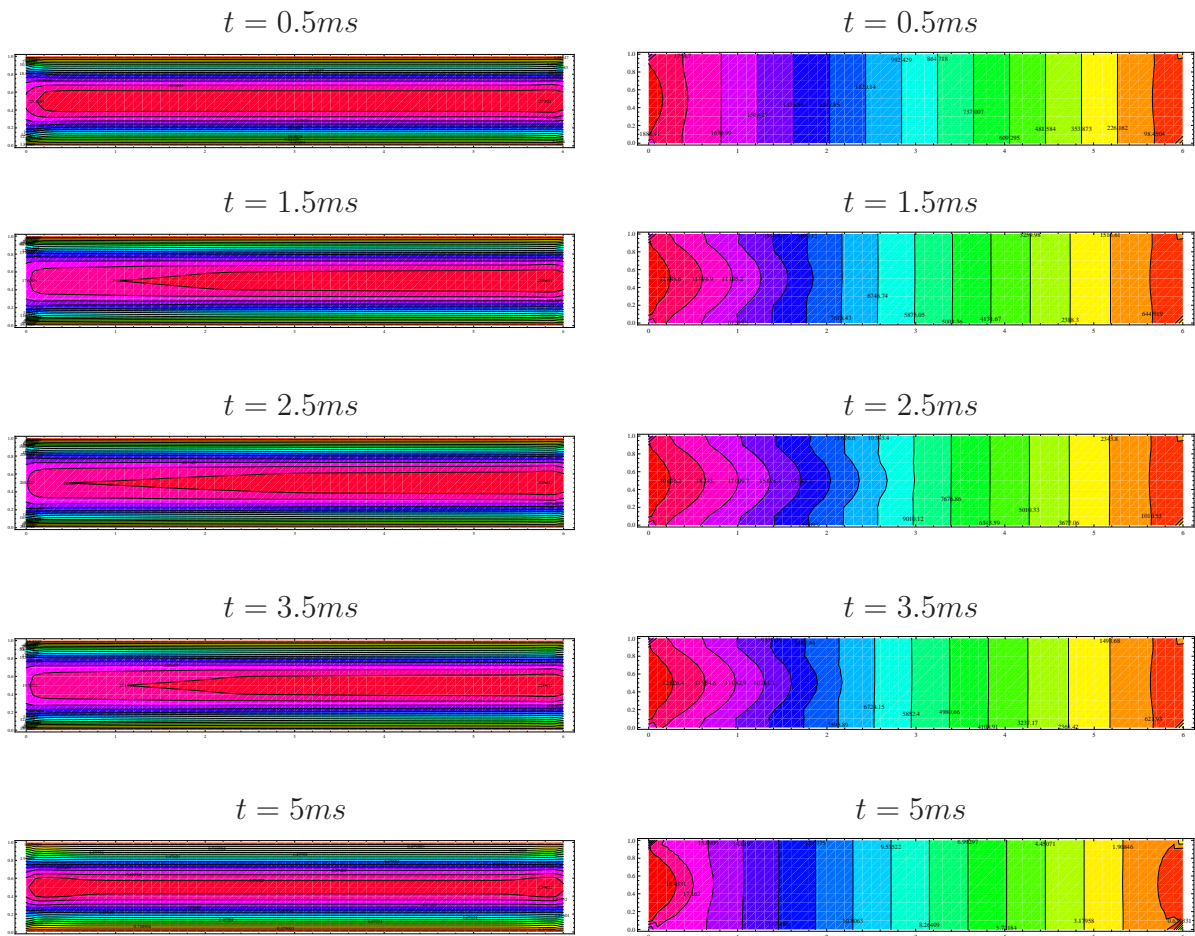


Figure 5.16: Contour plots of u_1 (on the left) and of pressure (on the right) at different instants of time, in a straight pipe.

The following plots show the action of each component of velocity over the displacement of the fluid. Both lead the fluid into the center of the pipe and towards the downstream.

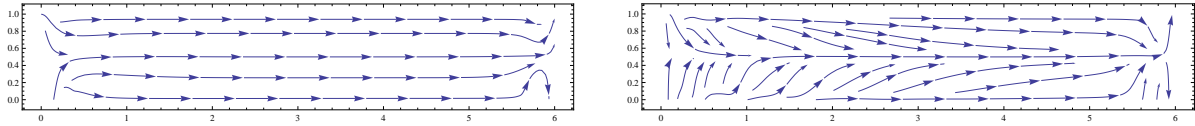


Figure 5.17: *The representative vectorial field of each component of velocity, in a straight pipe.*

These behaviors are visible at any instant of time. However the maximum magnitude is reached at time $t = 2.5 \text{ ms}$ and $t = 7.5 \text{ ms}$ corresponding to the maximum value of the pressure at the inlet tube, and the minimum value of the magnitude of the normal speed occurs at instant times $t = 5 \text{ ms}$ and $t = 10 \text{ ms}$, which is when the inlet pressure is zero. In fact, the magnitude of normal velocity have the same sinusoidal behavior of inflow (figure 5.18).

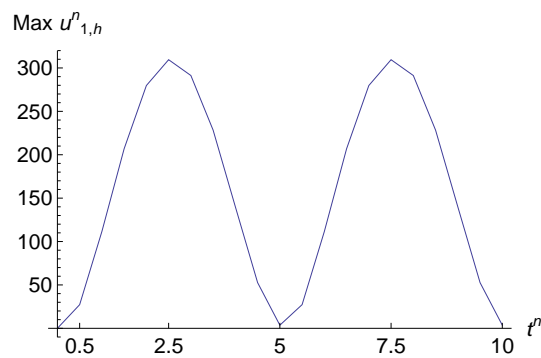


Figure 5.18: *Variation of magnitude of the normal velocity in function of time, in a straight pipe.*

We can observe a propagation of pressure along the pipe. The increase and decrease of parabolic profile is directly related with the increase and decrease of inlet impulse (Figure 5.16 - column at the right).

The pressure varies on inlet keeping constant over time at the outlet. This means that the wave of inlet impulse is not strong enough to travel until the end of pipe, finishing by dissipate.

The whole flow pattern is shown in figure 5.19 as instantaneous streamlines and the velocity vector plots. The behavior is the same along the time. We can observe an unidirectional flow laminar type (flow where there is a minimum of agitation of

the fluid layers). For each time, we can observe the adjacent streamlines are equally distant which suggests a constant average speed and constant volume flow rate.

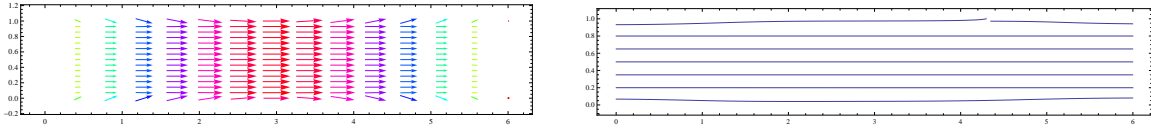


Figure 5.19: *The representative vector plot (on the left) and the streamlines (on the right), in a straight pipe.*

To confirm that, we computed the volume flux of fluid crossing a vertical line S_i of the mesh, corresponding to the position $x_i = ih$, $i = 0, \dots, 60$ and $h = 0.1\text{cm}$, on the axis, i.e.,

$$\mathcal{Q}^n(x_i) = \int_{S_i} \mathbf{u}_h^n \cdot \mathbf{n} dy = \int_{S_i} u_{1,h}^n dy \quad (5.12)$$

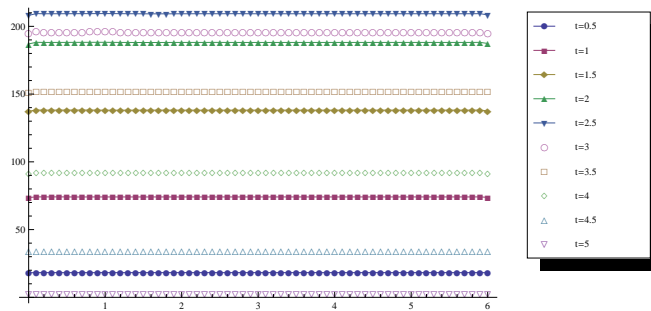


Figure 5.20: *The volume flux of fluid $\mathcal{Q}^n(x_i)$, at different times, in a straight pipe.*

The behavior of velocity and pressure at $t \in [5\text{ms}, 10\text{ms}]$ repeats comparatively to the qualitative behavior at $t \in [0\text{ms}, 5\text{ms}]$

5.2.6 Flow in a deformed pipe

In this subsection we choose a pipe with deformation on the upper wall as analogy of the pathological situations in cardio vascular system. To simulate an abnormal narrowing of a blood vessel, usually called stenosis, we define the upper wall with a concave deformation. To simulate a dilation of the vascular wall, designated as aneurysm, we define a convex deformation on the upper wall.

Concave deformation of the upper wall

We take a pipe with a concave deformation of the top wall. We consider the kinematic viscosity $\nu = 1$ and the same time step $\Delta t = 0.01ms$. The mesh is unstructured of diameter $h = 0.160605\text{ cm}$, being $h_{min} = 0.0554262\text{ cm}$ the diameter of the smallest element. The mesh is formed by 1948 elements with 1070 nodes \mathbb{P}_1 and 2679 nodes \mathbb{P}_2 .

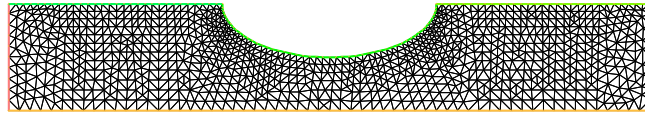


Figure 5.21: *Unstructured mesh employed, in a pipe with concave deformation of the upper wall.*

The figures below shows the normal and tangential velocity (cm/s) at three instants of time significant for their behaviors close to the stenosis.

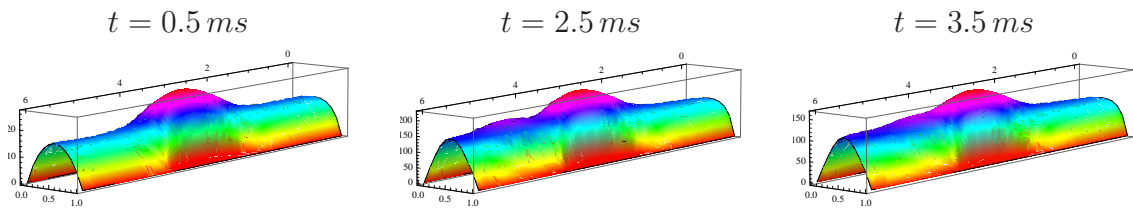


Figure 5.22: *Normal velocity at different instants of time, in a pipe with concave deformation of the upper wall.*

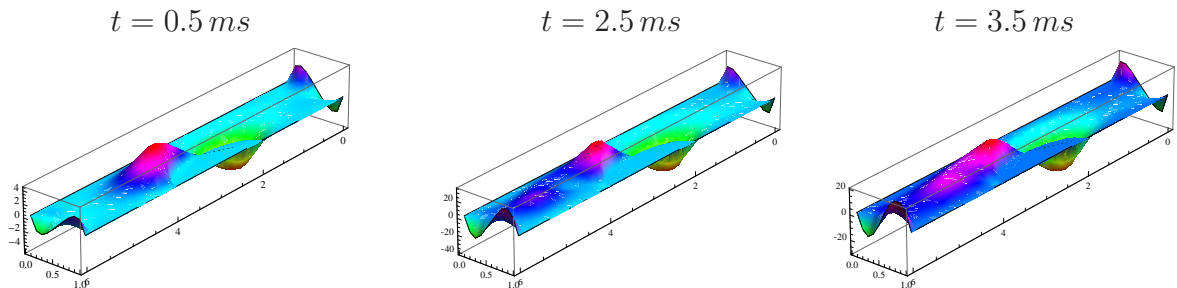


Figure 5.23: *Tangential velocity at different instants of time, in a pipe with concave deformation of the upper wall.*

Observe that the tangential velocity has an antisymmetric behavior relatively to the axis of symmetry of stenosis. The minimum values are reached at the first half of the narrowing and the maximum values are reaching in the other half part. The following plots shows the action of each component of velocity over the displacement of the fluid. While the normal velocity pushes the fluid against the upper wall slightly towards the downstream, the tangential velocity has the opposite behavior in the first half of the pipe and then reversing their action.

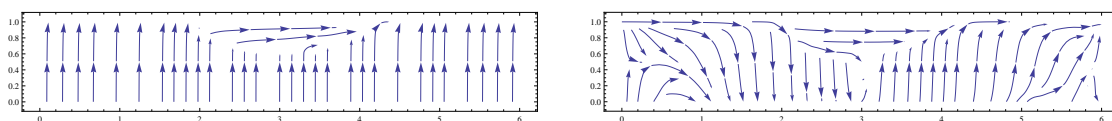


Figure 5.24: *The representative vectorial field of each component of velocity, in a pipe with concave deformation of the upper wall.*

The pressure decreases abruptly on stenosis.

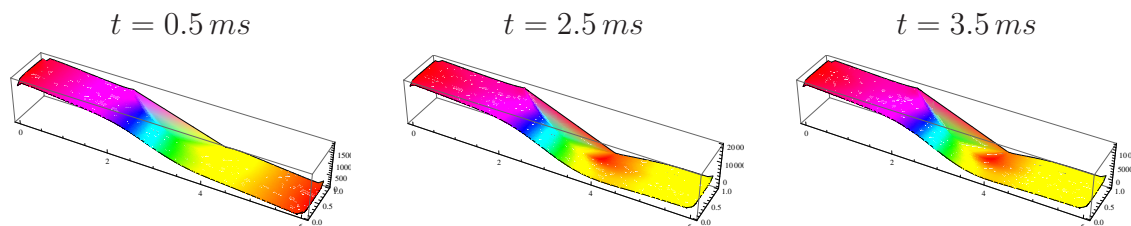


Figure 5.25: *Pressure at different instants of time, in a pipe with concave deformation of the upper wall.*

We computed the averaged quantities on each vertical line S_i of the mesh, corresponding to the position $x_i = ih$, $i = 0, \dots, 60$ and $h = 0.1cm$, on the axis. In particular, we computed the diameter of the pipe and the averaged pressure at each time:

$$\mathcal{A}(x_i) = meas(S_i) \quad \bar{p}^n(x_i) = \frac{1}{\mathcal{A}(x_i)} \int_{S_i} p_h^n dy$$

The figure 5.26 shows the averaged pressure at different instants. It is clear from this plot that the propagating inlet impulse is associated to this quantities.

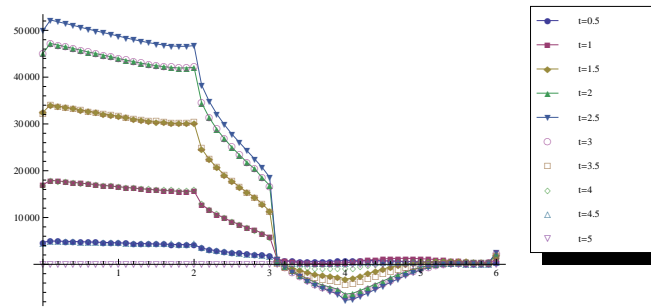


Figure 5.26: The average pressure of fluid $\bar{p}^n(x_i)$, at different times, in a pipe with concave deformation of the upper wall.

As in the case of a straight tube the magnitude of the velocity also increases with increase in the input pulse. Values vary significantly with the distance in area of stenosis and also in time during the period of the inlet impulse. It reaches the maximum value in narrowing at the same time as maximum of inlet impulse occurs (see streamlines - figure 5.27). The minimum value is reached behind the stenosis.

As can be observed in the vector field in the corners of the stenosis exerts some tension, which being much higher at the right where a recirculation arises and it increases with the growth of inlet impulse and decreases as the input pulse reduces.

The proximity of streamlines inside the stenosis indicate the increase of average velocity, as we refer before, and the decrease of volume flux as we can confirm with the figure 5.28.

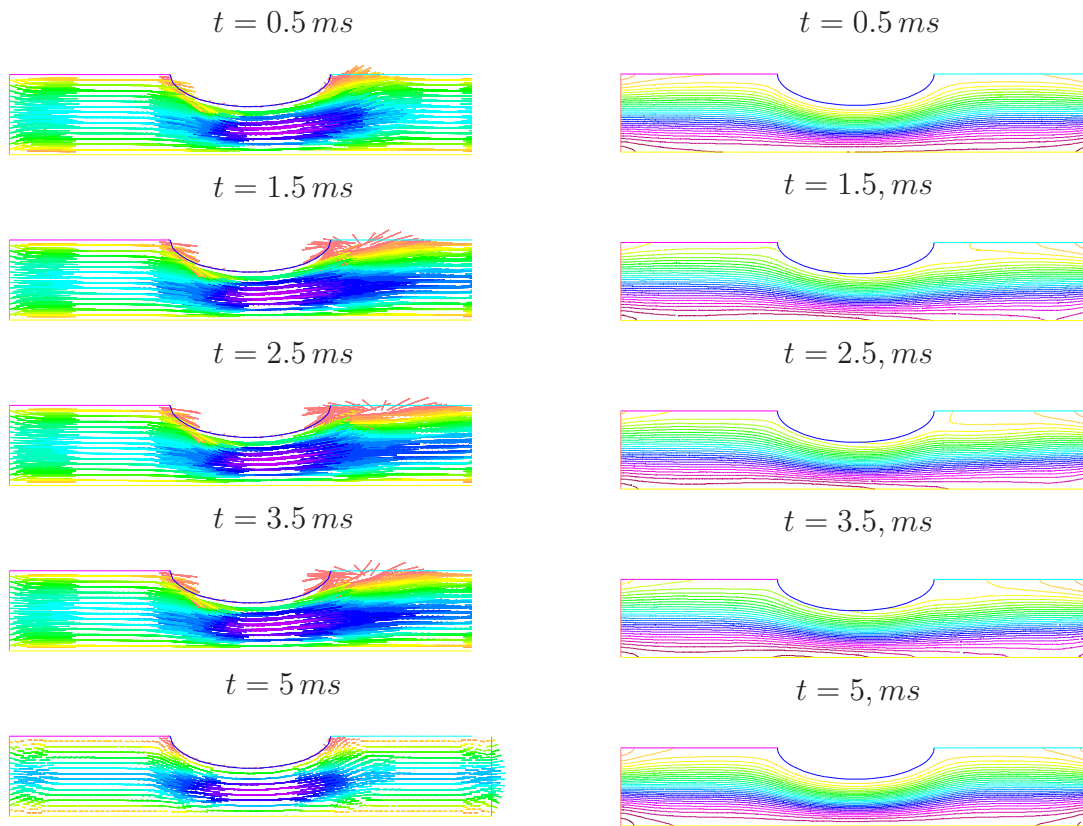


Figure 5.27: The whole flow pattern: velocity vector plots and streamlines at five different times, in a pipe with concave deformation of the upper wall.

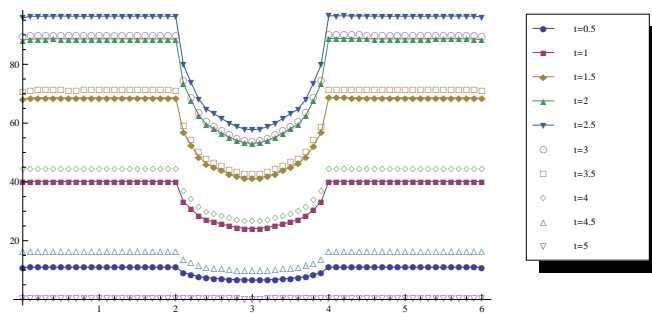


Figure 5.28: The volume flux of fluid $Q^n(x_i)$, at different times, in a pipe with concave deformation of the upper wall.

Convex deformation of the upper wall

We take a pipe with a convex deformation of the top wall. We consider the kinematic viscosity $\nu = 1$ and the time step $\Delta t = 0.01ms$, as before. The mesh is unstructured with diameter $h = 0.153968\text{ cm}$, being $h_{min} = 0.0664441\text{ cm}$ the diameter of the smallest element. The mesh is formed by 1582 elements with 867 nodes \mathbb{P}_1 and 3315 nodes \mathbb{P}_2 .

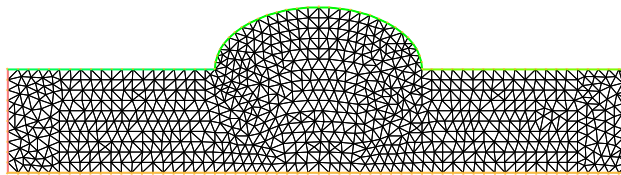


Figure 5.29: *Unstructured mesh employed, in a pipe with convex deformation of the upper wall.*

Here we observe two distinct flows. One inside the dilatation part and other in the straight pipe. Inside the aneurysm we observed the formation of recirculation of flow. As we can see from the vector plots, there is a big tension on the wall due to the deceleration of the local velocity. This recirculation does not travel out of the bulged region, it remains within the aneurysm. This recirculation increases with the inlet impulse and the center of vortex moves to the center of dilation for decreasing its intensity and vanishes remaining inverse flows when the inlet impulse weakens.

For other way the flow in the pipe has minimum of agitation. It is laminar type. The magnitude of velocity decreases in pipe in the area of the aneurysm.

From the streamlines we observe the waves of inlet impulse. In the zone of dilation the streamlines are spaced, which allows us to conclude that a decrease average speed and an increasing volume flux in this place, as we can see in figure 5.31.

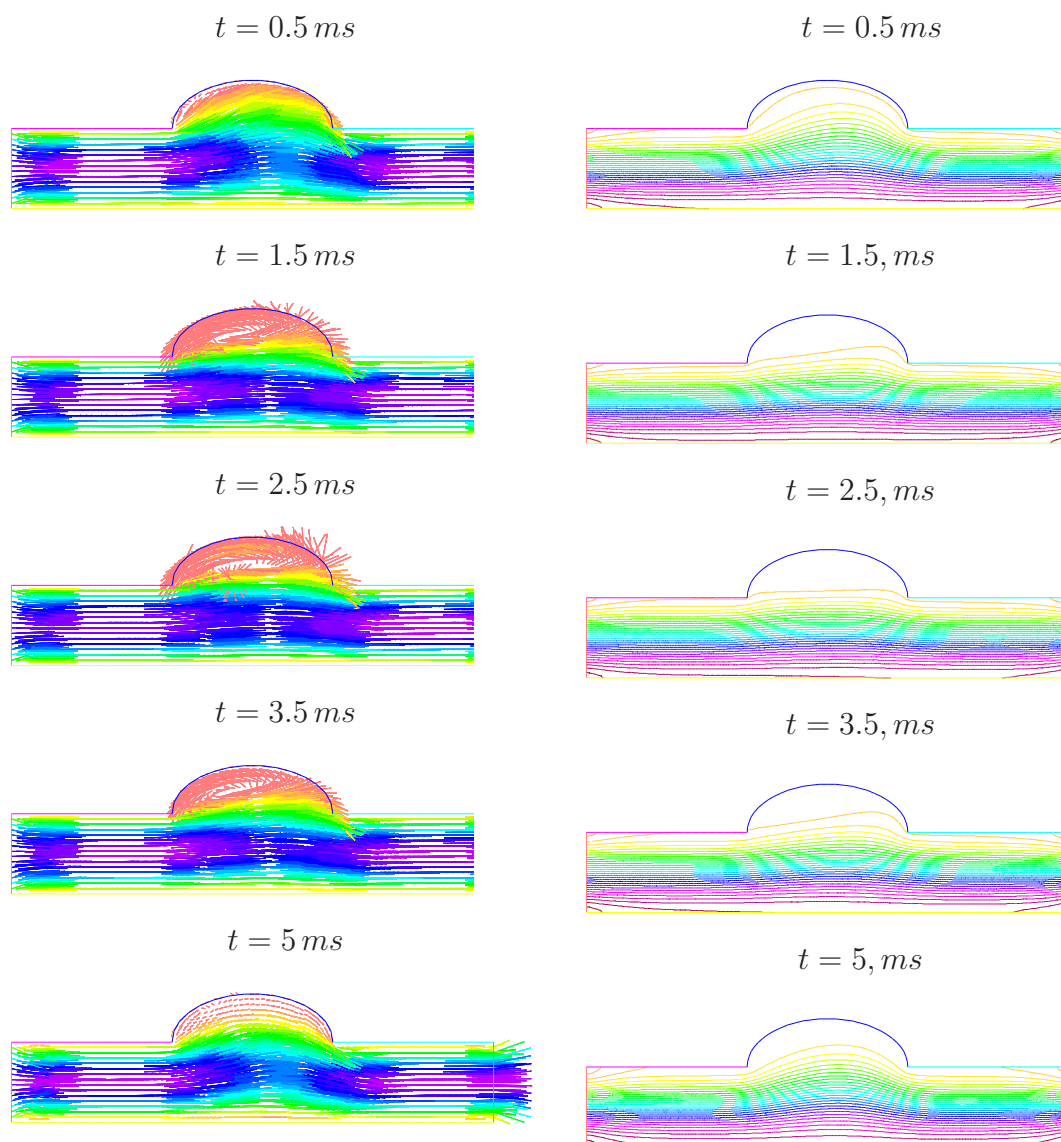


Figure 5.30: *The whole flow pattern: velocity vector plots and streamlines at five different times, in a pipe with convex deformation of the upper wall.*

The behavior of components of velocity and pressure are qualitatively the same along the time. The normal velocity is lower in the region of dilation. We continue to observe antisymmetric behavior of the tangential velocity, this time, in relation to the axis of symmetry of zone rounded, assuming the maximum value before of deformation contrary to what happens with the narrowing of the field (deformation concave).

The following plots show the action of each component of velocity over the displacement of the fluid. While the normal velocity pushes the fluid against the upper wall,

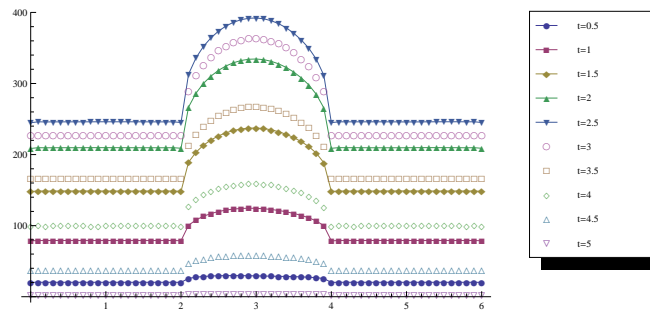


Figure 5.31: The volume flux of fluid $Q^n(x_i)$, at different times, in a pipe with convex deformation of the upper wall.

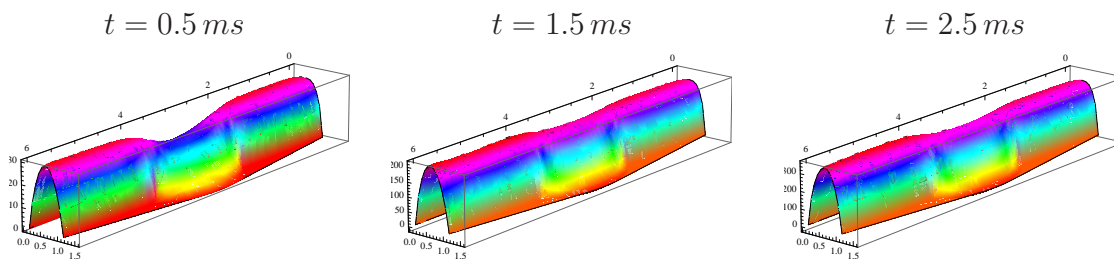


Figure 5.32: Normal velocity at different instants of time, in a pipe with convex deformation of the upper wall.

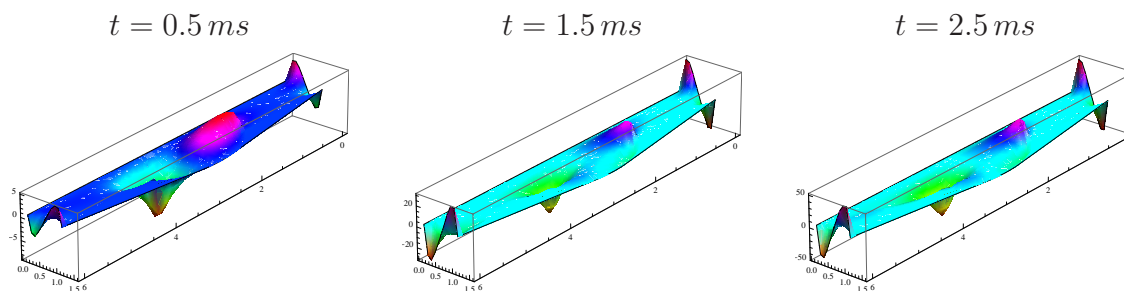


Figure 5.33: Tangential velocity at different instants of time, in a pipe with convex deformation of the upper wall.

the tangential velocity has four distinct actions. First pushes the fluid to the center of the pipe to then pushes in the direction of expansion. Within the aneurysm pushes out the fluid after and then it transports down to the outlet.

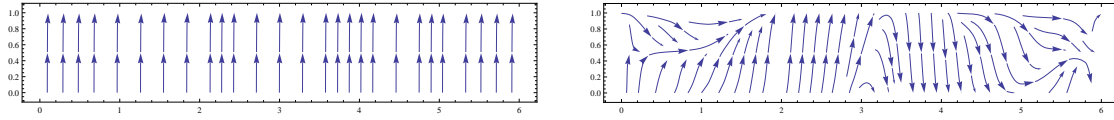


Figure 5.34: *The representative vectorial field of each component of velocity, in a pipe with convex deformation of the upper wall.*

The magnitude of the pressure varies according to the variation of the input pulse, decreasing from upstream to downstream, remaining virtually unchanged at the end of the tube.

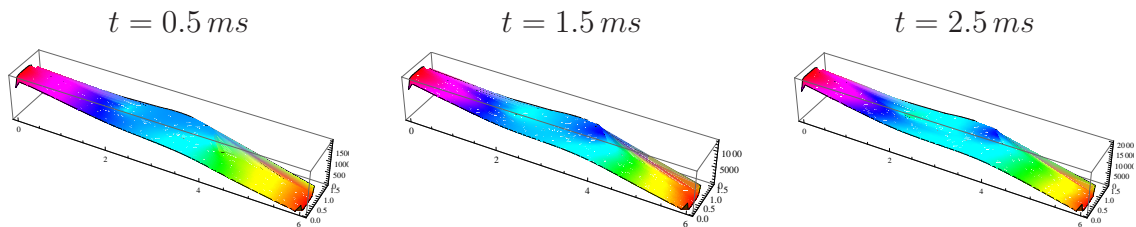


Figure 5.35: *Pressure at different instants of time, in a pipe with convex deformation of the upper wall.*

We can better verify this behavior taking into account the variation of the average pressure along the tube.

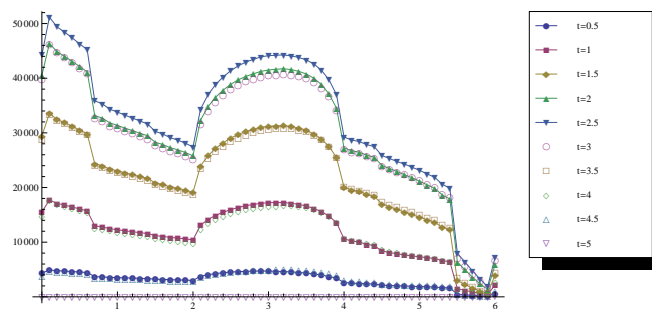


Figure 5.36: *The average pressure of fluid $\bar{p}^n(x_i)$, at different times, in a pipe with convex deformation of the upper wall.*

Chapter 6

Conclusions

The objective of this dissertation was the analysis and numerical approximation of the nonstationary problem that models the motion of incompressible Newtonian fluids in different geometries. We present results of existence and uniqueness of solution both for continuous problem and approximate problem. We also deduced energy estimates for both problems. We present estimates of the a-priori error. The numerical simulations to these problems were obtained computationally, by implementing the Finite Element Method. The method Hood-Taylor was applied to the unsteady Navier Stokes equations, and the corresponding linear system was solved by the direct method of Crout. For this problem, we approach the evolution in time of the solution, following the method of Characteristics Galerkin. The choice of solver and validation of the numerical method was made by considering the problem of Kim-Moin in square domain $\Omega = [0.25, 1.25] \times [0.5, 1.5]$ for which it was considered for a refine mesh and a coarse mesh with several times steps. We compared the results obtained by Crout method and Conjugate Gradient method taking into account errors analysis and the CPU time.

With a view to possible future work, we made an approach of modeling of blood flow with an unsteady Navier-Stokes problem with a pulsatile flow, in different geometries for which we can establish analogy with existing cardio vascular systems. The boundary conditions considered attempted to describe the conditions in the model of blood flow.

By comparing the simulations results from their velocity, velocity vectors, pressure, streamlines and volume flux many differences can be noted due to geometry of the domain.

The type of Newtonian fluid flow is dependent on the geometry.

Bibliography

- [1] R.A. Adams, *Sobolev Spaces*, Academic Press, New York (1975).
- [2] E. Becker, G. Carey and J. Oden, *Finite Elements. An Introduction. Vol.1*, Prentice Hall, Inc., Englewood Cliffs, New Jersey (1981).
- [3] S.Brenner and L. R. Scott, *The Mathematical Theory of Finite Element Methods*, Springer-Verlag, New York (1994).
- [4] H. Brézis, *Analyse fonctionnelle*, Masson (1983).
- [5] H. Brézis, *Functional Analysis Sobolev Spaces and Partial Differential Equations*, Springer (2011).
- [6] G. F. Carey and J.T. Oden, *Finite elements. Vol. VI. Fluid mechanics.*, The Texas Finite Element Series, VI. Prentice Hall, Inc., Englewood Cliffs, New Jersey (1986).
- [7] P. G. Ciarlet, *Mathematical Elasticity: Three-dimensional elasticity, Vol. 1* Springer-Verlag, North-Holland (1988).
- [8] A. J. Chorin and J. E. Marsden, *A Mathematical Introduction to Fluid Mechanics* 3ed., Springer (2000).
- [9] C. R. Doering and J. D. Gibbon, *Applied analysis of the Navier-Stokes equations*, Cambridge University Press, (1995).
- [10] G. Duvaut, *Mécanique des Milieux Continus*, Masson (1990).

-
- [11] G. P. Galdi, *An Introduction to the Mathematical Theory of the Navier-Stokes Equations: Linearized Steady Problems*, Springer Tracts in Natural Philosophy, Vol. 38, Springer, New York (1994).
- [12] G. P. Galdi, *An Introduction to the Mathematical Theory of the Navier-Stokes Equations: Nonlinear Steady Problems*, Springer Tracts in Natural Philosophy, Vol. 38, Springer, New York (1994).
- [13] V. Girault and P. A. Raviart, *Finite Element Approximation of the Navier-Stokes Equations*, Lecture Notes in Math., 749, Springer-Verlag, Berlin (1979).
- [14] R. Glowinski, *Numerical Methods for Nonlinear Variational Problems*, Springer (2008)
- [15] M. Griebel, T. Neunhoeffler and H. Regler *Algebraic multigrid methods for the solution of the NavierStokes equations in complicated geometries*, International Journal for Numerical Methods in Fluids, Vol. 26, Issue 3, 281301, 1998.
- [16] J. Heywood, R. Rannacher and S. Turek *Artificial Boundaries and flux and Pressure Conditions for Incompressible Navier-Stokes Equations*, International Journal for Numerical Methods in Fluids 22: 325–352 (1996).
- [17] J. Iannelli, *Characteristics Finite Element Methods in Computational Fluid Dynamics*, Springer (2006).
- [18] C. Johnson, *Numerical Solutions of Partial Differential Equations by the Finite Element Method*, Cambridge University Press (1987).
- [19] B. Lucquin and O. Pironneau, *Introduction au Calcul Scientifique*, Masson (1996).
- [20] M. Marion and R. Temam, *Navier-Stokes Equations: Theory and Approximation*, Handbook of Numerical Analysis, Vol. VI, P.G. Ciarlet and J.L. Lions(ed), Elsevier Science B.V. (1998)
- [21] Y. Nakayama, R.F. Boucher, *Introduction to Fluid Mechanics*, Butterworth-Heinemann (2000).

- [22] M. A. Olshanskii, *A low order Galerkin finite element method for the Navier-Stokes equations of steady incompressible flow: a stabilization issue and iterative methods*, Comput. Methods Appl. Mech. Engrg. 191, 55155536, 2002.
- [23] R. Owens and T.N. Phillips, *Computational Rheology*, Imperial College Press, London (2002).
- [24] A. Quarteroni and A. Valli, *Numerical Approximation of Partial Differential Equations*, Springer-Verlag (1994).
- [25] K. R. Rajagopal, On boundary conditions for fluids of differential type, A. Sequeira (ed.) *Navier-Stokes Equations and Related Non-Linear Problems*, Plenum Press, 273-278, 1995.
- [26] P. A. Raviart and J. M. Thomas, *Introduction à l'analyse numérique des équations aux dérivées partielles*, Masson (1983).
- [27] W. Rudin, *Real and Complex Analysis*, McGRAW-HILL (1970).
- [28] Y. Saad, *Iterative Methods for Sparse Linear Systems*, (Second edition) Society for Industrial and Applied Mathematics, Philadelphia (2003).
- [29] J. Serrin, *Mathematical Principles of Classical Fluid Mechanics*, in S. Flugge and S. Truesdell, editors, *Handbuch der Physik*, Vol. VIII, Springer-Verlag, Berlin (1969).
- [30] E. J. Shaughnessy, I.M.Katz and J.P.Schaffer, *Introduction to Fluid Mechanics*, Oxford University Press (2005)
- [31] V. A. Solonnikov, *Estimates for solutions of nonstationary Navier-Stokes equations*, Journal of Mathematical Sciences, Vol. 8, Number 4, 467-529 (1973).
- [32] R. Temam, *Navier-Stokes Equations and Nonlinear Functional Analysis*, Society for Industrial and Applied Mathematics (1983).
- [33] R. Temam, *Navier-Stokes Equations. Theory and Numerical Analysis*, 3rd ed. North-Holland, Amsterdam (1984).

- [34] R. Verfürth, A posteriori error estimators for the Stokes equations, *Numer. Math.*, 55, 309-325, 1989.
- [35] J. Yeh, *Real Analysis, Theory of Measure and Integration, Second Edition*, World Scientific Publishing Co. Pte. Ltd. (2000).
- [36] K. Yosida, *Functional Analysis, Sixth Edition* Springer-Verlag (1980).
- [37] O. C. Zienkiewicz and R. L. Taylor *Finite Element Method: The Basis Vol. I, Fifth Edition*, Butterworth-Heinemann (2000).
- [38] O. C. Zienkiewicz and R. L. Taylor *Finite Element Method: Fluid Dynamics Vol. III, Fifth Edition*, Butterworth-Heinemann (2000).

Appendix: Some basic results

Review on metrics spaces

Let V be real vector space.

Let $(\cdot, \cdot) : V \times V \rightarrow \mathbb{R}$ satisfying $\forall u, v, w \in V$ and $\lambda \in \mathbb{R}$:

$$(u + v, w) = (u, w) + (v, w)$$

$$(\lambda u, v) = \lambda(u, v)$$

$$(u, v) = (v, u)$$

$$u \neq 0 \Rightarrow (u, u) > 0$$

then (\cdot, \cdot) is said to be a *scalar product* on V .

Given a vector space V with a scalar product $(\cdot, \cdot)_V$ we can define the *norm* of vector $v \in V$ as

$$\|v\|_V = \sqrt{(v, v)_V}.$$

We recall that any scalar product verifies the *Cauchy-Schwarz inequality*

$$|(u, v)| \leq \|u\|_V \|v\|_V, \quad \forall u, v \in V \tag{A-1}$$

and the parallelogram law

$$\|u + v\|_V^2 + \|u - v\|_V^2 = 2\|u\|_V^2 + 2\|v\|_V^2 \quad \forall u, v \in V. \tag{A-2}$$

The pair $(V, \|\cdot\|)$ is called *normed vector space*.

We define a *metric* associated with the norm as

$$d(u, v) = \|u - v\|_V.$$

So, every normed vectorial space is a *metric space*.

Supposing V is a normed vectorial space. Let $\{u_m\}_{m=1}^{\infty} \subset V$ be a sequence. Then the sequence is said to be *Cauchy sequence* if it satisfies

$$\lim_{n,m \rightarrow \infty} \|u_m - u_n\|_V = 0$$

A metric space V is a *complete space* when all Cauchy sequence in V is convergent.

A complete normed vector space V is said to be a *Banach space*.

A vectorial space V with the scalar product $(\cdot, \cdot)_V$ and complete for the norm $\|\cdot\|_V = \sqrt{(\cdot, \cdot)_V}$ is called *Hilbert space*.

Let $l(\cdot) : V \rightarrow \mathbb{R}$ be a linear form, *i.e.*,

$$l(\alpha v + \beta w) = \alpha l(v) + \beta l(w), \quad \forall \alpha, \beta \in \mathbb{R}, v, w \in V \quad (\text{A-3})$$

then $l(\cdot)$ is said to be bounded if

$$\exists c_l > 0 \text{ such that } |l(v)| \leq c_l \|v\|_V, \quad \forall v \in V \quad (\text{A-4})$$

Remark:

We can also say that a linear functional $l(\cdot)$ is continuous when it is bounded.

Let $a(\cdot, \cdot) : V \rightarrow \mathbb{R}$. If $\forall \alpha, \beta \in \mathbb{R}, \forall u, v, w \in V$

$$\begin{aligned} a(\alpha v + \beta w, u) &= \alpha a(v, u) + \beta a(w, u), \\ a(u, \alpha v + \beta w) &= \alpha a(u, v) + \beta a(u, w), \end{aligned}$$

then $a(\cdot, \cdot)$ is bilinear. This bilinear form is symmetric if

$$a(u, v) = a(v, u) \quad \forall u, v \in V$$

Review on differential operators

For the following, we consider $\Omega \subseteq \mathbb{R}^3$.

Gradient operator

Let $u : \Omega \rightarrow \mathbb{R}$ be differentiable in Ω . The gradient of u defines a vector field on Ω , denoted by ∇u , as follows

$$\nabla u = \left[\frac{\partial u}{\partial x_j} \right]_{j=1,\dots,3} = \begin{bmatrix} \frac{\partial u}{\partial x_1} \\ \frac{\partial u}{\partial x_2} \\ \frac{\partial u}{\partial x_3} \end{bmatrix}. \quad (\text{A-5})$$

The vector field $\mathbf{u} : \Omega \rightarrow \mathbb{R}^3$ is differentiable if all components are differentiable. The gradient of \mathbf{u} is a tensor field defined by $\nabla \mathbf{u} = \left[\frac{\partial u_i}{\partial x_j} \right]_{3 \times 3}$, i.e.,

$$\nabla \mathbf{u} = \begin{bmatrix} \frac{\partial u_1}{\partial x_1} & \frac{\partial u_1}{\partial x_2} & \frac{\partial u_1}{\partial x_3} \\ \frac{\partial u_2}{\partial x_1} & \frac{\partial u_2}{\partial x_2} & \frac{\partial u_2}{\partial x_3} \\ \frac{\partial u_3}{\partial x_1} & \frac{\partial u_3}{\partial x_2} & \frac{\partial u_3}{\partial x_3} \end{bmatrix}.$$

Divergence operator

Let $u : \Omega \rightarrow \mathbb{R}^3$ be differentiable in Ω . Then the divergence of u is a scalar defined by

$$\nabla \cdot \mathbf{u} = \sum_{i=1}^3 \frac{\partial u_i}{\partial x_i}.$$

Let $\mathbf{T} : \Omega \rightarrow \mathbb{R}^{3 \times 3}$ be a tensor field. A tensor field is differentiable if all of its components are differentiable. For a differentiable tensor field \mathbf{T} the divergence defines as vector field as follows,

$$(\nabla \cdot \mathbf{T})_i = \sum_{j=1}^3 \frac{\partial T_{ij}}{\partial x_j}, \quad i = 1, 2, 3.$$

i.e.,

$$\nabla \cdot \mathbf{T} = \begin{bmatrix} \frac{\partial T_{11}}{\partial x_1} + \frac{\partial T_{12}}{\partial x_2} + \frac{\partial T_{13}}{\partial x_3} \\ \frac{\partial T_{21}}{\partial x_1} + \frac{\partial T_{22}}{\partial x_2} + \frac{\partial T_{23}}{\partial x_3} \\ \frac{\partial T_{31}}{\partial x_1} + \frac{\partial T_{32}}{\partial x_2} + \frac{\partial T_{33}}{\partial x_3} \end{bmatrix}$$

Laplacian operator

For a scalar real smooth function $u : \Omega \rightarrow \mathbb{R}$ we denote the Laplacian of u as

$$\Delta u = \nabla \cdot (\nabla u) = \sum_{j=1}^3 \frac{\partial^2 u}{\partial x_j^2}. \quad (\text{A-6})$$

For a real smooth vector field function, the Laplacian is a vector field whose components are the Laplacian of the components of \mathbf{u} , is defined by

$$\Delta \mathbf{u} = [\Delta u_1, \dots, \Delta u_d]^t,$$

where t denote the transpose.

Vector identities and notations

Taking a scalar p and a vector field \mathbf{u} , then

$$\nabla \cdot (p\mathbf{u}) = \nabla p \cdot \mathbf{u} + p \nabla \cdot \mathbf{u}. \quad (\text{A-7})$$

where $\nabla p \cdot \mathbf{u} = \sum_{i=1}^3 \frac{\partial p}{\partial x_i} u_i$.

Taking a vector field \mathbf{u} and a tensor \mathbf{T} , then the component i ($i = 1, \dots, 3$) of the product $\mathbf{T} \cdot \mathbf{u}$ is given by

$$(\mathbf{T} \cdot \mathbf{u})_i = \sum_{j=1}^3 T_{ij} u_j. \quad (\text{A-8})$$

The double dot operation between two tensors defines the matrix inner product is defined as

$$\mathbf{S} : \mathbf{T} = \sum_{i=1}^3 \sum_{j=1}^3 S_{ij} T_{ji}. \quad (\text{A-9})$$

In \mathbb{R}^2 all previous definitions extend naturally.

We define the directional derivative of a scalar field u on Ω along the normal direction as

$$\frac{\partial u}{\partial \mathbf{n}} = \nabla u \cdot \mathbf{n}.$$

Let \mathbf{A} be square matrix. We say that \mathbf{A} is symmetric if

$$\mathbf{A}^T = \mathbf{A}.$$

We say that \mathbf{A} is positive definite if, for all non-zero vector \mathbf{x} in \mathbb{R}^3

$$\mathbf{x}^T \mathbf{A} \mathbf{x} > 0$$

Some equalities

Let \mathbf{u} be a vector field function on Ω such that $\nabla \cdot \mathbf{u} = 0$, then

$$2\nabla \cdot \mathbf{D}(\mathbf{u}) = 2\nabla \cdot \left[\frac{1}{2} (\nabla \mathbf{u} + (\nabla \mathbf{u})^t) \right] = \nabla \cdot (\nabla \mathbf{u}) + \nabla \cdot (\nabla \mathbf{u})^t = \Delta \mathbf{u} + \nabla (\nabla \cdot \mathbf{u}) = \Delta \mathbf{u}. \quad (\text{A-10})$$

We have $\nabla \cdot (\nabla \mathbf{u})^t = \nabla (\nabla \cdot \mathbf{u})$ since

$$[\nabla \cdot (\nabla \mathbf{u})^t]_i = \sum_{j=1}^3 \frac{\partial}{\partial x_j} \frac{\partial u_j}{\partial x_i} = \sum_{j=1}^3 \frac{\partial}{\partial x_i} \frac{\partial u_j}{\partial x_j} = \frac{\partial}{\partial x_i} \sum_{j=1}^3 \frac{\partial u_j}{\partial x_j} = [\nabla (\nabla \cdot \mathbf{u})^t]_i \quad (\text{A-11})$$

Taking into account the property of summations we obtain the following equality

$$\begin{aligned}
\int_{\Omega} \mathbf{D}(\mathbf{u}) : \mathbf{D}(\mathbf{v}) &= \int_{\Omega} \frac{1}{2} [\nabla \mathbf{u} + (\nabla \mathbf{u})^t] : \frac{1}{2} [\nabla \mathbf{v} + (\nabla \mathbf{v})^t] \\
&= \frac{1}{4} \int_{\Omega} \sum_{i,j=1}^3 \left(\frac{\partial u_i}{\partial x_j} + \frac{\partial u_j}{\partial x_i} \right) \left(\frac{\partial v_i}{\partial x_j} + \frac{\partial v_j}{\partial x_i} \right) \\
&= \frac{1}{4} \int_{\Omega} \sum_{i,j=1}^3 \left(\frac{\partial u_i}{\partial x_j} \frac{\partial v_i}{\partial x_j} + \frac{\partial u_j}{\partial x_i} \frac{\partial v_i}{\partial x_j} + \frac{\partial u_i}{\partial x_j} \frac{\partial v_j}{\partial x_i} + \frac{\partial u_j}{\partial x_i} \frac{\partial v_j}{\partial x_i} \right) \\
&= \frac{1}{4} \int_{\Omega} \sum_{i,j=1}^3 \left(\frac{\partial u_i}{\partial x_j} \frac{\partial v_i}{\partial x_j} + \frac{\partial u_j}{\partial x_i} \frac{\partial v_i}{\partial x_j} + \frac{\partial u_j}{\partial x_i} \frac{\partial v_i}{\partial x_j} + \frac{\partial u_i}{\partial x_j} \frac{\partial v_i}{\partial x_j} \right) \tag{A-12} \\
&= \frac{1}{2} \int_{\Omega} \nabla \mathbf{u} : \nabla \mathbf{v} + \frac{1}{2} \sum_{i,j=1}^3 \frac{\partial u_j}{\partial x_i} \frac{\partial v_i}{\partial x_j} \\
&= \frac{1}{2} \int_{\Omega} \nabla \mathbf{u} : \nabla \mathbf{v} + \frac{1}{2} \int_{\Omega} (\nabla \mathbf{u})^t : \nabla \mathbf{v} \\
&= \int_{\Omega} \frac{1}{2} (\nabla \mathbf{u} + (\nabla \mathbf{u})^t) : \nabla \mathbf{v} \\
&= \int_{\Omega} \mathbf{D}(\mathbf{u}) : \nabla \mathbf{v}
\end{aligned}$$

Remark that using (3.14) and the Green's formula (theorem 3.1.2) we have, for all $\mathbf{u} \in \mathbf{V}$,

$$\begin{aligned}
\int_{\Omega} \mathbf{D}(\mathbf{u}) : \mathbf{D}(\mathbf{v}) &= \int_{\Omega} \mathbf{D}(\mathbf{u}) : \nabla \mathbf{v} = \\
&= - \int_{\Omega} \nabla \cdot \mathbf{D}(\mathbf{u}) : \mathbf{v} + \int_{\partial \Omega} (\mathbf{D}(\mathbf{u}) \cdot \mathbf{n}) \cdot \mathbf{v} = \tag{A-13} \\
&= - \int_{\Omega} \nabla \cdot \mathbf{D}(\mathbf{u}) : \mathbf{v}, \quad \forall \mathbf{v} \in \mathbf{V}.
\end{aligned}$$

But,

$$\int_{\Omega} \nabla \cdot \mathbf{D}(\mathbf{u}) : \mathbf{v} = \int_{\Omega} \nabla \cdot [\nabla \mathbf{u} + (\nabla \mathbf{u})^t] : \mathbf{v} = \int_{\Omega} \nabla \cdot (\nabla \mathbf{u}) : \mathbf{v} = \int_{\Omega} \nabla \mathbf{u} : \nabla \mathbf{v} \tag{A-14}$$

as consequence of (2.21) and Green's formula.

Then, we conclude

$$\int_{\Omega} \mathbf{D}(\mathbf{u}) : \mathbf{D}(\mathbf{v}) = \int_{\Omega} \nabla \mathbf{u} : \nabla \mathbf{v}. \tag{A-15}$$